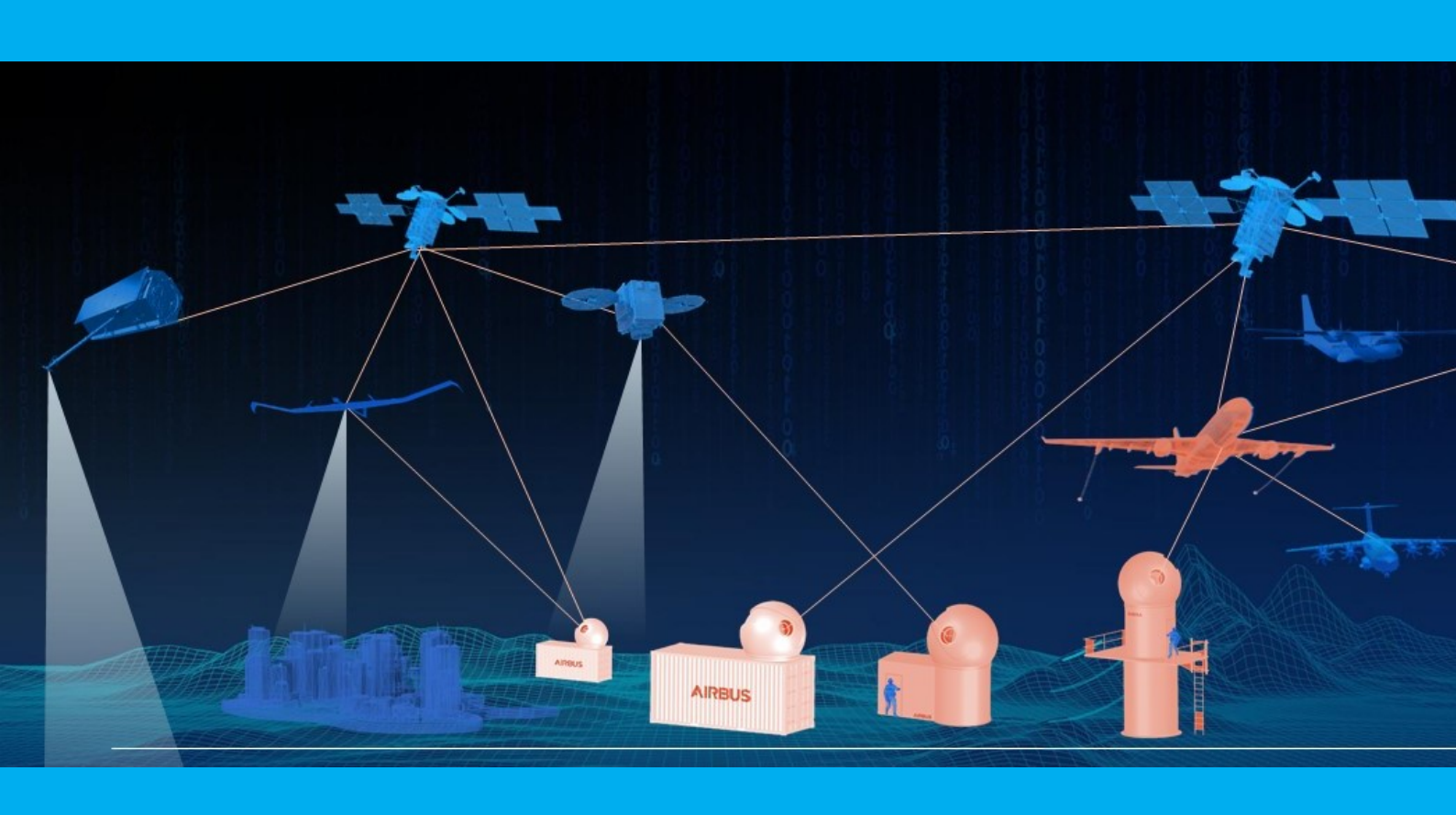
Thesis

Link Selection model for Endto-End Free-Space-optical Airto-Space laser communication services

Jari Stensen

Supervisors Rudolf Saathof (TU Delft) Remco den Breeje (AirbusDSNL)





Thesis

Link Selection model for End-to-End Free-Space-optical Air-to-Space laser communication services

by

Jari Stensen

to obtain the degree of Master of Science at the Delft University of Technology, to be defended publicly on Monday July 15, 2024.

Student number: 4666380

Project duration: November 13, 2023 – July 15, 2024

Thesis committee: Dr. ir. E. Mooij, TU Delft, Chairman

Dr. S. Gehly,

TU Delft, Second Chair

Tu Delft, Supervisor

ing. R. den Breeje, Airbus Netherlands, External

An electronic version of this thesis is available at http://repository.tudelft.nl/.



Contents

	List of Figures	
Lis	et of Acronyms	vii
	Introduction	1
2	Theory & Method	3
۷	2.1 Problem Description 2.1.1 Physical Environment 2.1.2 Time Domain 2.1.3 Client Requirements 2.2 Optimization Strategy	3 3 3 4 4
	2.3 LP Formulation	4 5 5 5
3	Implementation 3.1 Model Input. 3.2 Model Prerequisites. 3.2.1 AC/SC propagation 3.2.2 Physical level. 3.3 Performance Parameters 3.3.1 Availability. 3.3.2 Bit Error Rate. 3.3.3 Cost. 3.3.4 Latency 3.3.5 Throughput 3.4 Model Integration. 3.4.1 Visibility 3.4.2 Applicability 3.5 Model Settings	6 6 6 7 7 7 7 8 8 9 9 9 9
4	4.1 Performance	
5	Conclusion	12
Αp	ppendix	14
A	Research Objectives	15
В	Model Philosophy	16
С		20 20 22 22

Contents

	C.3 Masking. 2 C.4 Model Settings 2 C.4.1 Falling satellite module 2 C.4.2 Outperforming satellite module 2 C.4.3 Single Satellite Module 2	24 24 24
D	Linear Programming Formulation	26
Е	Link Selection Model Overview E.1 Overview	27 28
F	F.0.1 Mission and service time analysis 2 F.0.2 Falling satellite setting 2 F.0.3 Outperforming satellite setting 3 F.0.4 Performance score translated to selected satellite 3 F.0.5 Control performance parameter 3 F.0.6 Isolated performance parameter 3 F.0.7 Unit 404 to 409 3 F.1 Verification Overview 3	29 30 32 32 35
G	Variable Description 4 G.1 Greek Variables 4 G.2 Latin Variables 4	
Η	Definitions 4 H.1 Availability 4 H.2 Bit Error Rate 4 H.3 Cost 4 H.4 Latency 4 H.5 Throughput 4 H.6 Time instances 4	16 16 16
Ι	Configuration file 4	18

List of Figures

1.1	Communication terminals	2
3.2 3.1	Accumulated availability over the remaining visible time instances for 8 satellites for an 80 minute mission. High level link selection optimization model overview	7 7
3.3	The accumulated Bit Error Rate performance over the remaining visible time instances for 8 satellites for an	
3.4	80 minute mission	8
3.5	Propagation Latency Performance for 8 satellites on a 80-minutes mission	9
3.6	Throughput performance averaged over the remaining availability time for 8 satellites for an 80 minute mission	9
4.1	Active satellite (green) over time including performance score for 1 orbital planes with 14 satellites per plane	10
4.2	Active satellite (green) over time including performance score for 2 orbital planes with 14 satellites per plane	11
4.3	Accumulated link performance over complete mission time for 1 orbital plane with 14 satellites per orbit (t_M)	11
4.4	Active satellite (green) over time including performance score for 2 orbital planes with 14 satellites per plane	11
4.5 4.6	Link performance over time for 1 orbital plane with 14 satellites per orbit	11 12
	High level overview of model section entered with no active satellite	17
	High level overview of model section entered with active satellite	18
В.3	High level overview of model section entered with active satellite and equal list of applicable satellites	19
	Trade-off of all considered optimization algorithm	21
C.2	Two dimensional view of system geometry to demonstrate satellite visibility[4]	22
	Visibility and accumulated visibility over the mission time for a 14 and 28 satellite configuration	23
C.4	Bit mapping of masking analysis for different pod placements on commercial aircraft with T-tail and wingtips configuration	24
		24
	High level overview of link selection model coding structure	27
E.2	Detailed overview of link selection model coding structure	28
F.1	Active satellite and accompanied performance over time resulting from falling satellite setting verification	30
F.2	Satellite visibility and link selection for a 28 satellite configuration	31
F.3	Performance scores of 4 subsequent time instances of a 28 satellites simulation configuration showing a link	
Е4	switch	31
F.4	Mission simulation with a 28 satellites configuration while the availability performance parameter weight set	22
F.5	to 1	32
1.5	set to 1	33
F.6	Mission simulation with a 28 satellites configuration while the data transfer latency performance parameter	55
1.0	weight set to 1	33
F.7	Mission simulation with a 28 satellites configuration while the propagation latency performance parameter	
	weight set to 1	34
F.8	Mission simulation with a 28 satellites configuration while the throughput performance parameter weight set	_
го	to 1	34
F.9	Availability Performance including normalization and penalization	35 36
1.10	DIL ETTUT RALE I CHUTHIANCE INCIUUNIN NUTHIANZAUUN AND DENAME AND DENAME I CHUTHIANCE INCIUUNIN NUTHIANZAUUN AND DENAME I CHUTHIANCE INCIUUNIN NUTHIANZAUUN AND DENAME I CHUTHIANZAUUN	ათ

List of Tables

4.1	Mission performance of simulated case studies	12
F.1	Overview of performed unit tests, convergence analysis and validation on the mission level of the link selection model	37
F.2		39
F.3	Overview of performed unit tests, convergence analysis and validation on the link level of the link selection	
	model	39
F.4	Overview of performed unit tests, convergence analysis and validation on the access level of the link selection model	39
F.5	Overview of performed unit tests, convergence analysis and validation on the performance level of the link	
E6	selection model	40
1.0	tion model	41
F.7	Overview of performed unit tests, convergence analysis and validation on the input level of the link selection	
	model	41
G.1	Description of Greek Variables	42
G.2	Description of Latin Variables	43
	Description of Variables (1/2)	44
G.4	Description of Variables (2/2)	45

List of Acronyms

low-earth orbit.

LEO

ALCT	airborne laser communication terminal.	LOS LP	line-of-sight. Linear Programming.			
ASL	air-to-space links.	MMM	Modified multi-scale method.			
BER	bit-error-rate.	OGS	optical ground station.			
ECI	Earth-Centered-Inertial.	OSI	Open Systems Interconnection.			
FSO	Free-space-optics.	Q	Quality factor.			
GEO GSL	geostationary orbit. ground-to-space links.	RF RX	radio-frequency. the receiver terminal.			
HAP HMM	high altitude platform. Heterogeneous multi-scale method.	TLE TPA TPCWM	two-line element. Tracking, Point and Acquisition. Time-parallel compound wavelet method.			
ISL	inter-satellite-links.	TX	the transmitter terminal.			

UAV

Unmanned Aerial Vehicle.

Introduction Thesis

Free-space-optics (FSO) satellite communication is garnering significant interest due to its superior advantages over the traditional radio-frequency (RF) satellite communication methods. These advantages include reduced latency, enhanced channel capacity, bolstered security, and lower demands on mass and power [1]. Their are numerous of future applications of FSO communications, among which are deep-space communication, and data relay services for both geostationary orbit (GEO) and low-earth orbit (LEO) satellite constellations [2]. The latter is particularly noteworthy for its potential to dramatically boost high-speed internet access and global connectivity. Multiple of these constellations are already in place, for example the Starlink and OneWeb constellations [3]. Consequently, assuring an optimal link selection for FSO communication services between an airborne airborne laser communication terminal (ALCT) and LEO constellations is an essential step toward maximizing the benefits of this emerging service. However it is difficult to model these missions, as the scope is very broad with many physical processes occurring at different timescales. In order to be able to evaluate such missions, a comprehensive model needs to be in place which is able to asses the performance of the potential FSO communication links. However, to optimize this potential performance a link selection model needs to be in place which is able to select the link with the best performance from a mission perspective. In earlier work, it was investigated how link selection could be used for hybrid FSO and RF communication links. Several other studies focused on the performance of the FSO in data relay networks, hybrid systems or data package queuing [4, 5, 6, 7, 8]. However, none of these models focus on the use case of a link between an ALCT and a LEO constellation.

Therefore, the aim of this thesis is to develop an optimization strategy that is able to model the FSO link selection process between an ALCT and a LEO constellation from a physical and client based perspective, increasing the link quality on mission level performance. A Linear Programming (LP) formulation is proposed, which determines the optimal link by maximizing the objective function. This objective function consist of client input weights and accompanying performance parameters. These performance parameters are evaluated from a physical point of view and comprise of Availability, Bit Error Rate, Cost, Propagation Latency, Data Transfer Latency and Throughput. These performance parameters are defined based on their physical relevance after which they are translated to their mathematical counterpart. These performance parameters and the client weight form the cost function, which in combination with a set of constraints and the decision variable, which states which satellite is made active at what point is time, are able simulate the link selection decision process at mission level. This thesis is performed from November 2023 until July 2024 as a collaboration between the TU Delft (Space engineering track) and Airbus Netherlands, and can be seen as the continuation of the work performed by Wieger Helsdingen[9], who started building an End to End model simulating the performance of a FSO communication link. The thesis is initiated by the UltraAir program, which concerns the development of an FSO communication service between aircraft and satellite constellations [10]. Therefore, a mission between one aircraft and different satellite constellations is chosen as use case during this research. The main contributions of this thesis are:

- Provide a link selection optimization model to improve the link quality performance for an airborne ALCT and LEO constellation mission
- Extend the end-to-end model that allows preliminary analysis and verification of the performance of global FSO communication missions with satellite constellations.
- Insightful analysis into the behaviour of the introduced performance parameters for different types of use cases

The thesis is written as a scientific paper and will therefore consist out of two parts. Namely, the general thesis setup with all the required nomenclatures, an introduction, a main part which is presented as scientific paper, an appendix with all supporting work and additional information that is not included in the scientific paper but is relevant for the thesis, and a conclusion. The main part, the scientific article consist out chapter 1, to 5. After the scientific article the appendix will provide all material required to provide the reader with the full scope explored within this thesis. In Appendix A the research objectives, question and goals will be stated, after which in Appendix B the philosophy behind the model will be put in place. In Appendix C all supporting material from a model and physical perspective will be provided, following into a complete mathematical description of the model in Appendix D and a high level model overview in Appendix E. In Appendix F the verification process and their results will be stated. Appendix G will describe all used variables, Appendix H will provide all important definitions, whereas Appendix I will provide the input from a hardware and atmospheric perspective for the model. The final chapter will provide the overarching conclusion of this thesis including future recommendations.

Link Selection model for End-to-End Free-Space-optical Air-to-Space laser communication services

Jari Stensen
Aerospace Engineering
Delft University of Technology
Delft, The Netherlands

Abstract - Free-space-optics (FSO) satellite communication is characterized by its capacity to enable data transfer at high bandwidths, low latency, and enhanced security levels. These characteristics enable FSO communication services using satellite constellations as to be a pivotal technology for significantly increasing global connectivity. To make use of this high potential the link selection process of global FSO satellite communication services between an airborne laser communication terminal (ALCT) and a satellite constellation must be optimized. However, such an optimization is complex and computational expensive as there are multiple physical processes which need to be translated to a realistic optimization strategy. To correctly map those a set of performance parameters is created overarching the physical and geometrical performance but also the mission input. To overcome this challenge, an Linear Programming (LP) formulation is proposed that consists of a decision variable deciding if a satellite is made active or not, an objective function based on a cost function derived from the performance parameters combined with client input and a set of constraints based on the mission physical environment and time domain. Independent of the number of satellites available within the constellation the model is able to make a sophisticated choice when to switch from one link to another. This was tested for two 80-minute missions with the same ALCT and input configurations, namely with the SDA constellation with 1 and 2 orbital planes, resulting in a 86.11%, 85.26% availability respectively, and a 10.12 and 9.87 Tbits accumulated throughput respectively. Using the LP formulation as backbone of the link selection model, it is possible to efficiently provide information required to determine which link needs to be selected between an ALCT and satellite constellation.

Chapter 1

Introduction

According to Nielsen's law of internet bandwidth, global capacity demand is increasing by 50% each year[11, 12]. Free-space-optics (FSO) satellite communication services can contribute significantly to global internet coverage and high capacity connections, making it highly relevant with this rapidly increasing demand in mind. Additionally, compared to current satellite radio-frequency (RF) communication, FSO technology holds significant benefits with respect to capacity, latency, cost, and security [1]. Because of this, FSO satellite communication is a growing area of interest [2], resulting into models being developed to evaluate the performance of ground-to-space links (GSL) [13, 14, 15, 16, 17, 18], air-to-space links (ASL) [19] and inter-satellite-links (ISL) [20].

In addition, the deployment of low-earth orbit (LEO) satellite

constellations is expanding rapidly and more relay hubs are created. For example, Telesat (\pm 2000 sat), OneWeb (\pm 7000 sat), SpaceX (\pm 4500 sat) and Amazon (\pm 3000 sat) are planning to get large constellations in place [3]. This is contributing to the ability to build a complete FSO communication network [21, 4].

The first step to use the FSO communication potential in combination with the increase in LEO satellite deployment, is to be able to efficiently model such a communication service between a airborne laser communication terminal (ALCT) and a satellite constellation. In literature, models are developed to analyze link channels with atmospheric turbulence and platform vibrations [15, 18, 22, 23], models that include transported bit processes [13, 14, 24] and models that use link budgets to approximate performance [14, 24]. In addition, a more sophisticated model tries to include relative platform dynamics, atmospheric variations, atmospheric turbulence and platform dynamics into one overarching End-to-End model [9]. However, the link selection process used in this model is static, meaning that once a link is established between an ALCT and a satellite, this link is kept untill the satellite disappears on the other end of the horizon. The set of satellites which are available to establish a link with are denoted by the set of i spanning all satellite numbers. The static link selection process is a serial method and a more advanced optimization can be implemented by making use of a cost function. Namely, the performance of the link drops significantly at lower elevation angles, due to increase in geometrical link length and atmospheric density, and therefore keeping a link till it disappears on the other 2 1. Introduction

end of the horizon hurts the overall mission performance.

There are models within the FSO communications area which are applying a link selection scheme. For example, in Hassan et al. [25] a statistical delay Quality-of-service scheme for joint power allocation and relaying link selection is proposed. It optimizes the relay and aggregation node assignment by applying a mixed non-linear-programming formulation, which is solved using a Langragian dual decomposition and weight matching techniques. Zhou et al. [6] addresses a joint relay selection and power allocation problem, aiming to maximize network-wide throughput within a given power budget while having a limited number of FSO transceivers. The problem is also formulated as mixed integer nonlinear programming, and both centralized and distribution algorithms based on bipartite matching and convex optimizations are proposed. It is shown that these algorithms significantly outperform non-cooperative schemes. Korçak and Alagöz formulate in [4] an optimization problem to match high altitude platform (HAP)s and satellites such that the utilization of the HAPs is maximized together with the average elevation angle, including a method to avoid frequent switching of the optical link by favouring the active link. This problem is solved by applying a linear programming formulation with the objective function defined as maximizing the product of the number of HAPs served by the elevation angle.

Barsimantov and Nikulin are comparing three different control algorithms to optimize for the link efficiency in [8]. They proposed a gradient minimization, a logarithmic step minimization and division step minimization. From laboratory experiments that emulated the fSONA link, it was concluded that the gradient minimization method could not ensure the performance of the link, while the logarithmic minimization and division step minimization were found to be stable.

In Nadeem et al. [26] a comparison between three different implementation methods of switch-over algorithms is provided for optimal bandwidth utilization and maintaining availability in a hybrid FSO/Wireless LAN architecture. A power hysteris, with two different thresholds was deemed unsuccessful as it showed to many switches during the simulation. The delayed switching, with one threshold but with a waiting period of T seconds, outperformed the power hys-

teris and the third method, namely filtering. In the end it was shown that a combination of the power hysteris and delayed switching led to an availability close to 99.999%. Bag et al. [27] also proposed a link switching algorithm for hybrid FSO/RF-FSO link adaption. A single and dual FSO threshold scheme were simulated, from which it was concluded that the dual FSO threshold outperformed the single FSO threshold in terms of outage probability, average biterror-rate (BER) and average throughput. To conclude the provided literature review, to the best of our knowledge there is no optimization model in place within our defined physical and time domain to control the link selection process between ALCT and a LEO.

Such optimization model needs to be able to accurately translate the mission physical environment, time domain and client requirements into a set of performance parameters based on which it can optimize the link selection. A trade-off has been performed between switch-over, control and linear programming algorithms after which it was concluded that the linear programming algorithm is most suitable. This linear programming algorithm consist of (1) a decision variable, which decides which satellite is made active at what point in time. (2) An objective function which needs to be maximized in order to find the optimal solution. (3) A formalized optimization framework in the form of a cost function. This cost function is made out of the set of performance parameters and their corresponding client weight. (4) A set of constraints which bound the solution to be within the defined physical environment and time domain. The model will focus on an ASL, more specifically from any ALCT to a LEO constellation, communication mission. However, the model is built in such a modular and versatile way that it is able to be extended for any future user cases.

To start modelling this Linear Programming (LP) formulation and translate all client based and physical components into their intended use, the problem with its corresponding physical environment and time domain is described in section 2.1, after which all components of the LP formulation will be described in section 2.3. In chapter 3 an in-depth explanation about the numerical implementation of all components together comprising the link selection model is given. The implemented model is simulated on two different

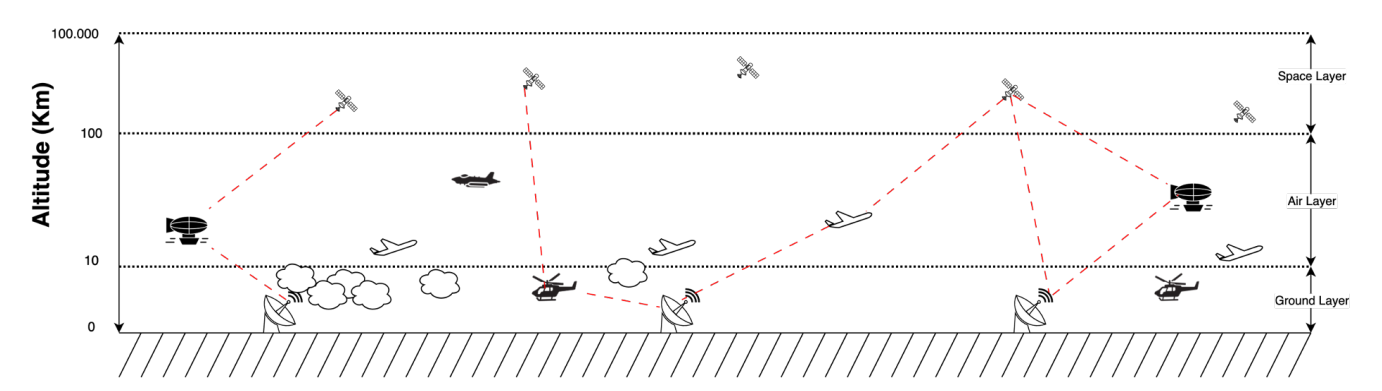


Figure 1.1: Problem visualization of relay creation by providing a hubs within the air-layer comprising of Airborne Laser Communication terminals

use cases, spanning from a low to an high satellite coverage, of which the results are shown and discussed in chapter 4. Chapter 5 will mention the main conclusion of the implemented LP model and provide recommendations for future research.

Chapter 2

Theory & Method

2.1 Problem Description

The problem under investigation focuses on a global FSO communication service facilitating connectivity between an ALCT and satellite constellation, providing an alternative routing direction for ground to space communications. The air-layer functions as a relay hub within which the communication signal can circumvent cloud obstructions, as visualized in Figure 1.1 The analysis is confined primarily to the physical layer, the lowest layer within the Open Systems Interconnection (OSI) model [28]. This study models an FSO signal, or laser-based connection, spanning from the the transmitter terminal (TX) to the the receiver terminal (RX). The model integrates both uplinks and downlinks, covering the communication and acquisition phases. The latter phase involves calibration of the pointing systems of both terminals to establish communication. One constraint to the communication is that the satellite is assumed to be the endgoal of the communication service. In order to improve the quality of the acquisition and communication phase, an optimization strategy needs to be applied to the link selection process. This optimization strategy on the link selection process needs to make sure that the best link at all instances of time within the mission is chosen. To make the problem better addressable it is divided into 3 components, the physical environment, the involved time domain and the client requirements.

2.1.1 Physical Environment

In order to find the best link between an ALCT and a satellite constellation it must be known how these two entities behave as individuals but also how they move with respect to one another. It must be noted that this research focuses on ALCT's and a LEO constellation. However, for future studies the model could be extended to include ground stations and geostationary orbit (GEO) constellation or deep space links.

An airborne ALCT is a communication system flying around at a specific altitude. Examples of ALCTs are any type of

aircraft such as an Unmanned Aerial Vehicle (UAV)'s, a commercial plane, or a HAP. For this specific research it is required to know the flight route of the ALCT, the cruise altitude and the number of optical heads. The flight route and altitude are important because the relative movement compared to the satellites must be tracked, given that the change in elevation and azimuth angle between the ALCT and satellite constellation are of significant importance for the link quality. The number of optical heads affects the acquisition time of starting a new link. Given that the ALCT only has 1 optical head it needs to hold the connection with the current link until the point it is told that it needs to switch to another link, after which it starts the Tracking, Point and Acquisition (TPA) process. This process usually can range between 5 to 60 seconds, with an equivalent downtime, dependent on the hardware and assembly used as explained in chapter 3 of Near-Earth Laser Communications by H. Hemmati [29]. If an ALCT holds two or more optical heads, it can use one of its optical heads to already start the acquisition process while still holding the previous link. In such case the acquisition process can be assumed to be instantaneous and no downtime on the communication occurs.

A LEO constellation is a group of satellites arranged within a framework in which they can work together to provide comprehensive coverage across a wide area. The main reason to make use of a LEO constellation is the reduced communication latency as a result of their lower orbit altitude, compared to GEO constellations, which allows for 70 times more round trips of data for a LEO communication service. It is important to know the the following aspects of a LEO constellation. (1) Number of orbital planes: the number of distinct paths around the Earth. A constellation comprises of multiple planes to ensure coverage and redundancy. (2) Number of satellites per orbital plane: the number of satellites within each distinct orbital plane. The total number of satellites in a constellation is calculated by multiplying the number of satellites per orbital plane with the number of orbital planes. (3) Inclination: The orbital planes are usually inclined at specific angles relative to the equator, depending on the desired coverage. Polar orbits, which have an inclination close to 90 degrees, allow satellites to pass over the poles and cover higher latitudes. Furthermore, it is important to know the phasing between each plane and the altitude of each orbit.

2.1.2 Time Domain

The above explained ALCT's and LEO constellations need to be placed within the right time domain. In this section all mathematical expressions will be given for each time stamp and index.

The **mission time** (t_M) is defined as the time the ALCT reaches cruising altitude till the point in time it starts to decent. The reason being that it can be assumed that during the climb and descent phase of the ALCT cloud interference can occur and thus no optical links can be established due to this interference as explained in chapter 2 from Free Space Optical Communication, 2018, Kaushal [30]. It is envisioned

4 2. Theory & Method

that one of the use cases of these ALCT's is going to be as a data relay point which forwards the signal from an optical ground station (OGS) to the next hub.

$$t_M = t_{M,end} - t_{M,start} (2.1)$$

The **service time** (t_S) is defined as the combined time of all operational links within the mission time. From a mathematical point of view it is defined as shown in Equation 2.2, where t_{L_i} is the link time.

$$t_S = \sum_{i=0}^{i} t_{L_i} \tag{2.2}$$

$$t_S \le t_M \tag{2.3}$$

The loss from mission to service time is the accumulated acquisition time and outage periods during which a link was selected but was not available as it did not have a positive link margin. The service time is therefore always equal or smaller than the mission time as shown in Equation 2.3.

The **visible time** is defined as the time that the satellite is visible for the ALCT. If the satellite is within line-of-sight (LOS) of the ALCT the elevation angle is assumed to be larger than zero. In reality, this angle can be slightly negative due to the altitude of the aircraft with respect to the surface of the earth. This physical visibility is defined based on a derivation provided by Korcak and Alagoz [4], which is further explained in Appendix C.

$$t_{V_i} = t_{V_i,e} - t_{V_i,s} (2.4)$$

2.1.3 Client Requirements

Potential clients in the field of FSO communication have several mission drivers when evaluating service offerings, namely (1) link availability, (2) link quality, and (3) link financial cost. Link availability is a pivotal concern, encompassing not only the global coverage but also the percentage of time during a mission that the communication link remains accessible. In terms of link quality, clients assess various parameters including throughput, which is constrained by capacity as per the Shannon-Hartley theorem [31], BER defining the number of bit errors at the receiving end, and latency which is the delay of transferring bits from a transmitter to a receiver, all of which significantly impact the efficacy of data transmission. As the market for laser communication in space becomes more commercialized, the induced costs are becoming more relevant. It is anticipated that end-users will incur costs based on the duration of connectivity to a satellite, along with a one-time fee for establishing the link. This evolving cost framework underscores the need for FSO communication solutions that balance performance with affordability, catering to the growing demand for reliable and cost-effective satellite communication services.

2.2 Optimization Strategy

Three different optimization strategies were assessed to decide which would be best suitable for the defined problem.

The first strategy is a (1) Switch-over algorithm [32], which is designed to manage transitions between different operational modes or system states, ensuring seamless handoffs in processes such as network routing, control systems, or data management. These algorithms prioritize reliability and minimal transition time, often used in scenarios requiring high availability or low fault tolerance. Next, a (2) control algorithm which is typically used in engineering systems where regulation of variables such as temperature, speed, or position is required. They compute control inputs that drive a system towards a desired state. The last assessed strategy is a (3) Linear programming algorithm [33] which solves optimization problems where the objective function and the constraints are linear. These algorithms, such as the Simplex method or interior-point methods, are fundamental in operations research, economics, and scheduling tasks. An extensive trade-off has been performed, which is described in section C.1, after which it was concluded that the LP formulation would be most suitable given that its modular setup allows for future extensions of the model while finding a nearoptimal solution.

2.3 LP Formulation

An LP formulation consist of a decision variable, objective function and the constraints it is bounded to. Based on the provided problem description in section 2.1, these components will be derived.

2.3.1 Performance Parameters

The set of defined performance parameters is shown below in matrix 2.5, and it consist out of an availability (\hat{Q}_{A_i}), BER (\hat{Q}_{BER_i}) , cost (\hat{q}_{C_i}) , data transfer latency (\hat{Q}_{DTL_i}) , propagation latency (\hat{q}_{PL_i}) and throughput parameter (\hat{Q}_{R_i}) . The nomenclature used is a capital Q for performance parameters which are an assessment over future time indices, and lower case q is used for performance parameters which are derived at an instantaneous point in time. The performance parameters are individual components with a suffix to indicate the specific performance target. They all show diverse behaviour and are expressed in different units, therefore they will be normalized to a value between 0 and 1. The normalized performance parameters are indicated by \hat{q} or \hat{Q} , dependent on the parameter itself. For the mathematical notation detailing the individual performance parameter, t_i is used to indicate the time at point j, t_{acq} is the acquisition time and the subscript 'e' and 's' are used to indicate the 'end' and 'start' of a time interval.

Normalized Performance Parameters

$$Q_{i} = \begin{bmatrix} Q_{A_{i}} \\ \hat{Q}_{BER_{i}} \\ \hat{q}_{C_{i}} \\ \hat{Q}_{DTL_{i}} \\ \hat{q}_{PL_{i}} \\ \hat{Q}_{R_{i}} \end{bmatrix}$$

$$(2.5)$$

The first mission driver mentioned in subsection 2.1.3, the link availability, addresses that a client would like to increase

2.3. LP Formulation 5

its global coverage. This can be achieved in two ways. First, the client can increase the number of ALCTs it has available, while making sure these ALCTs are able to link to more satellite constellations or deploy a constellation of their own. Second, the client can make use of a link selection model which optimizes the availability between the ALCT and satellite constellation. This can be included within the LP formulation as the Availability \hat{Q}_{A_i} performance parameter. This performance parameter, if prioritized, makes sure that the total link time as a percentage of mission time is maximized.

The second mission driver mentioned is the link quality, ensuring that given an available link exists, the performance of that link is as optimal as possible. This quality factor can be divided into three components and therefore multiple performance parameters are introduced. The first physical performance parameter takes into account the physical BER. The BER is the number of bit errors divided by the total number of transferred bits during a studied time interval as explained in chapter 5 from Free Space Optical Communication, 2018, Kaushal [30]. If the BER performance parameter \hat{Q}_{RER} is prioritised the link selection model will make sure that the time instances with a high Bit Error Rate are minimized. The second quality component is the latency, which can be divided into two separate performance parameters, namely propagation latency \hat{q}_{PL_i} and data transfer latency \hat{Q}_{DTL_i} . If the propagation latency is prioritised the link selection model will make sure that the distance between the ALCT and satellite is smallest during a link switch. If the data transfer latency is prioritised the link selection model will make sure that the average data transfer delay over all future time instances is minimized. The third quality component is the throughput, which is defined as the number of bits transferred during a studied time interval. This results in the throughput performance parameter \hat{Q}_{R_i} , and if prioritised the link selection model will make sure that the accumulated throughput of the mission is maximized.

The last mission driver is the link cost, which is modelling the financial impact of such a communication mission. A cost performance parameter is introduced \hat{Q}_{C_i} , which if prioritised the link selection model will make sure that the overall mission cost will be minimized.

2.3.2 Link Switching Penalty

The aforementioned Linear Programming algorithm should be applied repeatedly in both a periodic manner, meaning at a predefined ΔT and an event driven manner, which ensures that the change in visibility matrix is accounted for. Zooming in at these aspect it must be considered that frequent switching of the link between ALCT and satellite may result is a small gain in terms of performance parameters but does not compensate for the cost of the switching operation. Thus, it is better to avoid frequent switching and favor the existing link in the optimization algorithm. This can be done by introducing a penalty to inactive links as the acquisition time needs to be taken into account for each specific performance parameter apart from the propagation latency. The latency parameter is dependent on the distance between

the ALCT and satellite i. Therefore, it not influenced by a propagation over time compared to the other performance parameters. Furthermore, for the cost performance parameter a time penalty does not make sense. Instead, the fixed costs, the cost to establish a link, are serving as acquisition costs and can therefore be used as a penalty on the cost performance.

2.3.3 Client input

Each of the mentioned performance parameters in subsection 2.3.1, can be prioritised or omitted by the client by applying a certain weight to this specific performance parameter. These weights are summarized in matrix 2.6, and combined with the performance parameter matrix 2.5 they form the cost function as shown in Equation 2.12.

Client Input Matrix

$$A = \begin{bmatrix} \alpha_A \\ \alpha_{BER} \\ \alpha_C \\ \alpha_{DLT} \\ \alpha_{LP} \\ \alpha_R \end{bmatrix} = \begin{bmatrix} \text{Availability Weight} \\ \text{Bit Error Rate Weight} \\ \text{Cost Weight} \\ \text{Data Transfer Latency Weight} \\ \text{Propagation Latency Weight} \\ \text{Throughput Weight} \end{bmatrix}$$

$$(2.6)$$

2.3.4 High-level LP overview

Decision Variable

The backbone for an LP algorithm is its decision variable. For this use case, the decision variable E_i^T represents whether a link between the ALCT and satellite i has been made active. The mathematical notation is shown in Equation 2.7 below.

$$E_i^T = \begin{cases} 1 & \text{If link is selected between ALCT and satellite i} \\ 0 & \text{Otherwise} \end{cases}$$
 (2.7)

Constraints

The appropriate constraints need to be defined. The first constraint of the LP-formulation is to make sure that the sum of all active link times is less or equal to the total mission time. This is mathematically shown in Equation 2.8.

$$\sum E_i t_{L_i} \le t_M \tag{2.8}$$

Following this logic, there also must be a constraint which assures that the sum of all separate link times is equal to the total service time. This is shown in Equation 2.9.

$$\Sigma t_{L_i} = t_S \tag{2.9}$$

The second constraint is introduced to make sure that only 1 link is active at each instance of time, as in this study it is assumed that the ALCT holds a one-to-one relationship with a specific satellite. In future studies, it could be interesting to look into one-to-many mission setups. This needs to be in place as it is assumed the ALCT's only have 1 or 2 optical heads. Ensuring that if an ALCT has 1 optical head, it is

bound to 1 link; if an ALCT has 2 optical heads, it can have 1 link and the other ALCT is used to establish the next link which reduces the Acquisition, Tracking and Pointing time.

$$\Sigma E_i^T \le 1 \tag{2.10}$$

Looking at the client input matrix, the summation of $\alpha_1 - \alpha_6$ must be equal to 1 at all times while only using real values. If a client wants to omit certain criteria from the objective function it can simply apply a 0 value to one of the input parameters, or it can optimize a specific criteria setting that value to a 1 while setting the other weights to zero.

$$\alpha_A + \alpha_{BER} + \alpha_C + \alpha_{DTL} + \alpha_{PL} + \alpha_R = 1 \tag{2.11}$$

Objective Function

The combination of the performance parameters as specified in subsection 2.3.1, with the client input from subsection 2.3.3, lead to the cost function J. The mathematical notation is shown in Equation 2.12.

$$J_{i}(t_{j}) = A \cdot Q_{i}$$

$$= \left(\alpha_{A} \cdot \hat{Q}_{A_{i}} + \alpha_{BER} \cdot \hat{Q}_{BER_{i}} + \alpha_{C} \cdot \hat{q}_{C_{i}} + \alpha_{DTL} \cdot \hat{Q}_{DTL_{i}} + \alpha_{PL} \cdot \hat{q}_{PL_{i}} + \alpha_{R} \cdot \hat{Q}_{R_{i}}\right)(t_{j})$$

$$(2.12)$$

The objective function can be defined with the introduction of the decision variable and the general time instance specification, as shown in Equation 2.14. This objective function will maximize the given cost function over the defined mission time.

$$\max_{i} \sum_{i=1}^{t_{m}} E_{i}(t_{j}) \Big(\alpha_{A} \cdot \hat{Q}_{A_{i}} + \alpha_{BER} \cdot \hat{Q}_{BER_{i}} + \alpha_{C} \cdot \hat{q}_{C_{i}} + \alpha_{DTL} \cdot \hat{Q}_{DTL_{i}} + \alpha_{PL} \cdot \hat{q}_{PL_{i}} + \alpha_{R} \cdot \hat{Q}_{R_{i}} + \Big)$$
(2.14)

The entire mathematical LP formulation combining the decision variable, the constraints and the objective function, is written out in Appendix D.

Chapter 3

Implementation

The above explained theory and method resulting in the LP formulation will be the base for the link selection model. However, the model consist of multiple components spanning from a client driven input module to a desired outcome.

In Appendix E a detailed visualization is shown of how the model is composed. In Figure 3.1 a high level overview is provided. It is worth mentioning that various components can be adjusted based on either the client preferences or the available propagation strategies. Note, all figures showing the performance parameter behaviour are calculated on 96 timestamps with a 50s time-step spanning a t_M of 80 minutes with a LEO constellation of 2 orbital planes, with 4 satellites in each orbit on an inclination of 85.00 °or visualization purposes. On the left axis, the satellite index is assigned to each individual satellite, spanning from 1 to 8.

3.1 Model Input

The model input parameters can be defined in five distinctive categories, describing what information needs to be available in advance. These parameters consist out of (1) Airborne Laser Communication Terminal in which it must be stated what type of aircraft is evaluated UAV, commercial plane or HAP. Furthermore, the flight route information must be available and the number of optical heads needs to be specified. The next category is the (2) Satellite Constellation information, focusing on orbit altitude, inclination, number of orbital planes and number of satellites per plane. An addition to this could be a constellation with multiple shells, meaning satellite planes at different orbital altitudes. Given this information the two-line element (TLE) information can be extracted from a publicly available source and the satellite position can be propagated over time. Finally, it is important to get specifications about the (3) Hardware used onboard of the ALCT and satellite and the (4) Environmental conditions. Last but not least the (5) client input should be provided. This entails the weights it wants to assign to each performance parameter, the required BER and throughput. The required BER (BER_{req}) is the worst BER which is accepted by the client from a hardware perspective [Bits/s]. The required throughput (R_{req}) is the number of bits received over a studied instance of time as per client input, which can be converted to an average required bits at a specific time index [Bits/[time]].

3.2 Model Prerequisites

3.2.1 AC/SC propagation

The ALCT and satellite propagation is done based on the model provided by Helsdingen et al. [9]. The aircraft propagation is obtained from an open source database, which provides the state vectors of the flight routes containing speed, longitude, latitude, altitude and time [34]. For the propagation of the satellites, the software tool TUdat is used, which is an in-house TU delft developed module [35, 36]. Propagation is performed within the Earth-Centered-Inertial (ECI) frame and the initial position can either be selected manually or extracted from real positional data. For the manual selection, the model inputs as mentioned in section 3.1 are the driving components. For the real positional data, TLE sets are retrieved from Celestrak [37, 38].

3.3. Performance Parameters 7

3.2.2 Physical level

The physical output, which needs to consist out of the BER, throughput and power received is calculated by making use of the Modified Multi-scale Method proposed by Helsdingen et al. [9]. This Modified multi-scale method (MMM) is based on a Heterogeneous multi-scale method (HMM) and Time-parallel compound wavelet method (TPCWM), in which physical processes spanning from macro-scale level (1 minute to days) to micro-scale level (100 milliseconds). An estimation of power received is done by composing the link budget, which takes all gains and losses into account. This estimation gets multiplied with all micro-scale induced losses, resulting in the real power received. The BER is computed by modulation schemes which parameterize the analytical relations between a Quality factor (Q) and BER. From a simulation of fluctuating BER values, the average BER can be computed by integrating over the BER probability density function of the fading channel. With this BER the actual throughput can be calculated, by subtracting the number of faulty bits per time step from the transmitted number of bits per time step.

3.3 Performance Parameters

3.3.1 Availability

The availability performance parameter is defined as follows: given a specific time index it will be checked for each upcoming instance of time if the P_{RX} is larger than the link power threshold P_{thr} which is derived from the Required Bit Error Rate stated by the client. The mathematical expression is shown in Equation 3.1 including the penalty applied if the link is not active ($E_i=0$) and its normalization in Equation D.4. The availability performance parameter is normalized with respect to the maximum time ($t_{V_{max}}$) that a satellite within constellation k is visible to the ALCT .

$$Q_{A_{i}}(t_{j}) = \begin{cases} \sum_{t_{j}}^{t_{V_{i},e}} q_{A_{i}}(t), & \text{if } E_{i}(t_{j}) = 1\\ \sum_{t_{j}+t_{acq}}^{t_{V_{i},e}} q_{A_{i}}(t), & \text{if } E_{i}(t_{j}) = 0 \end{cases}$$
where $q_{A_{i}}(t_{j}) = \begin{cases} 1, & \text{if } P_{RX,i}(t) > P_{thr}\\ 0, & \text{otherwise} \end{cases}$ (3.1)

$$\hat{Q}_{A_i}(t_j) = \frac{Q_{A_i}(t_j)}{t_{V_{max}}}$$
 (3.2)

From this performance parameter the maximum availability time (t_{A_i}) of the satellites within constellation k can be retrieved, meaning the maximum duration that satellite i has an available link with an ALCT. This will be used for subsequent calculations. The implemented availability performance behaviour is shown in Figure 3.2. It can be seen that the slope is constantly decreasing as the time increases. This behaviour makes sense, as the number of time instances where the P_{RX} is larger than the threshold is at its maximum at the start of the link visibility and decreases with each instance of time. The normalized and penalized performance parameter behaves in the exact same manner, as can be seen in Figure F.9.

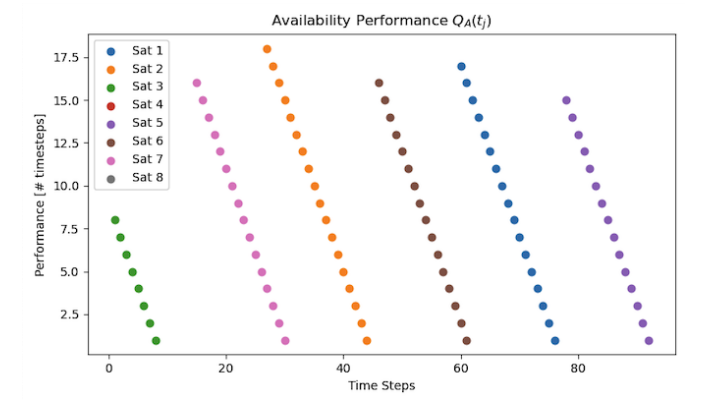


Figure 3.2: Accumulated availability over the remaining visible time instances for 8 satellites for an 80 minute mission

3.3.2 Bit Error Rate

The definition of the Bit Error Rate performance parameter is as follows: the number of future time indices for satellite i at which the actual throughput (R_{act_i}) is larger or equal then the required throughput (R_{req}) . The mathematical expression is shown in Equation 3.3 including the penalty applied if the link is not active $(E_i=0)$ and its normalization in Equation D.6. The Bit Error Rate performance parameter is normalized with respect to the time that satellite i is available to the ALCT, as derived from the previous performance parameter.

$$Q_{BER_i}(t_j) = \begin{cases} \sum_{t_j}^{t_{A_i,e}} q_{BER_i}(t), & \text{if } E_i(t_j) = 1\\ \sum_{t_j+t_{acq}}^{t_{A_i,e}} q_{BER_i}(t), & \text{if } E_i(t_j) = 0 \end{cases}$$
(3.3)

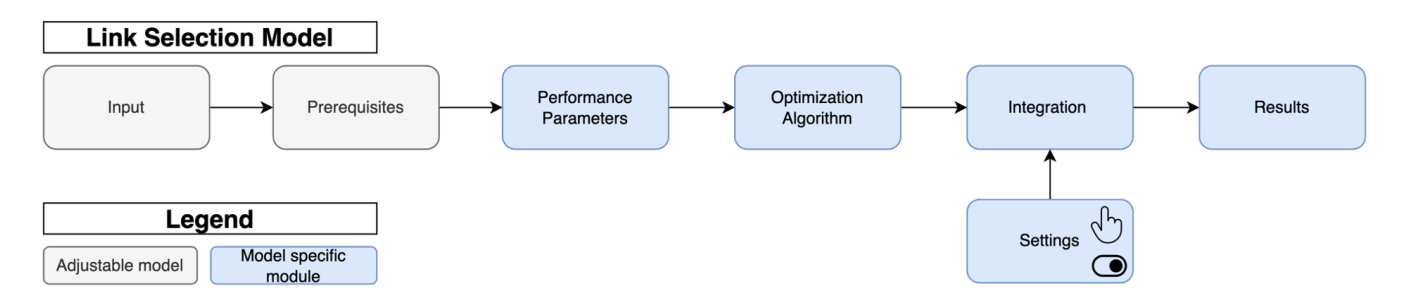


Figure 3.1: High level link selection optimization model overview

8 3. Implementation

where
$$q_{BER_i}(t_j) = \begin{cases} 1, & \text{if } R_{act,i}(t) >= R_{req}(t) \\ 0, & \text{otherwise} \end{cases}$$
, $t_j \le t \le t$

$$\hat{Q}_{BER_i}(t_j) = \frac{Q_{BER_i}(t_j)}{t_{A_{max}}}$$
(3.4)

In Figure 3.3 the performance of the BER parameter is shown. It can be seen that the BER performance is constantly decreasing as the time increases. This behaviour makes sense, as the number of time instances where the actual throughput matches the required throughput is at its maximum when the satellite becomes visible and decreases with each future time step. The normalized and penalized performance parameter behaves in the exact same manner, as can be seen in Figure F.10.

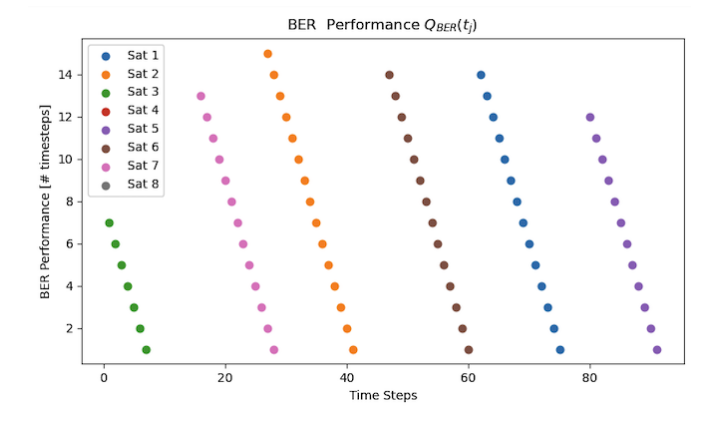


Figure 3.3: The accumulated Bit Error Rate performance over the remaining visible time instances for 8 satellites for an 80 minute mission

3.3.3 Cost

To quantify the cost performance parameter, the variable cost (C_{var_k}) is evaluated. The variable cost is the amount paid per studied instance of time, to make a link with a satellite i in constellation k. The mathematical expression is shown in Equation 3.5 including the penalty applied if the link is not active ($E_i = 0$) and its normalization in Equation D.6. The penalty is not based on t_{acq} , as seen in previous calculations, but consists of the fixed costs (C_{fix_k}) that needs to be paid to establish a link with satellite i in constellation k. The normalization is therefore also different, as it subtracts the ratio of variable cost of satellite i over the maximum variable cost within the available constellations from 1. For the normalized penalized calculation it subtracts the ratio of variable cost of satellite i over the maximum variable cost within the available constellations from 1 plus the ratio of fixed cost of satellite i over the maximum fixed cost within the available constellations from 1. For the current implementation only 1 constellation is modelled which results in an equal performance for all satellites, and therefore a flat line if the cost performance is plotted. Given that the model is setup such that it seeks for distinctive performance between different satellites, modelling the cost performance of all satellites in the same constellations results into a score of 0 for all satellites.

$$q_{C_i} = \begin{cases} C_{var_k} & \text{if } E_i(t_j) = 1\\ C_{var_k} + C_{fix_k} & \text{if } E_i(t_j) = 0 \end{cases}$$
(3.5)

$$\hat{q}_{C_{i}} = \begin{cases} \left(1 - \frac{C_{var_{k}}}{C_{var_{max}}}\right) & \text{if } E_{i}(t_{j}) = 1\\ \frac{1}{2}\left(1 - \frac{C_{var_{k}}}{C_{var_{max}}}\right) + \frac{1}{2}\left(1 - \frac{C_{fix_{k}}}{C_{fix_{max}}}\right) & \text{if } E_{i}(t_{j}) = 0 \end{cases}$$
(3.6)

3.3.4 Latency

Data transfer latency

To quantify the data transfer latency performance parameter, the following calculation will be performed: given a specific time index it will be calculated what the average propagation latency, which is derived from dividing the distance between the ALCT and satellite i (d_{ALCT-S_i}) by the speed of light (c-S), over all future time indices. The mathematical expression is shown in Equation 3.7 and its normalization in Equation D.10.

$$Q_{DTL_i}(t_j) = \begin{cases} \sum_{t_j}^{t_{A_i,e}} q_{PL_i}(t), & \text{if } E_i(t_j) = 1\\ \sum_{t_j+t_{ac_q}}^{t_{A_i,e}} q_{PL_i}(t), & \text{if } E_i(t_j) = 0 \end{cases}$$
(3.7)

where
$$q_{PL_i}(t_j) = \frac{d_{ALCT-S_i}(t_j)}{c_s}, t_j \le t \le t_{A_i,e}$$

$$\hat{Q}_{DTL_{i}}(t_{j}) = \frac{Q_{DTL_{i}}(t_{j})}{q_{PL_{min}}(t_{j})}$$
(3.8)

In Figure 3.4 the performance and the normalized performance of the data transfer latency is shown. The normalized performance is the scaled inverse of the actual performance. This behaviour is expected as from the calculation described above it can be concluded that the minimum data transfer latency corresponds to maximal performance.

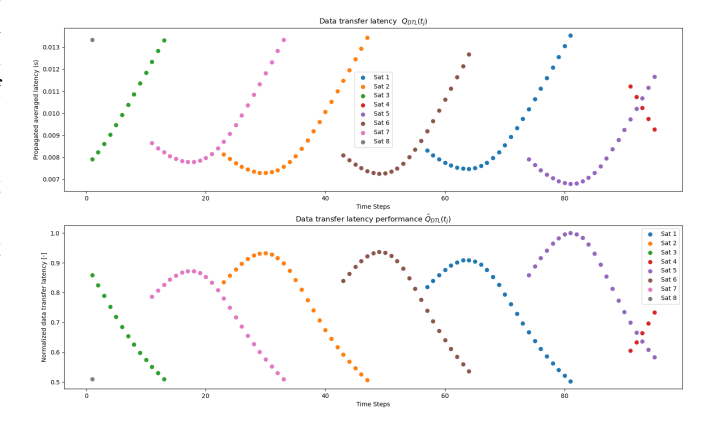


Figure 3.4: Data Transfer Latency Performance for 8 satellites on a 80-minutes mission

Propagation latency

To quantify the propagation latency performance parameter, the following calculation will be performed: given a specific time index it will be calculated what the distance between the ALCT and satellite i (d_{ALCT-S_i}) is divided by the speed

3.4. Model Integration 9

of light (c - S). It must be noted that latency consist out of more factors such as transmission delay, data package queuing delay etc. However, these factors are deemed to be equal for all links and therefore are not a distinctive quality parameter. The mathematical expression is shown in Equation 3.9 and its normalization in Equation D.12.

$$q_{PL_i}(t_j) = \frac{d_{ALCT-S_i}(t_j)}{c_s}$$
 (3.9)

$$\hat{q}_{PL_i}(t_j) = 1 - \frac{q_{PL_i}(t_j)}{q_{PL_{min}}}$$
(3.10)

With,

$$q_{PL_{min}} = \frac{d_{LCT-S_{min}}}{c_s} \tag{3.11}$$

In Figure 3.5 the performance and the normalized performance of the propagation latency is shown. The normalized performance is the scaled inverse of the actual performance. This behaviour is as expected given that based on calculation provided above it can be concluded that the minimum propagation latency corresponds to maximal performance.

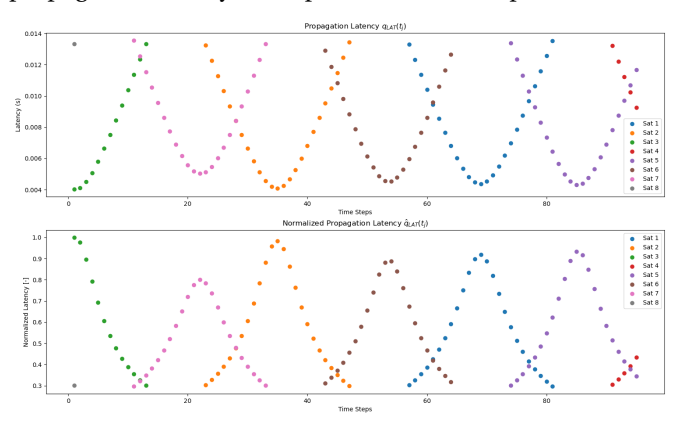


Figure 3.5: Propagation Latency Performance for 8 satellites on a 80-minutes mission

3.3.5 Throughput

To quantify the throughput performance parameter, the following calculation will be performed: given a specific time index it will be calculated what the average throughput will be for satellite i for all future time indices. The mathematical expression is shown in Equation 3.12 including the penalty applied if the link is not active ($E_i = 0$) and its normalization in Equation D.15. The throughput performance parameter is normalized with respect to the required throughput (R_{req}) provided by the client as an input.

$$Q_{R_i}(t_j) = \begin{cases} \sum_{t_j}^{t_{A_i,e}} q_{R_i}(t_j), & \text{if } E_i(t_j) = 1\\ \sum_{t_j+t_{acq}}^{t_{A_i,e}} q_{R_i}(t_j), & \text{if } E_i(t_j) = 0 \end{cases}$$
(3.12)

where $q_{R_i}(t_i) = R_{act,i}(t)$, $t_i \le t \le t_{A_i,e}$

$$\hat{Q}_{R_i}(t_j) = \frac{Q_{R_i}(t_j)}{R_{req}(t_{A_i,e} - t_j)}$$
(3.13)

In Figure 3.6 the performance of the throughput parameter is shown. The behaviour shows a relatively low first instance of the throughput performance per satellite i, the next index it moves to its highest value after which it gradually decreases over time. This behaviour is expected, as the first and last time instances of visibility time per satellite are correlated to the lowest elevation angles. These low elevation angles negatively affect the number of bits received, but that effect decreases after the first time instances of a visibility period and increases again at the end of the visibility period.

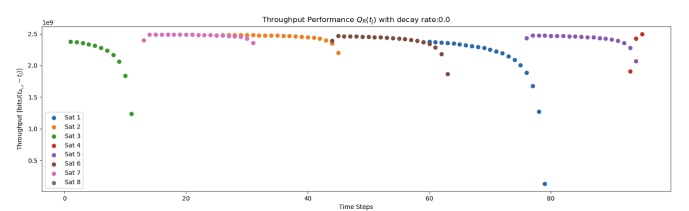


Figure 3.6: Throughput performance averaged over the remaining availability time for 8 satellites for an 80 minute mission

3.4 Model Integration

3.4.1 Visibility

With input (1) and (2) from section 3.1 and the AC/SC propagation as explained in section 3.2 a visibility matrix can be created, by making use of the flight route and TLE propagation data. Meaning, which satellite i is visible for the ALCT at every instance of time within the total mission time (t_M) . The constraints for satellite i being visible for the ALCT at time T are specified in subsection 2.1.1. The results from scanning which satellite is visible at what time will be stored in matrix 3.14. If satellite i is visible to ALCT, $V_i^t = 1$, otherwise $V_i^t = 0$.

Visibility Matrix
$$V_i^T = \begin{bmatrix} V_1^{t_{M,s}} & \dots & V_1^{t_{M,e}} \\ \vdots & \ddots & \vdots \\ V_i^{t_{M,s}} & \dots & V_i^{t_{M,e}} \end{bmatrix}$$
(3.14)

3.4.2 Applicability

A visible satellite does not per se mean that it is also feasible to include it into the set of satellites that are applicable to establish a link with. Only the set applicable satellites (A_i^T) at a specific instance of time will be used for the link selection. This set of applicable satellites matrix is created identically as the visibility matrix however after applying two selection criteria. Namely an applicability check based on elevation angle and a masking analysis. This set of constraints on the applicability can be extended further if deemed needed for other use cases.

Elevation Angle

As explained in subsection 2.1.1, it has been concluded by multiple researchers that low elevation angles lead to lower FSO link performance, due to the longer distance from ALCT to satellite and propagation at lower altitudes forcing the

laser to go through denser atmosphere, compared to looking directly upwards. The threshold used within this research is set at 10°, making sure the lowest elevation angles are omitted for selections.

active if after the performed pre-selection mentioned above, or in general, only 1 satellite is applicable.

Masking

To be able to setup a link a physical optical head needs to be present on the ALCT. Given that the optical head cannot always be fully integrated within the design of the aircraft, there is a chance that certain viewing angles are blocked. Therefore, a masking module is built within the link selection module, removing satellites from the set of applicable satellites as their combined elevation and azimuth angle overlap with a blockage from the ALCT's perspective. Two example cases are shown in section C.3

3.5 Model Settings

The model is built in such a modular way that it is able to become less computational expensive by turning certain functions off. The downside is that this leads to not all applicable satellites being included in the link selection analysis and therefore it could results in a less optimal link selected. Furthermore, it leads to omitting the calculation of the performance parameters for all satellites for all time steps. The below described settings have the capability of removing certain satellites at certain time steps from the link selection process, as it is concluded that it is cumbersome to propagate the performance of these satellites.

The first setting is the (1) falling satellite mode, which entails that an applicable satellite gets removed from the applicable set when its overall performance has decreased for 4 subsequent time instances. As explained in subsection 2.1.1 a satellite is either rising, exactly above the ALCT, or falling from a geometrical point of view. After translating this geometrical movement to the overall performance of a satellite, it can be seen from the behaviour of the visualizations in section 3.3 that if the combined performance starts to decrease, it will never start to increase again. Therefore, if an inactive satellite has an decreasing performance lower than the currently active satellite, it can be assumed that it will never overtake the current active satellite again. The second setting is the (2) outperforming satellite mode, which entails that an applicable satellite gets removed when the sum of the latency and cost parameters plus the sum of the availability, BER and throughput weights is lower than the score of the currently active satellite. Namely, the latency performance parameters are retrieved from the geometrical output and the cost performance parameter is retrieved from the input, which are relative small computational efforts compared to the propagation of the physical output needed for the availability, BER and throughput performance. Thus when such a satellite does not outperform the active satellite with a perfect scoring on the computational expensive performance parameters (i.e. adding the weight of a parameter means it scoring a 1), it can be removed. The third setting is the (3) single satellite mode, which automatically makes a satellite

Chapter 4

Results and Discussion

The results of the model will be presented by demonstrating the link switching and physical performance of two different use cases. These use cases are chosen such that combined they show were the added value of the model is. The first use case comprises of one constellation with a relatively low satellite coverage and therefore no real satellite decision needs to be made. The second use case has an increased satellite coverage, forcing the model to make multiple decision between two or more satellite. For the two use cases a flight route of Oslo to Eneves is used. This ALCT, in the form of a commercial aircraft, is equipped with 1 optical head where it is assumed that $T_{acq} = 20s$. The simulation was run on a 50 second time interval. The hardware and atmospheric input values are specified in Appendix I. The required throughput (R_{req}) and BER (BER_{req}) is assumed to be 2.5 Gbps and 10e-6, and the performance parameters are weighted equally.

4.1 Performance

The first case simulates the SDA constellation, using only 1 orbital plane with 14 satellites orbiting at an inclination of 85.0°. The link selection performed is visualized in Figure 4.1. For each satellite within the constellation a dot is shown if it is applicable, this dot is red if the satellite is inactive and green if the satellite is active. The first and lasts dots for each satellite correspond to lower elevation angles and thus lower link performance.

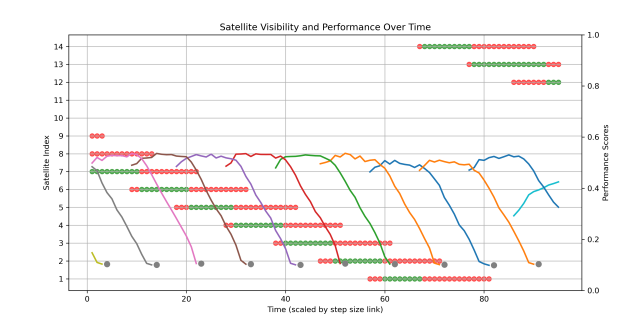


Figure 4.1: Active satellite (green) over time including performance score for 1 orbital planes with 14 satellites per plane

4.1. Performance

The behaviour of the simulation is promising as it is handing over the link, apart from the first connection, omitting low elevation angles. Namely, the general behaviour observed is that the link is handed over at the middle of the satellites its applicable time which corresponds with the third applicable time instance of the next satellite. This link selection translated to physical performance of the mission which is shown in Figure 4.2 and Figure 4.3. The difference between the two figures provided is that Figure 4.2 provides the relative behaviour at each time instance in terms of latency, throughput, cost and availability, while Figure 4.3 accumulates this behaviour.

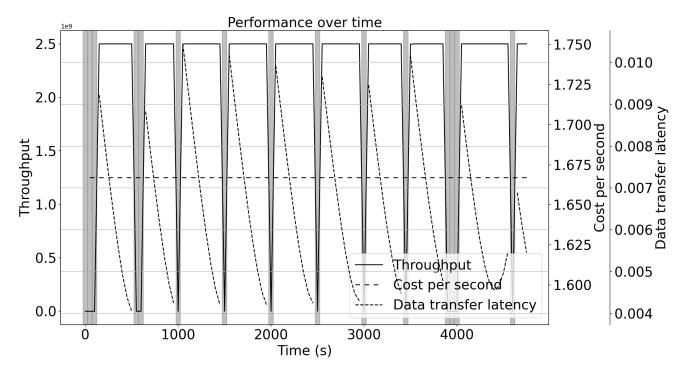


Figure 4.2: Active satellite (green) over time including performance score for 2 orbital planes with 14 satellites per plane

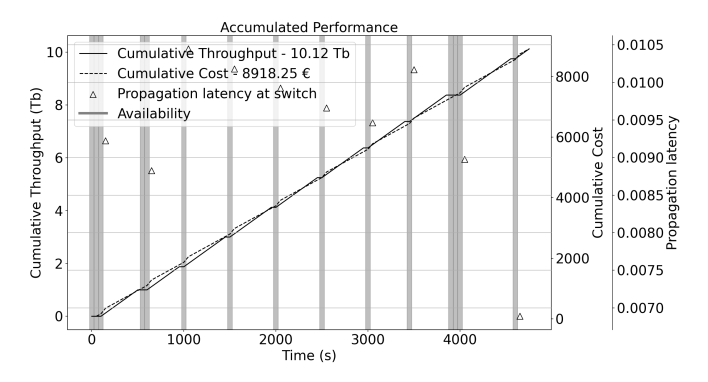


Figure 4.3: Accumulated link performance over complete mission time for 1 orbital plane with 14 satellites per orbit (t_M)

The cost is constant over time and is therefore an constant increasing line in the accumulated figure. There is a jump in the accumulated cost every time a new link is established due to the fixed cost that need to be payed to acquire a new link. Within the model it is assumed that the variable cost need to be payed independent if the link is available or not, and therefore never the cost over time never goes to zero. The throughput over time is zero when the link is unavailable and is in the neighbourhood of 2.5 Gb/s when the link is available. Therefore, the accumulated graph shows an gradually increasing throughput over time, however with flat instances when the link is unavailable. The mission has a total of 10.12 Tb accumulated throughput. The availability is shown by a grey background in the figures, within this grey area it can be observed the throughput over time is zero and at the end of the grey period a jump in the cost is induced. The data propagation latency is shown in Figure 4.2, which is the propagation latency at that point in time. It can be observed that the handover of the link in the middle of the

applicable time of a satellite corresponds to the behaviour seen in data transfer latency as it reaches its minimum right before a new link is initiated. In the accumulated link performance the propagation latency is provided, presenting the time required to find a new link apart from the acquisition time.

The second simulated case, also makes use of the SDA constellation. However, in this case 2 orbital planes are used and thus a total of 28 satellites are modelled.

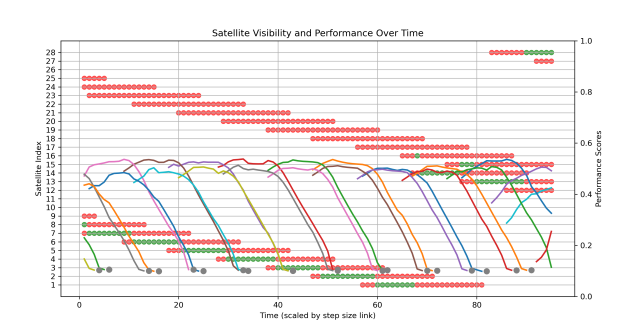


Figure 4.4: Active satellite (green) over time including performance score for 2 orbital planes with 14 satellites per plane

The same behaviour as the first simulation is observed, where the first instances of applicable time per satellite are omitted but the link is handed over neatly from satellite to satellite. The second orbital plane, indicated by the satellites indices ranging from 15 to 28 is not used at the beginning of the mission. Given that their azimuth angle, and therefore there relative distance to the ALCT is larger the first orbital plane holds the satellites with the preferred connection. This changes once the mission has prolonged and at time instance 67 the model decides to hand over the link to the subsequent satellite within the second orbital plane.

The accumulated and performance over time are provided in Figure 4.5 and 4.6. This simulation resulted in an accumulated throughput of 9.87 T bits, and an availability of 85.26%.

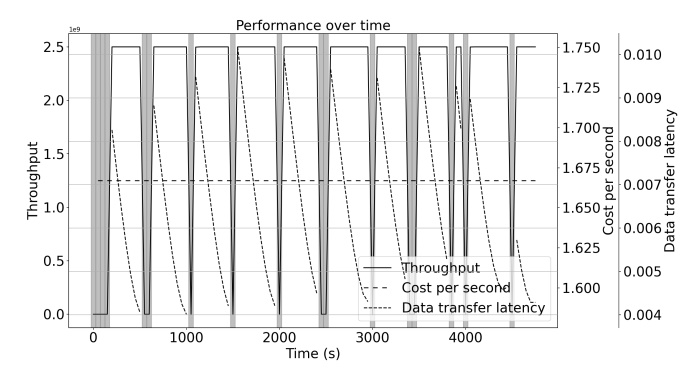


Figure 4.5: Link performance over time for 1 orbital plane with 14 satellites per orbit

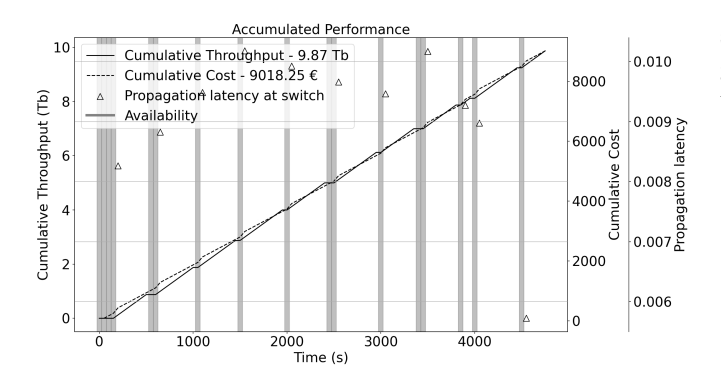


Figure 4.6: Accumulated link performance over complete mission time (t_M) for 2 orbital planes with 14 satellites per orbit

The simulation inputs and performance are summarized in Table 4.1, where also the average link time, the service time and the number of different links is provided.

Table 4.1: Mission performance of simulated case studies

Mission Input	Case 1	Case 2	
Number of orbital planes	1	2	
Number of satellites per plane	14	14	
Orbit inclination [degrees]	85	85	
Orbit altitude [km]	1200	1200	
Mission Performance			
Number of links	10	11	
Service time [min:s]	68:52	68:13	
Accumulated throughput [T bits]	10.12	9.87	
Availability [% of mission time]	86.11	85.26	

4.2 Validation

This model is validated against the static link selection model from Wieger et al. [9]. This model employs a link selection process based on two primary conditions: (1) the elevation angle between the satellite and the aircraft must be greater than 0°, and (2) the elevation rate must be positive, indicating a rising satellite. If a satellite meets both criteria, the satellite with the highest potential elevation angle is selected. Once the satellite descends below the horizon, the link is terminated, and the ALCT begins the search for a new satellite. Running the second simulation with this type of link selection scheme, an availability of 75.25% is reached and an accumulated throughput of 9.2T bits. Comparing to the provided two simulations, the developed link selection models shows relatively a 10% in terms of accumulated throughput and a 14.7% increase in availability.

Comparing this performance to link selection schemes for Radio-Frequency communication, it can be observed that the availability performance of such schemes is 99.999% while this model reaches an availability of around 86%. The reason that laser communication communication schemes can not yet reach such availability performance has first of all to do with the required acquisition time per link switch. Given that for each link, spanning approximately 7 minutes, already 20 to 50 seconds are needed for the next acquisition resulting in a 5-12% performance decrease. Furthermore,

some links are established at relatively too low elevation angles and can therefore result in an outage period which further decreases the availability performance.

Chapter 5

Conclusion

Free-space-optics (FSO) communication missions between airborne laser communication terminal (ALCT)'s and lowearth orbit (LEO) constellation are dependent on accurate link selection in order to unlock the full potential such missions. To achieve this, an optimization strategy in the form of an Linear Programming (LP) formulation is derived. This LP formulation is designed in such a way that it can be easily adjusted to other use cases, while having the physical potential performance of each available link included within its analysis. The LP optimization strategy consists out of a multiple parts. A decision variable stating if a satellite is made active at a specific instance of time. A set of performance parameters mapping the physical and geometrical performance while taking into account the induced costs. A client input assigning weights to these performance parameters, and a set of constraints bounding to the area in which the optimal solution needs to be found. To demonstrate the effectiveness of the proposed optimization strategy, two use cases are demonstrated spanning a low to high satellite coverage. These use cases show that the behaviour of the model is as it should be, omitting links with low elevation angle, while showing a 10% and 14.7% increase in availability and accumulated throughput compared to earlier implemented static link selection models.

Bibliography

- [1] Hemani Kaushal and Georges Kaddoum. Optical Communication in Space: Challenges and Mitigation Techniques. Tech. rep. 1. Jan. 2017, pp. 57–96. DOI: 10. 1109/COMST. 2016. 2603518.
- [2] Morio Toyoshima. "Recent Trends in Space Laser Communications for Small Satellites and Constellations". In: Journal of Lightwave Technology 39.3 (Feb. 2021), pp. 693–699. ISSN: 15582213. DOI: 10.1109/ JLT.2020.3009505.
- [3] Nils Pachler et al. "An Updated Comparison of Four Low Earth Orbit Satellite Constellation Systems to Provide Global Broadband". In: June 2021, pp. 1–7. DOI: 10.1109/ICCWorkshops50388.2021.9473799.
- [4] Omer Korcak and Fatih Alagoz. "Efficient networking in an integrated HAP and mobile satellite system with optical links". In: 2009 IFIP International Conference on Wireless and Optical Communications Networks. IEEE. 2009, pp. 1–5.
- [5] Wu Weiqiang, Zhang Qinyu, and Huang Siyao. "Optimization of TCP for HAPs Network". In: 2011 First International Conference on Instrumentation, Measurement, Computer, Communication and Control. 2011, pp. 666–669. DOI: 10.1109/IMCCC.2011.170.
- [6] Hui Zhou, Shiwen Mao, and Prathima Agrawal. "On relay selection and power allocation in cooperative freespace optical networks". In: Photonic Network Communications 29 (Feb. 2015). DOI: 10.1007/s11107-014-0465-z.
- [7] Md. Zoheb Hassan et al. "Statistical Delay-QoS Aware Joint Power Allocation and Relaying Link Selection for Free Space Optics Based Fronthaul Networks". In: IEEE Transactions on Communications 66.3 (2018), pp. 1124–1138. DOI: 10.1109/TCOMM.2017.2771524.
- [8] Ohad Barsimantov and Vladimir V. Nikulin. "Adaptive Optimization of a Free Space Laser Communication System Under Dynamic Link Attenuation". In: J. Opt. Commun. Netw. 3.3 (Mar. 2011), pp. 215–222. DOI: 10. 1364/JOCN.3.000215. URL: https://opg.optica.org/jocn/abstract.cfm?URI=jocn-3-3-215.
- [9] Wieger Helsdingen et al. "End-to-End model for freespace-optical Air-to-Space communication services".
- [10] Airbus en TNO ontwikkelen lasercommunicatieterminal voor vliegtuigen. URL: https://www.tno.nl/nl/newsroom/2021/04/airbus-tno-gezamenlijk-programma.

- [11] Nils Pachler et al. An Updated Comparison of Four Low Earth Orbit Satellite Constellation Systems to Provide Global Broadband. Tech. rep.
- [12] Jacob Nielsen. "Nielsen's Law of Internet Bandwidth". In: (Apr. 1998).
- [13] Mikhail S. Belen'kii, Kevin Hughes, and Vincent Rye. "Free-space laser communication model". In: Active and Passive Optical Components for WDM Communications IV. Vol. 5595. SPIE, Oct. 2004, p. 167. DOI: 10.1117/12.570496.
- [14] Ricardo Barrios et al. "Link budget assessment for GEO feeder links based on optical technology". In: International Journal of Satellite Communications and Networking 39.2 (Mar. 2021), pp. 160–177. ISSN: 15420981. DOI: 10.1002/sat.1371.
- [15] Dirk Giggenbach et al. Reference Power Vectors for the Optical LEO Downlink Channel. Tech. rep.
- [16] Otakar Wilfert and Zdenek Kolka. "Statistical model of free-space optical data link". In: Free-Space Laser Communications IV. Vol. 5550. SPIE, Oct. 2004, p. 203. DOI: 10.1117/12.558697.
- [17] G. Eswara Rao et al. "Free-space optical communication channel modeling". In: Smart Innovation, Systems and Technologies. Vol. 43. Springer Science and Business Media Deutschland GmbH, 2016, pp. 391–396. ISBN: 9788132225379. DOI: 10.1007/978-81-322-2538-6{_}41.
- [18] Ronald Parenti et al. "Modeling the PDF for the irradiance of an uplink beam in the presence of beam wander". In: Atmospheric Propagation III. Vol. 6215. SPIE, May 2006, p. 621508. ISBN: 0819462713. DOI: 10.1117/12.666547.
- [19] Niloofar Okati and Taneli Riihonen. "Downlink and Uplink Low Earth Orbit Satellite Backhaul for Airborne Networks". In: 2022 IEEE International Conference on Communications Workshops, ICC Workshops 2022. Institute of Electrical and Electronics Engineers Inc., 2022, pp. 550–555. ISBN: 9781665426718. DOI: 10.1109/ICCWorkshops53468.2022.9814585.
- [20] Hachemi Chenina, Djamel Benatia, and M'Hamed Boulakroune. "New modeling approach of laser communication in constellation and through atmospheric disturbances". In: Bulletin of Electrical Engineering and Informatics 10.4 (Aug. 2021), pp. 2088–2099. ISSN: 23029285. DOI: 10.11591/EEI.V1014.2792.
- [21] Franz Fidler et al. "Optical Communications for High-Altitude Platforms". In: IEEE Journal of Selected Topics in Quantum Electronics 16.5 (2010), pp. 1058–1070. DOI: 10.1109/JSTQE.2010.2047382.
- Fan Yang, Julian Cheng, and Theodoros A. Tsiftsis. "Free-space optical communication with nonzero boresight pointing errors". In: IEEE Transactions on Communications 62.2 (2014), pp. 713–725. ISSN: 00906778. DOI: 10.1109/TCOMM.2014.010914.130249.

14 Bibliography

[23] Hristo Ivanov et al. "Testbed Emulator of Satelliteto-Ground FSO Downlink Affected by Atmospheric Seeing Including Scintillations and Clouds". In: Electronics (Switzerland) 11.7 (Apr. 2022). ISSN: 20799292. DOI: 10.3390/electronics11071102.

- [24] Dirk Giggenbach, Marcus T. Knopp, and Christian Fuchs. "Link budget calculation in optical LEO satellite downlinks with on/off-keying and large signal divergence: A simplified methodology". In: International Journal of Satellite Communications and Networking (2023). ISSN: 15420981. DOI: 10.1002/sat. 1478.
- [25] Md. Zoheb Hassan et al. "Statistical Delay-QoS Aware Joint Power Allocation and Relaying Link Selection for Free Space Optics Based Fronthaul Networks". In: IEEE Transactions on Communications 66.3 (2018), pp. 1124–1138. DOI: 10.1109/TCOMM.2017.2771524.
- [26] G. Kandus. "Comparison of link selection algorithms for free space optics/radio frequency hybrid network". English. In: IET Communications 5 (18 Dec. 2011), 2751–2759(8). ISSN: 1751-8628. URL: https: //digital-library.theiet.org/content/ journals/10.1049/iet-com.2009.0469.
- [27] Banibrata Bag et al. "Performance Analysis of Hybrid FSO Systems Using FSO/RF-FSO Link Adaptation". In: IEEE Photonics Journal 10 (June 2018), pp. 1–17. DOI: 10.1109/JPHOT.2018.2837356.
- [28] Sumit Kumar, Sumit Dalal, and Vivek Dixit. THE OSI MODEL: OVERVIEW ON THE SEVEN LAYERS OF COMPUTER NETWORKS. Tech. rep., pp. 461–466. URL: www.researchpublish.com.
- [29] H. Hemmati. Near-Earth Laser Communications, Second Edition. Optical Science and Engineering. CRC Press, 2020. ISBN: 9780429532610. URL: https://books.google.nl/books?id=FPn2DwAAQBAJ.
- [30] Hemani Kaushal, Vk Jain, and Subrat Kar. Free Space Optical Communication. Jan. 2017. ISBN: 978-81-322-3689-4. DOI: 10.1007/978-81-322-3691-7.
- [31] Arun K. Majumdar and Jennifer C. Ricklin. Free-Space Laser Communications, Principles and Advances. Tech. rep. 2008. URL: http://springeronline.comlseries/4810..
- [32] Mahya Aghaee and William W. Hager. "The Switch Point Algorithm". In: SIAM Journal on Control and Optimization 59.4 (2021), pp. 2570–2593. DOI: 10.1137/21M1393315. URL: https://doi.org/10.1137/21M1393315.
- [33] Karen Aardal, Leo van Iersel, and Remie Janse. Optimization. Faculty of Electrical Engineering, Mathematic and Computer Science, 2023.
- [34] Xavier Olive. "traffic, a toolbox for processing and analysing air traffic data". In: Journal of Open Source Software 4.2475-9066 (2019).
- [35] Dominic Dirkx. Tudat mathematical model definition. Tech. rep. 2022. URL: https://tudat.tudelft.nl.
- [36] Dominic Dirkx et al. Tudat Space. 2022.

- [37] Cho Chang-Hwa. "NORAD TLE TYPE ORBIT DETER-MINATION OF LEO SATELLITES USING GPS NAVIGA-TION SOLUTIONS". In: (2002).
- [38] Kelso T.S. CelesTrak. 2023. URL: https://celestrak.org/.

Appendix A

Research Objectives

In this appendix the research objective from both the TU Delft and Airbus will be translated to the research question of this thesis and their accompanying research goals. These were defined in the initial stage and were therefore subject to multiple iterations over the course of the thesis.

Research Objective Airbus: What are the requirements for a Laser Communication Terminal to accommodate a certain link availability, throughput, latency and bit error rate.

Research Objective TU Delft: Define the communications service performance of the physical communications layer based on underlying physics.

These research objectives combined entail the larger goal behind this research project, of which the initial steps were taken by Wieger Helsdingen. His research focused on the development of an End-to-End model which is able to simulate the performance of an FSO communication mission with a LEO satellite constellation by efficiently combining all relevant physical processes [9]. This E2E model will therefore be used as a starting point of this research. The current model is build such that once a laser communication link between an airborne platform and LEO satellite is established, it will not change this link over the course of the satellite passing over the ALCT. However, as explained within chapter 1, the link quality drops at low elevation angles and thus it is important to switch to a subsequent link before the satellite reaches such low elevation angles. The below stated research question is defined to tackle the above described problem.

Research Question:

"What is the impact of an optimization model on the link selection process between an airborne laser communication terminal and a Low-Earth Orbit constellation, such that it provides an improved user case-based simulation performance in terms of link quality 1 , link availability and link financial cost of the E2E 2 laser communication, while modelling all relevant 3 physical processes."

In order to answer this question, it is necessary to formulate several sub-goals that are more specific and provide more background to the overall research project. Below the three sub-goals are formulated accompanied by several elaborately questions.

Research Goals:

- 1. Model the link performance parameters, which will be used to asses the mission level performance of the free-space optical communication mission between an airborne laser terminal and a satellite constellation.
 - (a) Which parameters are already modelled within the End-to-End model? Which parameters should/could be added to map the performance more elaborately?
 - (b) What are the inter-dependencies between these performance parameters?
 - (c) How can these parameters be modelled such that a link selection can be made for any specific mission type?
- 2. Formulate a cost function to model the link selection based on the link performance parameters.
 - (a) Which methods can be used to make such cost function?

¹Link Quality consist of Bit Error Rate, Throughput and Latency

²This is an E2E model within the defined user case

³Relevant processes consist out of relative platform dynamics, atmospheric variations, atmospheric turbulence and platform dynamics

- (b) How to integrate the performance parameters into the cost function?
- (c) How to integrate the client preference to be able to tweak the link selection process based on their specific use case?
- 3. Simulate the performance of the optimization model, integrate within the E2E model and compare the results
 - (a) How should this performance be visualized?
 - (b) How to maintain versatility within the model?
 - (c) How to perform a comparison analysis to asses whether the optimization model has added value?

Appendix B

Model Philosophy

The model created can be used in different ways, and therefore it is important to discuss the philosophy behind the model. As mentioned in Appendix A, the model is an extension on the E2E model created by Wieger Helsdingen, however could be part of a broader mission scope if the definition of E2E is put to the test. In this chapter the integral model setup will be discussed after which this is translated to 2 different "how to use the model" philosophies. Thereafter, the potential model and use case extensions are discussed answering sub-question 1a-1c and 3b as defined in Appendix A.

The model consist of six different coding layers which are glued together. The high-level and detailed overview of the model are visualized in Figure E.1 and Figure E.2. From these figures it can be seen that the first layer is the (1) input-layer. This input layer comprises of a JSON configuration file. Within this configuration file all inputs, as explained in section 3.1, can be specified and adjusted for different use cases. These different use cases can span from commercial to verification purposes. An example of such a JSON configuration file is provided in Appendix I. To start a simulation, a configuration file needs to be selected. The second layer is the (2) model prerequisites layer, which consists out of a set of modules generating data which is not model specific. Therefore, these modules can be adjusted based on client preferences or different research resources. The main components are geometrical propagation of the ALCT and satellite and the calculation of the potential physical performance of a link. The current model prerequisites are build from the source code taken from the prior performed research by Wieger et al., but if it is preferred to use other propagation tools or physical performance estimators the model allows for it as long as it generates the aforementioned output in the detailed overview. The third layer is the (3) performance parameter layer, in which all performance parameters are calculated including their normalization and penalized values. Currently, there are six performance parameters included, however for future use it could be required that additional performance parameters are added (or parameters are removed). Within the current model the six performance parameters together form the performance score. However, within the JSON configuration file it is possible to specify the set of performance parameters used for the propagation of the performance score and thus is subject to chance for other use cases. If it is required to add a new performance parameter, a python class needs to be created which calculates the performance parameter at each instance of time. The required output of such a class is a set of four variations based on that specific performance parameters consisting out of the physical output, the normalized performance, the penalized performance and the normalized penalized performance. It must be noted that stating within the JSON configuration file which performance parameters to include in the model is something fundamentally different than applying weights to these performance parameters. If a performance parameter is added or removed, also the accompanying weight needs to be specified or removed while still staying within the constraints of the LP formulation.

The current model setup is such that an important distinction needs to be made between the six performance parameters. Namely, the way how they are propagated has significant effect on the computational effort required to calculate them. The cost performance parameter is simply based on the input provided on the variable and fixed cost of all constellations available to establish a link with, and therefore the computational effort is very low. The two latency performance parameters (data transfer and propagation) are solely dependent on the geometrical output, more specific the distance between the ALCT and the satellite. These distances are propagated within the relative movement prerequisite and therefore easily

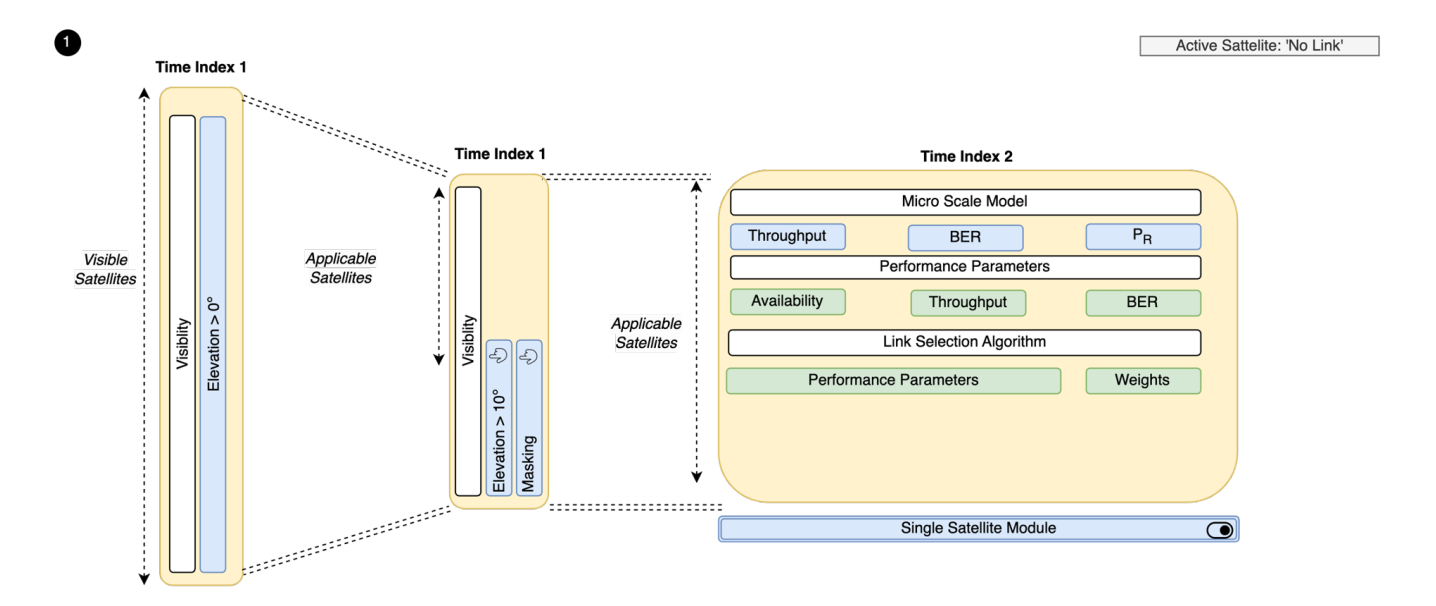


Figure B.1: High level overview of model section entered with no active satellite

accessible and require low computational effort. The propagation for the availability, bit error rate and throughput performance parameter is significantly more computational intensive, as it involves a Monte Carlo simulation. This Monte-Carlo simulation gives an accurate simulation of the P_{RX} and bit-error-rate (BER) over the entire span of the mission. These physical performance can be converted to the availability, BER and throughput performance parameter at a specific instance of time. Within section 3.3 it is explained why it is needed to calculate the physical performance over the entire mission span, to generate the performance parameter at a specific instance of time.

The fourth layer is the **(4) settings layer**, in which it can be specified what modules to be turned on or off. These settings have significant impact on the computational effort required to run the simulation. They are mentioned in section 3.5 and will be further explained in section C.4. Furthermore, within the JSON configuration file shown in Appendix I each setting can be turned "ON" or "OFF". The fifth layer is the **(5) optimization algorithm**, which selects the best link to be made active based on the selected performance parameters at each instance of time.

The above five layers combined form all the necessities needed to generate the required results. However, these layers need to be integrated such that the data flows in the right direction. Namely, given the input and settings, the selected performance parameters are maximized in order to be able to optimize the link quality, availability and cost for the selected mission use case. To be able to perform the optimization, it is important that the model enters the correct section of the code while looping through each instance of time. This is needed to take into account the current state of the mission. Before the model starts looping through the mission time, the cost, data transfer, and propagation performance parameter are calculated and stored for all instances of time, as their computational effort is insignificant. This timestep is an important feature of the model. Namely, the customer can define himself what the Δt is between two consecutive time indices. The larger the timestep the less computational effort is required as it simply has to perform fewer iteration, however this could lead to a missed optimal switching point.

The model can enter three different loops, which are visualized in Figure B.1, B.2, B.3. The status of the currently active satellite and the set of applicable satellites (A_i^T) at that specific instance of time is leading in which loop gets entered. Namely, given that it is the first instance of time, or an outage period has occurred in which no link was selected, the model enters the loop with the current active satellite in the "No Link" status. This section of the model is visualized in Figure B.1 and indicated in the overview by the '1' in the left corner.

Within this section of the model all applicable satellites will be evaluated independent on what settings are turned on, which starts with the calculation of the availability, bit error rate and throughput physical performance by performing the earlier mentioned Monte-Carlo simulation. This physical performance will be converted to the performance parameters for the specific instance of time. With all the performance parameters calculated (i.e. taking the performance values at the specific time instance from the stored data transfer, propagation and cost parameter), the optimization algorithm can check which satellite performs best and select that one to become active.

Given that a satellite was selected in the previous time index, the model enters the loop where the current active satellite is a

18 B. Model Philosophy

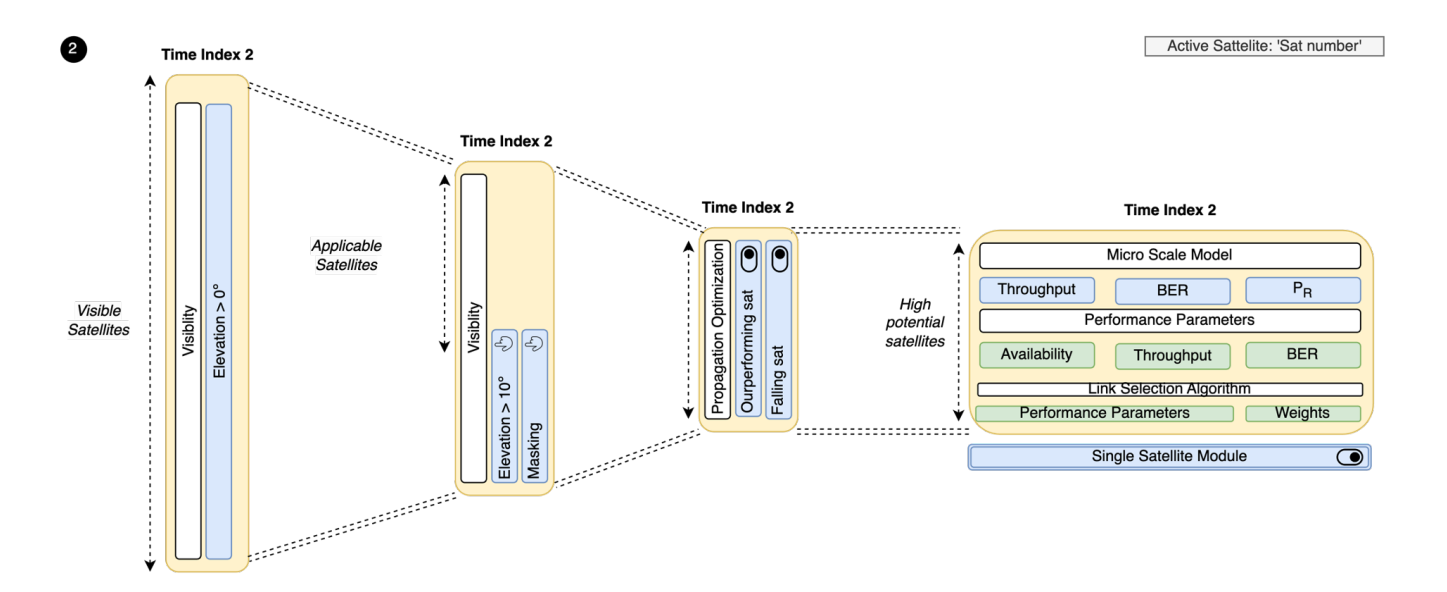


Figure B.2: High level overview of model section entered with active satellite

"satellite number". This section of the model is visualized in Figure B.2. Dependent on the settings turned on, the list (or the reduced list) of applicable satellites will be used to propagate the physical performance by making use of the Monte-Carlo simulation. This will once again propagate the physical performance for the entire mission span, which is converted to the availability, BER and throughput performance parameter at that specific instance of time. The optimization algorithm performs the link selection again and dependent on the combined performance scores, either the same satellites remains active or a new satellites gets selected.

The third section the model can enter is visualized in Figure B.3. This section is entered if a satellite was selected in the previous time index and the set of applicable satellites is identical (in terms of satellite index numbers) as the previous time index. Given that the set of applicable satellites is identical as the previous time index, the list of physical performance generated at the previous time index can be used to calculate the performance parameters. It must be noted that the physical performance of the previous time index will be removed, such that the remaining set of physical performance is only reflecting the current time index and all future ones. This is also shown in the visualization by stating that the physical performance list is taken [1:], which is a python syntax for keeping the list equal while removing the first instance of that specific list.

After the model has completed all timestamps, it creates a new folder with use case and timestamp references in which all mission results are stored. This result folder is the final layer shown in overview provided in Figure E.1. The results stored consist of a set of graphs, some animations, and various CSVs with numerical output. This **(6) results folder** is the sixth and last layer of the model and the set of graphs and csv files generated can be used for further mission analysis.

From the above explanation it can be concluded that the model is quite complex and computational expensive. In order to suit multiple user philosophies the settings module allows the user to make the model less computational expensive. From our point of view there are two ways of using this model. First of all, the **A-priori** mission analysis setup in which a simulation is performed in advance of the mission itself. This will allow the user to make the model as computational expensive as the computational facilities allow. The results of the simulation can be used to pre-program the ALCT. Furthermore, given the commercialization of the FSO communication market, it is expected that within a couple of years customers need to "reserve" a time slot with a satellite operator to establish a link. These reservations can then be made prior to the mission. The second use case is the **Ad-hoc** solution setup in which the model is simulated during the mission if any discrepancies occur in link establishment, reservation or routing. This means that the model needs to be simulated while the mission is in operation, and therefore it is required to minimize the computational effort as it is expected the computational availability is limited onboard of the ALCT. This can be done by turning on all settings explained in section C.4, which removes a lot of calculations that are needed to achieve the final bit of accuracy but are cumbersome if a short term estimate is needed. However, even with all settings turned on, the model has a relatively high computational effort to be simulated during a mission. Therefore, it is important that the model is further improved which will allow the model to be ready for future use case extension.

The first improvement to save computational effort is to elaborate the copying of the physical performance. Namely, in the current model setup, only if the set of applicable satellites is exactly equal compared to the previous time instance, the

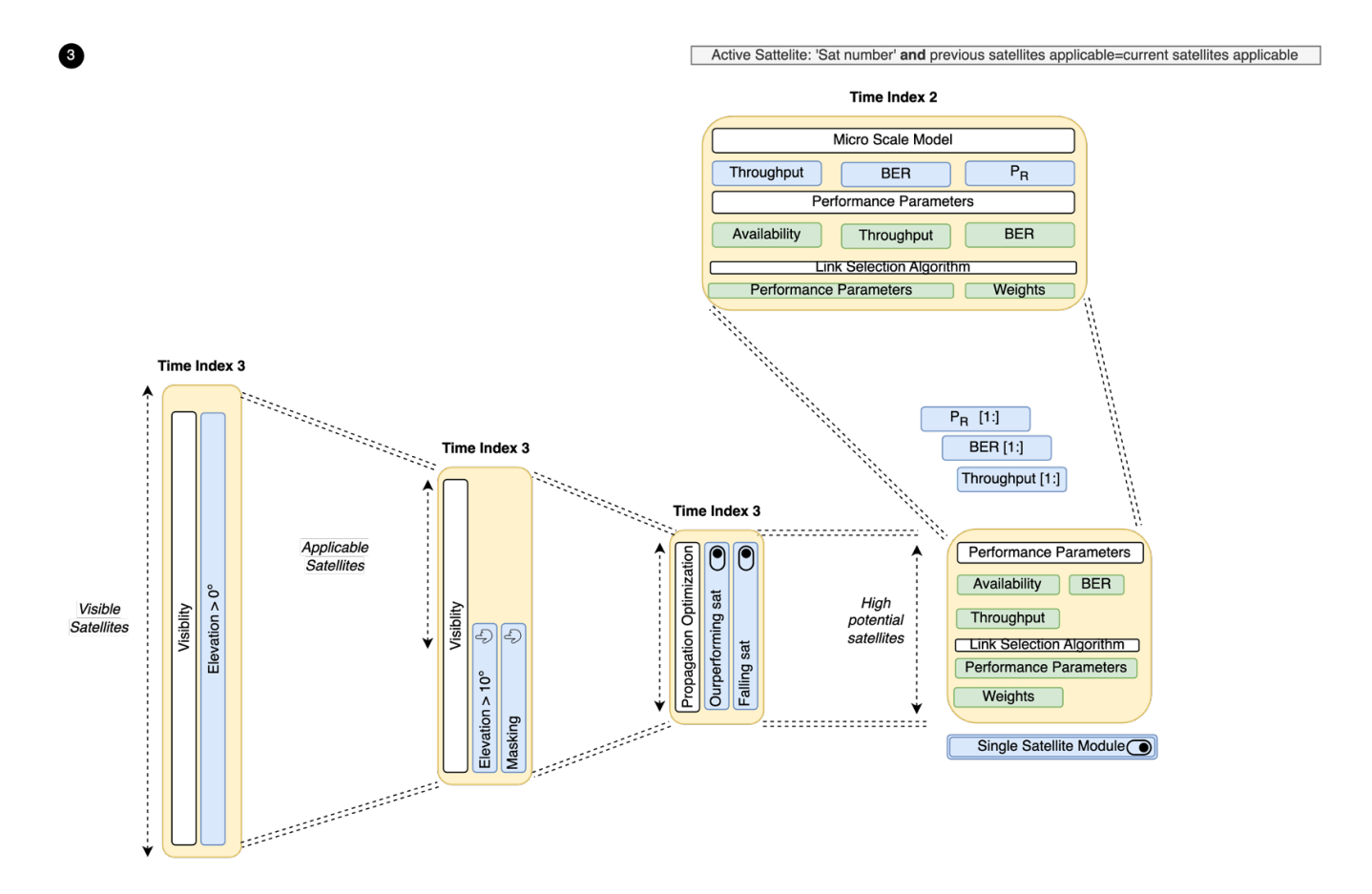


Figure B.3: High level overview of model section entered with active satellite and equal list of applicable satellites

physical output is used as calculated in the previous time instance calculated. The condition that the set of applicable satellites must be equal to the previous time instances should be converted to a condition which checks if a specific satellite was applicable in the previous time instance, and if so use the physical performance accordingly. Furthermore, a control performance parameter should be introduced, which chooses what satellite to be made active based on readily available data like the distance between the ALCT and satellite or elevation angle. This control performance parameter could be integrated as a dominant factor when a satellite needs to be made active within a short time interval. Moreover, to make the model more complete it should be able to include multiple constellations within the simulation. Currently only 1 different constellation is modelled, resulting in an equal cost performance for all satellites within the simulation. However, a satellite should be assigned to a specific constellation within the input source code. In general, a user is able to create or upgrade the settings or pre-selection methods by himself, given that they suit the purpose of the model.

The current setup of the model is such that it is able to make an assessment between an air to space link, more specifically a LEO link. In order to be able the model the entire routing network, i.e. from ground to space and back by making use of a mash network of different airborne ALCTs, the model need some refinement. Either it can be decided to incorporate this model into an existing ground to space routing model, or further extend this model such that it also entails the calculations incorporating those communication layers.

Appendix C

Supporting Material

In this appendix all supporting material needed to provide the reader with the full scope of the thesis is addressed. The scientific paper mentions various design choices, model explanations, physical components as taken for granted, while elaboration is required to fully understand the completed process. Therefore, firstly the performed trade-off will be explained, stating the criteria used to asses the different optimization algorithms, and what arguments were found to decide to initiate an LP formulation. Thereafter, the landscape is further elaborated on by providing a mathematical approach how the visibility is defined. This is followed by an explanation about the masking module, and the model settings.

C.1 Trade-off

The optimization algorithms that were analysed to answer question 2a from Appendix A are switch-over, control and linear programming algorithms. These three algorithms will be introduced briefly, after which they will be compared based on a set of trade-off criteria.

Switch-over algorithms can be found in multiple different forms, however they are all based on the same aspect. Namely, a threshold is defined and if this threshold is exceeded an action is performed. Practical application of this are hybrid FSO-RF systems or relay selection networks, in which due to cloud attenuation the primary FSO link has become insufficient and thus the link is switched to the RF or another FSO link. Furthermore, there are interesting differences how such a switch-over algorithms is applied. For example, it is possible to make use of a single, double and time based thresholds. In order to make model more stable filtering strategies can be implemented. All of these variants are mainly used to prevent frequent switching.

The next type of optimization algorithm assessed is the control algorithm. This algorithm is based on setting a desired setpoint, and the algorithm adjusts the control inputs to a system to converge and if reached maintain this setpoint. There are interesting variations how these control algorithms are applied. For example, adaptive control algorithms can adjust their parameters in real-time based on the system's behavior, while robust control algorithms are designed to perform well despite uncertainties and disturbances in the system. These variations are mainly implemented to enhance the performance, stability, and efficiency of the control system under different conditions.

The last algorithm assessed in the trade-off is the linear programming algorithm. To perform a linear programming optimization, an objective function is defined, which needs to be maximized or minimized, subject to a set of linear constraints. Practical applications of these algorithms include optimizing supply chains, allocating resources in manufacturing, and planning financial portfolios. There are interesting variations how these linear programming algorithms are applied to solve for different use cases. For example, dual simplex algorithms can be used when the initial solution is infeasible, but optimal solutions are sought through dual feasibility. Cutting-plane methods introduce additional constraints to iteratively refine the feasible region, improving the solution. These variations are mainly implemented to enhance the performance, efficiency, and applicability of linear programming algorithms across different scenarios.

To make an assessment which optimization algorithm is most suitable to the problem explained within section 2.1, 3 trade-off criteria are selected. Each algorithm is assigned a score scaled from 1-5 for each trade-off criteria. The criteria are accuracy, achievability, and versatility. They are all assigned a weight based on their relative importance, summing up to 100%. The accuracy criteria, which is prioritized with a weight of 50%, focuses on how closely the solution approximates the optimal solution. This emphasis is due to prior solutions in literature being viable but sub optimal. Versatility follows with a 33% weight, reflecting its importance for the expected expansion of the current model. This expansion ranges from the inclusion such as ground stations and geostationary orbit (GEO) constellation communication, and moreover the abil-

C.1. Trade-off

ity to adjust to different client requirements. Achievability, assigned a weight 17%, is considered less critical because it is assumed the implementation of all three algorithms is relatively straightforward, given that all are already existing optimization strategies. It is proven in literature that they are able to accommodate various problem types despite potential complexity and information availability differences.

		Switching	g Algorithm	Control	Algorithm	Linear Pr	ogramming
Criteria	Weight	Rating	Score	Rating	Score	Rating	Score
Accuracy	0,50	1	0,50	4	2,00	5	2,50
Achievability	0,17	4	0,67	3	0,50	3	0,50
Versatility	0,33	5	1,67	2	0,67	4	1,33
Final Score	1		2,83		3,17		4,33
Rank			3		2		1

Figure C.1: Trade-off of all considered optimization algorithm

To make the assessment which optimization strategy to use, each strategy has been assigned a score per trade-off criteria. The results are shown in Figure C.1. The switch-over algorithm, which is ideal for optimization problems characterized by severe fluctuations, is assigned a lower score of 1 for the accuracy criteria. This scoring reflects the algorithm's limited utility in scenarios where link quality is assumed to incrementally increase or decrease, typically resulting in only single transition (switch) per link. As mentioned, this research focuses on a problem where the relative position of the satellite compared to the ALCT is either rising or falling as explained in subsection 2.1.1. As such, it does not effectively predict or secure longterm optimal solutions, focusing instead on meeting immediate quality thresholds. In contrast, the control algorithm is expected to perform better due to its intrinsic behaviour to converge to a near-optimal solution and was therefore awarded a score of 4. The Linear Programming (LP) algorithm is highly favored with a score of 5 due to its expected precision. With a well-formulated and properly implemented model, the LP approach can achieve optimal results, significantly enhancing accuracy of the model. Regarding versatility, the control algorithm scores the lowest, with a value of 2. This rating is due to the requirement for distinct control algorithms tailored to each specific problem configuration. Conversely, both the switch-over and LP algorithms demonstrate greater flexibility. Modifications to these algorithms typically involve adjustments to constraints, objective functions, or switch-over metrics, which are considered to have a lesser impact on their overall adaptability. However, it must be noted that for a switch over algorithm the change in threshold is significant less effort compared to a potential change in objective function and therefore they are ranked with a 4 and 3, respectively. As for achievability, all algorithms perform commendably. However, the switch-over algorithm particularly excels, receiving the highest score of 5. This is attributed to its simplicity as the only requirement is the identification of a suitable metric and a corresponding threshold. This simplicity translates into lower complexity and easier implementation compared to the other algorithms, which receive a score of 3. Combining the weights of the trade-off criteria and the assigned scores it can be concluded that the LP algorithm is deemed most suitable to solve the earlier described problem, due to its modular setup and potential to find near-optimal solutions.

22 C. Supporting Material

C.2 Landscape

C.2.1 Visibility

To be able to establish a link between an ALCT and a satellite within an available constellation, the satellite must be visible to the ALCT. This visibility is defined based on a derivation provided by Korcak and Alagoz [4], and is visualized in Figure C.2. The setup used to explain the visibility criteria has three layers: Terrestrial layer, HAP layer, and satellite layer. The HAP layer as mentioned by Korcak and Alagoz is assumed to be equal to a hypothetical ALCT-layer. An ALCT H is said to be visible to a satellite S if the elevation angle between them exceeds the minimum elevation angle ε_{\min} . This implies that it is possible to establish an optical link between an ALCT and a satellite only if β does not exceed δ . This elevation angle is subject to change based on the use case and client preferences, namely a client can decide to increase or decrease the minimum elevation angle.

As can be seen from Figure C.2, OA is the distance between the center of the earth and a hypothetical position of an ALCT, whereas OS is the distance between the center of the earth and a hypothetical position of an satellite i. The result of applying the law of sines to OA and OS is shown in Equation C.1:

$$\frac{\sin(90 - \epsilon_{\min} - \delta)}{R_E + h_H} = \frac{\sin(90 + \epsilon_{\min})}{R_E + h_S}$$
 (C.1)

where R_E is the radius of the earth (6375 km), h_H is the height of the ALCT, and h_S is the height of the satellite. Equation C.2 is the result of extracting δ from Equation C.1:

$$\delta = 90 - \epsilon_{\min} - \arcsin\left(\frac{R_E + h_H \cdot \cos(\epsilon_{\min})}{R_E + h_S}\right)$$
 (C.2)

In Figure C.2, S' is the projection point of the satellite S on the ALCT layer. OS'H is an isosceles triangle, and by applying the law of sines once again, Equation C.3 provides a formulation for β :

$$\beta = 2 \cdot \arcsin\left(\frac{|S'H|}{2 \cdot (R_E + h_H)}\right) \tag{C.3}$$

It is possible to establish an optical link between a satellite and an ALCT while $\beta \leq \delta$. The β angle for a satellite-ALCT pair continuously changes due to the movement of the satellites. Based on the geometrical location of the satellites and ALCT's at each time unit, a visibility matrix can be retrieved representing which satellites are visible to the ALCT.

Looking closely at Figure C.2 it can be concluded that in this study a satellite is either rising, falling, or exactly above point S. A rising satellite means that its relative elevation angle is increasing with time, while a falling satellite means that the relative elevation angle is falling. It can be more or less assumed that the quality of an FSO communication link increases with increasing elevation angle, and thus

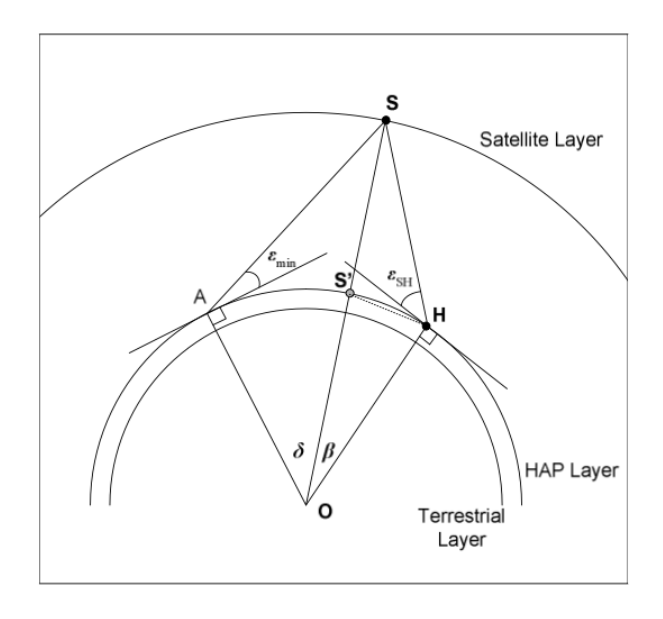


Figure C.2: Two dimensional view of system geometry to demonstrate satellite visibility [4]

achieving optimal link quality exactly above point S. This is due to the shorter distance from S' to S, and the path itself is less atmospherically dense on average as it moves directly in an outward direction of the atmosphere, compared to lower elevation angles where travel distance is longer and traveled distance is through denser atmosphere. To map this visibility derivation to the aforementioned use cases in chapter 4, Figure C.3 provides the visibility and the accumulated visibility over time. The upper two images are representing use case 1, which consist of 1 orbital plane with 14 satellites. It can be seen that the satellites are following one another and become visible one after another. For use case 2, the second orbital plane is clearly visible with an almost exact match in extra satellites visible compared to use case 1.

C.3. Masking 23

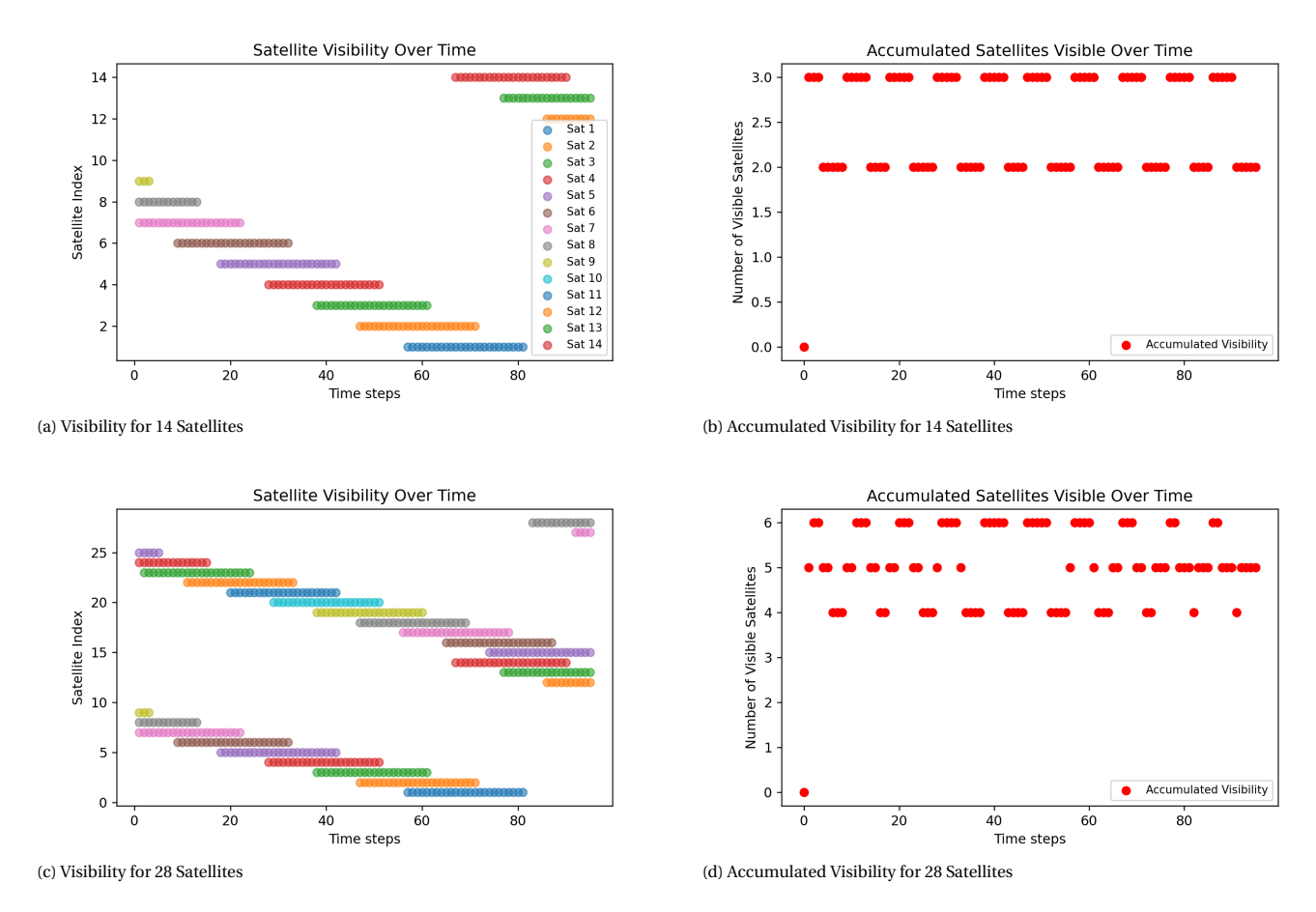


Figure C.3: Visibility and accumulated visibility over the mission time for a 14 and 28 satellite configuration

C.3 Masking

It is essential to choose a smart mounting location for the pod onto the ALCT, which can either be an commercial plane, Unmanned Aerial Vehicle (UAV) or a high altitude platform (HAP). The integration of the pod within the design of a flying object poses several challenges. One significant challenge is that the pod may not always be fully incorporated into the structural and aerodynamic design of the host vehicle. As a result, certain viewing angles from the pod may be obstructed by parts of the host vehicle itself, such as the fuselage, wings, or other structural components.

These obstructions can hinder the ALCT's ability to establish a line-of-sight communication link with satellites. To mitigate this issue, a masking module has been incorporated into the link selection model. The masking module dynamically assesses the visibility of satellites by calculating the combined elevation and azimuth angles relative to the ALCT's position. If these angles fall within regions identified as blocked by the host vehicle's structure, the respective satellites are excluded from the set of applicable satellites A_i^T . This process ensures that the communication link established by the ALCT is free from obstructions, thereby enhancing the reliability and quality of the optical link. In Figure C.4 two bit mappings are shown providing a masking analysis for two different location of pod mounting on a commercial plane. The commercial plane is a T-tail configuration and has wing tips. Green bits (areas) means that there is a line of sight outwards, a red bit means there is blockage due to a component of the aircraft.

The left image, Figure C.4a, is a bit mapping for a pod mounted on top of the fuselage. Therefore, if the pod looks to its left or right and slightly down, i.e. +90° or -90° (azimuth) and -10° (zenith), the pod sees the wings tips. If the pod looks backwards (+180° or -180°azimuth), it sees the T-tail. Furthermore, if the pod is looking directly in front of him it will see the fuselage up until a certain zenith angle, while looking slightly to the left or right already gives a clear line of sight, this results in the two extra red blocks at azimuth 0°, zenith 0°. Given that the pod is mounted on top of the fuselage it is impossible to look downwards, apart from some small negative zenith angles to the left or right, which are spanning the area between the fuselage and the wings.

The right image, Figure C.4b, is a bit mapping for a pod mounted in front of the left wing. Therefore, if the pod starts to look to its right side it sees the fuselage. The fuselage is visible from approximately 55° to 145° azimuth in between -30° and +30°

24 C. Supporting Material

zenith angle. Furthermore, just as with the previous case if the pod looks to its left side it sees the wingtip, the wing tip on the right side is behind the fuselage and therefore not visible from the bit mapping. Given that the pod is mounted in front of the wing it has a clear view of everything below it and above.

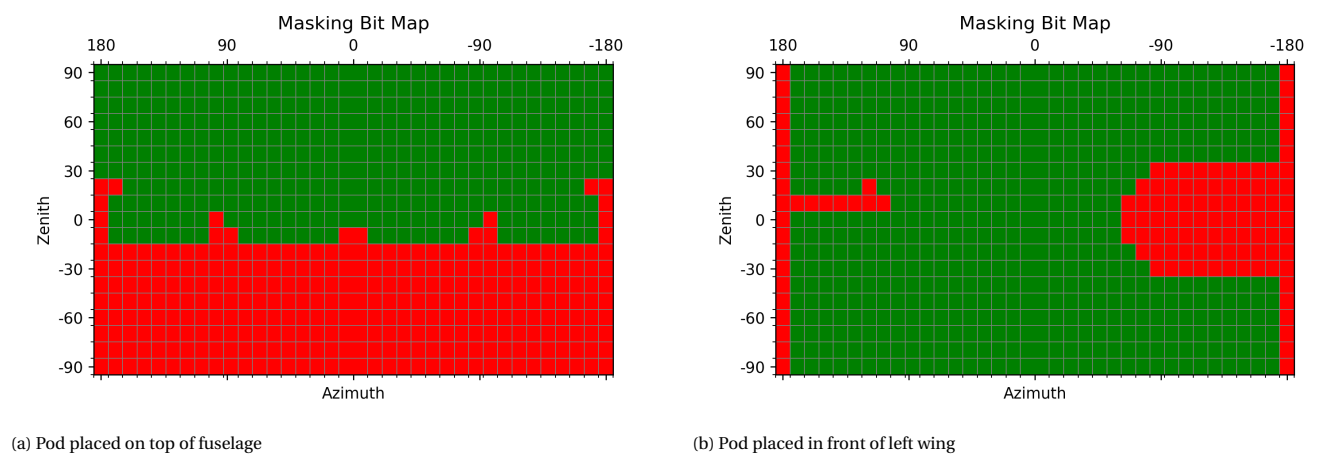


Figure C.4: Bit mapping of masking analysis for different pod placements on commercial aircraft with T-tail and wingtips configuration

C.4 Model Settings

The model consist out of multiple settings which can be turned on or off by adjusting its corresponding value in the input section. These settings are introduced to omit certain calculation which improve the computational efficiency model while maintaining its accuracy. It must be noted that the set of settings can be expanded by introducing new settings based on to be defined research/ mission optimization.

C.4.1 Falling satellite module

The first and most dominant setting is the falling satellite module. This setting removes applicable satellites from the analysis by looking at the performance scores of the past four time instances. The cost function J provides the result of the combined performance score at each instance of time. Looking at the combined behaviour of the six performance parameters separately, in combination with the geometrical behaviour where the satellite is either rising, above the ALCT or falling, it can be concluded that once the performance is dropping for multiple consecutive instances of time, it will never start to increase again. The separated behaviour of each performance parameter was shown in section 4.1 and will be further elaborated on in Appendix F. This behaviour is translated to the following mathematical condition as shown in Equation C.4.

if
$$J_i(t_{j-1}) < J_i(t_{j-2}) < J_i(t_{j-3}) < J_i(t_{j-4})$$
 then $i \notin A_i^T$ (C.4)

In order for the model to be able to continue this calculation after a satellite is removed from A_i^T , it stores its previous performance score to mimic the result given that no updated result is calculated. This results in a flat line in the performance of visible but non-applicable satellites, which can be observed in some of the subsequent plots.

C.4.2 Outperforming satellite module

As explained within Appendix B a distinction can be made between computational extensive and in-extensive performance parameters. The second setting makes use of this distinction by checking for the upcoming time step if the sum of the low computational extensive performance parameters $(Q_{DTL_i} + q_{PL_i} + q_{C_i})$ plus the weight of the high computational extensive performance parameters $(\alpha_A + \alpha_{BER} + \alpha_R)$ is smaller than the score of the satellite active at that specific instance of time. Namely, by adding the weights of the high computational cost it is assumed they score perfectly for those three criteria. The possibility of all three criteria scoring a 1 is very slim and thus by adding the weights an upper bound is defined. If this upper bound is lower than the score of the current active satellite it is cumbersome to include that specific satellite in the analysis as is it impossible it will outperform the current active satellite. The mathematical notation of this setting is provided in Equation C.5, and just as with the previous setting satellite i gets removed from the list of applicable satellites (A_i^T) if the condition is not met.

if
$$\left(Q_{DTL_i} + q_{PL_i} + q_{C_i} + \alpha_A + \alpha_{BER} + \alpha_R\right)(t_j) < J_i(t_{j-1})$$
 then $i \notin A_i^T$ (C.5)

C.4. Model Settings 25

C.4.3 Single Satellite Module

The single satellite module can be used if there is only one satellite applicable, in general or after a selection based on earlier performed settings. The model simply continues to the next instance of time while making the single satellite applicable active and performing no subsequent calculations. This is visualized within the performance graphs as a grey dot, indicating that the calculations are being cut-off at that specific instance of time.

Appendix D

Linear Programming Formulation

In Equation D.1 to D.14 the complete Linear Programming formulation is specified.

$$z(t_{j}) = \max \Sigma z_{i} = \max_{i} \quad \sum_{i}^{t_{m}} E_{i}(t_{j}) \left(\alpha_{A} \cdot \hat{Q}_{A_{i}} + \alpha_{BER} \cdot \hat{Q}_{BER_{i}} + \alpha_{C} \cdot \hat{q}_{C_{i}} + \alpha_{DTL} \cdot \hat{Q}_{DTL_{i}} + \alpha_{PL} \cdot \hat{q}_{PL_{i}} + \alpha_{R} \cdot \hat{Q}_{R_{i}} \right)$$
s.t.
$$\sum_{0}^{i} t_{L_{i}} \leq t_{M}$$

$$\sum_{0}^{i} t_{L_{i}} = t_{s}$$

$$\sum_{0}^{i} E_{i}(t_{j}) \leq 1$$

$$\alpha_{A} + \alpha_{BER} + \alpha_{C} + \alpha_{DTL} + \alpha_{PL} + \alpha_{R} = 1$$

$$E_{i}(t_{j}) \in [0, 1] \text{ and in } Z^{+}$$

$$\alpha_{A}, \alpha_{BER}, \alpha_{C}, \alpha_{DTL}, \alpha_{PL}, \alpha_{R} \in R^{+}$$

$$(D.1)$$

$$J_i(t_j) = \left(\alpha_A \cdot \hat{Q}_{A_i} + \alpha_{BER} \cdot \hat{Q}_{BER_i} + \alpha_C \cdot \hat{q}_{C_i} + \alpha_{PL} \cdot \hat{q}_{PL_i} + \alpha_{DTL} \cdot \hat{Q}_{DTL_i} + \alpha_R \cdot \hat{Q}_{R_i}\right)(t_j)$$
(D.2)

Availability

$$Q_{A_i}(t_j) = \begin{cases} \sum_{t_j}^{t_{V_i,e}} q_{A_i}(t), & \text{if } E_i(t_j) = 1\\ \sum_{t_j+t_{acq}}^{t_{V_i,e}} q_{A_i}(t), & \text{if } E_i(t_j) = 0 \end{cases}$$
(D.3)

where $q_{A_i}(t_j) = \begin{cases} 1, & \text{if } P_{RX,i}(t) > P_{thr} \\ 0, & \text{otherwise} \end{cases}$

$$\hat{Q}_{A_i}(t_j) = \frac{Q_{A_i}(t_j)}{t_{V_{max}}}$$
 (D.4)

Bit Error Rate

$$Q_{BER_{i}}(t_{j}) = \begin{cases} \sum_{t_{j}}^{t_{A_{i},e}} q_{BER_{i}}(t), & \text{if } E_{i}(t_{j}) = 1\\ \sum_{t_{j}+t_{acq}}^{t_{A_{i},e}} q_{BER_{i}}(t), & \text{if } E_{i}(t_{j}) = 0 \end{cases}$$
(D.5)

where $q_{BER_i}(t_j) = \begin{cases} 1, & \text{if } R_{act,i}(t) >= R_{req}(t) \\ 0, & \text{otherwise} \end{cases}, t_j \le t \le t_{A_i,e}$

$$\hat{Q}_{BER_i}(t_j) = \frac{Q_{BER_i}(t_j)}{t_{A\dots A}}$$
 (D.6)

Cost

$$q_{C_i} = \begin{cases} C_{var_k} & \text{if } E_i(t_j) = 1\\ C_{var_k} + C_{fix_k} & \text{if } E_i(t_j) = 0 \end{cases}$$
 (D.7)

$$\hat{q}_{C_i} = \begin{cases} \left(1 - \frac{C_{var_k}}{C_{var_{max}}}\right) & \text{if } E_i(t_j) = 1\\ \frac{1}{2} \left(1 - \frac{C_{var_k}}{C_{var_{max}}}\right) + \frac{1}{2} \left(1 - \frac{C_{fix_k}}{C_{fix_{max}}}\right) & \text{if } E_i(t_j) = 0 \end{cases}$$
(D.8)

Data Transfer latency

$$Q_{DTL_{i}}(t_{j}) = \begin{cases} \sum_{t_{j}}^{t_{A_{i},e}} q_{PL_{i}}(t), & \text{if } E_{i}(t_{j}) = 1\\ \sum_{t_{j}+t_{acq}}^{t_{A_{i},e}} q_{PL_{i}}(t), & \text{if } E_{i}(t_{j}) = 0 \end{cases}$$
(D.9)

where $q_{PL_i}(t_j) = \frac{d_{ALCT-S_i}(t_j)}{c_s}$, $t_j \le t \le t_{A_i, \epsilon}$

$$\hat{Q}_{DTL_i}(t_j) = \frac{Q_{DTL_i}(t_j)}{q_{PL_{min}}(t_j)}$$
 (D.10)

Propagation latency

$$q_{PL_i}(t_j) = \frac{d_{ALCT-S_i}(t_j)}{c_s}$$
 (D.11)

$$\hat{q}_{PL_i}(t_j) = 1 - \frac{q_{PL_i}(t_j)}{q_{PL_{min}}}$$
 (D.12)

With,

$$q_{PL_{min}} = \frac{d_{LCT - S_{min}}}{c_s} \tag{D.13}$$

Throughput

$$Q_{R_i}(t_j) = \begin{cases} \sum_{t_j}^{t_{A_i,e}} q_{R_i}(t_j), & \text{if } E_i(t_j) = 1\\ \sum_{t_j+t_{acq}}^{t_{A_i,e}} q_{R_i}(t_j), & \text{if } E_i(t_j) = 0 \end{cases}$$
(D.14)

where $q_{R_i}(t_j) = R_{act,i}(t)$, $t_j \le t \le t_{A_i,i}$

$$\hat{Q}_{R_i}(t_j) = \frac{Q_{R_i}(t_j)}{R_{reg}(t_{A_i,e} - t_j)}$$
(D.15)

Appendix E

Link Selection Model Overview

In this chapter two high level model overviews are provided to give a general understand how the model is created from a block code point of view. Figure E.1 is a zoomed out version of Figure E.2, which provides more detail.

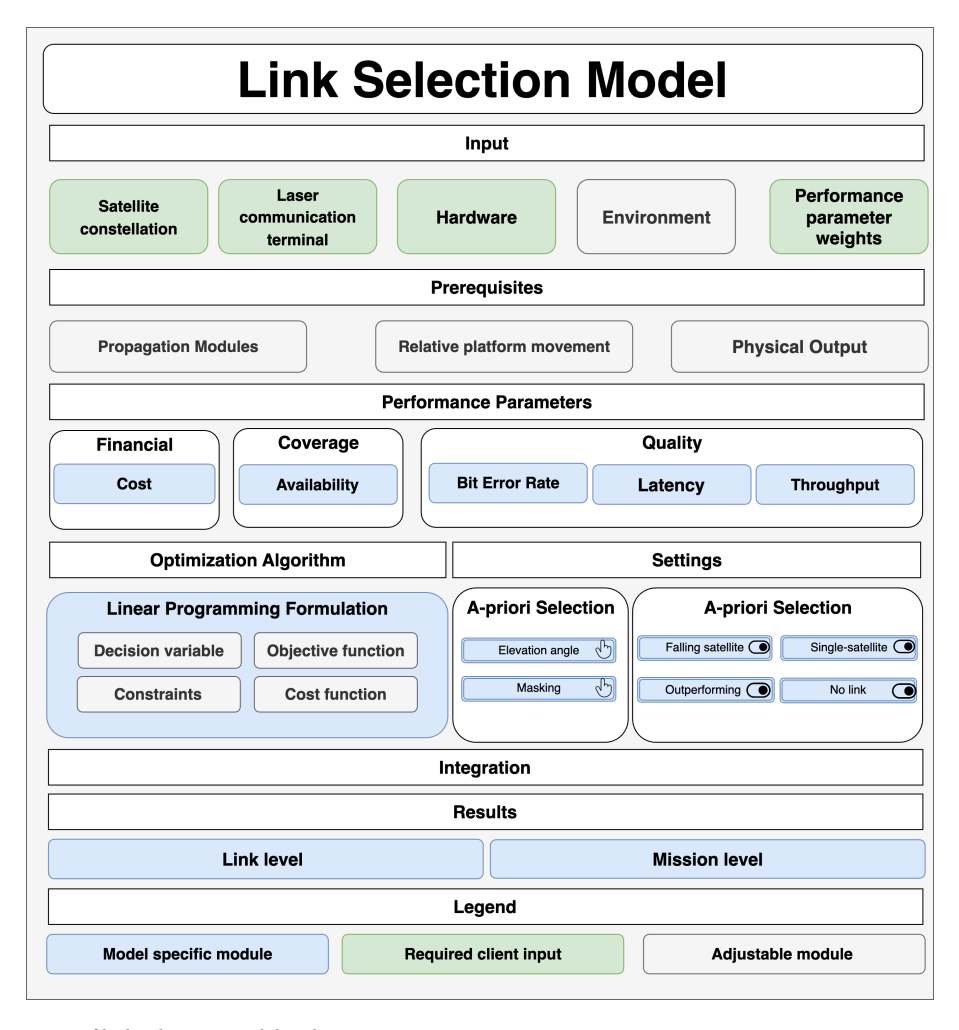


Figure E.1: High level overview of link selection model coding structure

E.1 Overview

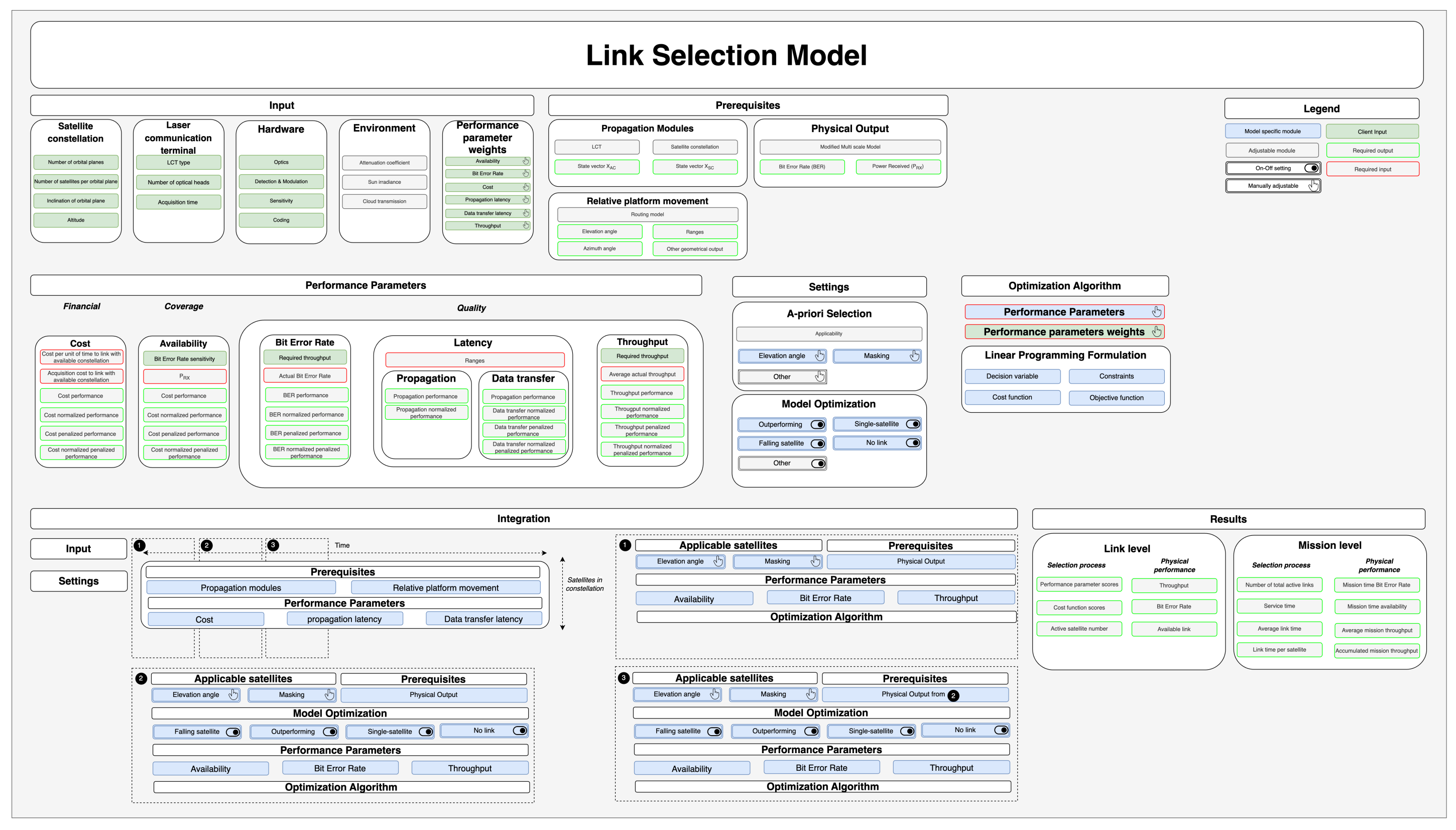


Figure E.2: Detailed overview of link selection model coding structure

Appendix F

Verification and Validation

To start the verification and validation process an extensive list has been compiled addressing all required tests to assure the model is performing as envisioned. This list is divided into levels, which indicates to what physical component the test is connected to. The levels span from mission to input level, and are all assigned an individual tag number. Two types of test are performed, unit test in which the functioning of a single module or definition is verified and convergence analysis in which combined behaviour of multiple modules or definitions are put to the test. Table E1-E7 provides an overview of all these tests. The first column states the tag number and the description of the test. The 'test' column specifies in more detail what kind of test was performed, and in the subsequent column the expected results is stated. Within the subsequent columns it is stated for each verification test the outcome of the test and in case the test was not successful which solution is suggested to be implemented. Note, it was observed that not every failure of a test was of fundamental importance to the correctness of the model, and therefore the proposed solution is not always implemented, but merely given as a potential solution to be implemented during further research. Some verification test generated results which where worth sharing and are therefore elaborated within this chapter. As can be seen, the list of verification test is quite extensive and therefore a priority scale from 1-3 was used to assure the most important test were performed prior to others. Thus, within the column "test performed" it is specified if the verification test was executed within the scope of this thesis, for future development it is recommended that the other verification test are performed to ensure the functioning of all components of the model.

F.0.1 Mission and service time analysis

The verification with respect to the mission and service time resulted in noteworthy conclusions. Within three test it was checked if the transformation between the time an ALCT is linked to a satellite corresponds with the output in terms of mission and service time. The constraints from a mathematical perspective are that the sum of the individual link times should be less or equal to the service time and the service time should be smaller or equal than the mission time. These constraints are adhered in terms of final mission output, however within some of the intermediate steps these constraints are violated. Namely, the simulation makes a satellite active at each instance of time if there is an applicable satellite. This was concluded by Unit-002, in which was stated that the length of the list of activated satellites is equal to the length of the time instances. However, accompanied with storing the index of the activated satellite the availability of that specific satellite at that specific instance of time is stored. This results in the end in an availability vector over the entire mission span. If a link switch occurs, i.e. two subsequent time indices with different satellite indices the availability is overwritten to make the subsequent instances of time unavailable according to the set acquisition time. Therefore, the test for **Unit-005** is not passed as the sum of activated satellites plus the number of different links is larger than the mission time, however the sum of time indices that an active available active satellites plus the number of different links is smaller or equal to the mission time. Furthermore, the test for Unit-102 and Unit-103 were not passed due to the same behaviour. The sum of time instances for all the separate links is larger than the service time, however the sum of time instances of the availability within each separate link equal than the service time. The average link time multiplied with the number of different links is larger than the service time, but the average available link time multiplied with the number of different links is equal to the service time. A proposed solution is to directly count the downtime if a switch in link occurs, but this was deemed not vital for the model to operate according to the set standards and is therefore left for future improvement.

F.0.2 Falling satellite setting

Unit-009 performed a check if there is significant difference in model output if the falling satellite setting was turned on. In terms of physical output the results were not per se very abnormal, however the progression of the performance scores of the last time instances showed large deviations from what was expected. In Figure F1 the behaviour is shown with the falling satellite mode turned on, with a 14 satellite configuration with a time step of 5 seconds.

30 F. Verification and Validation

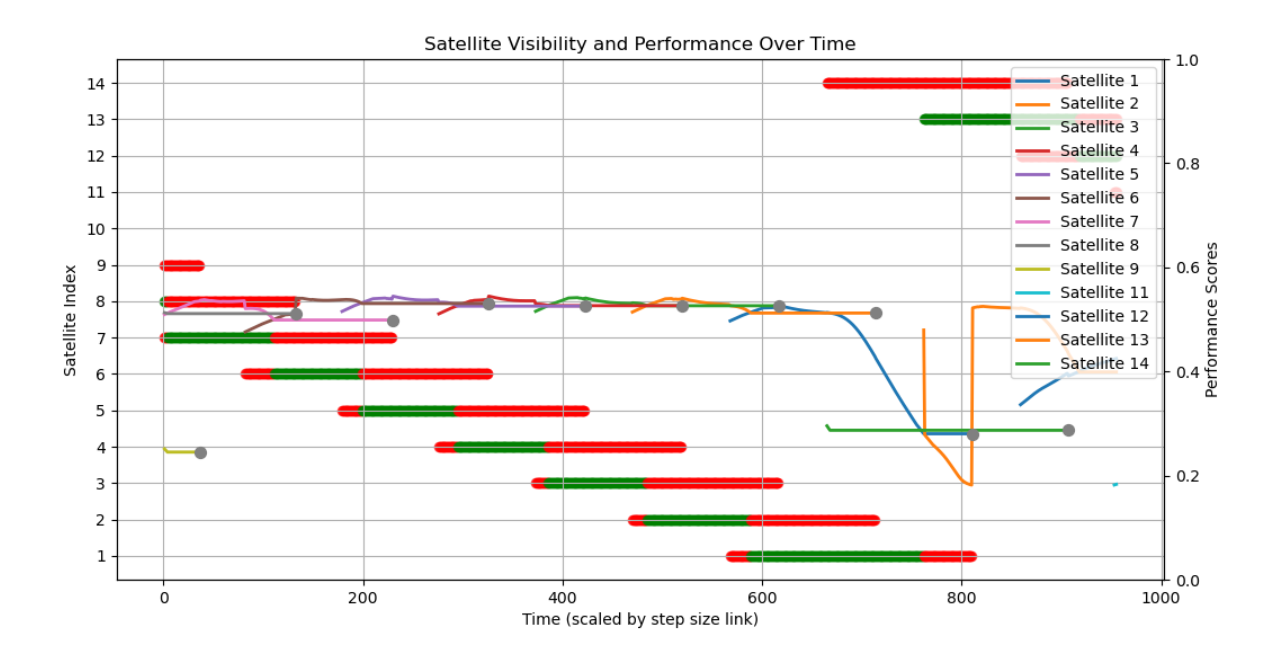


Figure F.1: Active satellite and accompanied performance over time resulting from falling satellite setting verification

As can be seen, everything seems to behave as expected up until time step 700. Satellite 1 stays active for an unusual long period of time while its performance, the blue line, is dropping significantly. Once satellite 13 becomes visible it is made active directly while its performance is also dropping, and after satellite 1 is not applicable anymore its performance increase to a more reasonable level. Based on the verification test performed the removal of satellites goes correctly, meaning that based on the set mathematical condition the falling satellites are removed. However, the translation of removing the correct accompanying physical output corresponding to the removed satellite went wrong. This results in the physical performance of a satellite being used to calculate the performance parameters of another satellite. This problem does not occur with the falling satellite setting turned off, as no removal of satellites occurs. From the plot it can also be concluded that this problem does not occur in the time steps before 700. This has to do with the fact that the removal of the physical performance goes sequentially, and thus if the index is simply reduced by one the physical performance is passed on to the following satellite index, which is correct. Only if multiple new satellites come into play, which occurs around timestamp 700 this passing on goes wrongly. In order for the settings module to operate correctly the allocation of physical performance need to be restructured within the source. It was deemed a fundamental task to implement this solution which was done by rewriting the physical performance assignment module, especially due to the fact that the computational gain is enormous based on the runtime of this configuration.

F.0.3 Outperforming satellite setting

Unit-010 performed a check if there is significant difference in model output if the outperforming satellite setting was turned on. The setting has been turned on in numerous simulation and based on all print statement not one satellite has been removed based on this condition, and thus no computational gain was achieved. Therefore it must be evaluated if the setting is required or needs an update, however this was not deemed vital for the model to operate according to the set standards and is therefore left for future improvement.

E.0.4 Performance score translated to selected satellite

One of the most important verification test of this model is to check if the model actually selected the satellite with the highest performance score. **Unit-101** performed this check by performing a simulation of 2 orbital planes with 14 satellites in each plane, like the setup for use case 2 as explained in chapter 4. The test was performed in an isolated environment meaning that the penalized values were not taken into account, and simply the focus was on does the right link gets selected. In Figure F.2 the visibility of each satellite can be seen and which satellite is made active at which point in time.

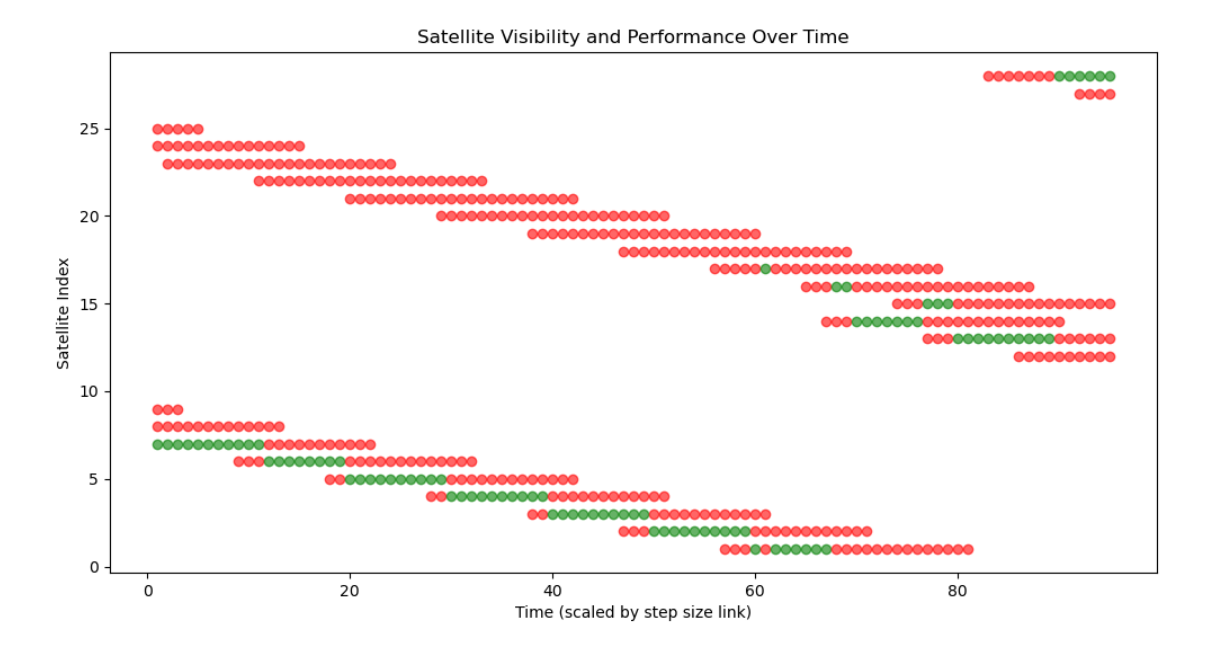


Figure F.2: Satellite visibility and link selection for a 28 satellite configuration

Lets focus on four subsequent timestamps ranging from 18 to 21. It can be seen from Figure E2 that during timestamp 18 and 19, satellite 6 is active and at timestamp 20 the link is passed onto satellite 5. Figure E3 shows the individual performance scores of all visible satellites. These performance scores are visualized with a stacked bar consisting out of the 6 separate performance parameters. On Figure E3a and Figure E3b it can be seen that satellite 6 has the highest performance score mainly due to a strong contribution of the data transfer and throughput performance. The active satellite is shown in these figures by the green border around the stacked bar, while the other stacked bars have a red border. In Figure E3c the link is switched to satellite 5 as the availability and throughput performance of this satellite is much better, and the overall performance of satellite six starts to drop. This is a visualization of 1 switch but this behaviour was observed for all link switches and therefore it was concluded that the model correctly selects the satellite with the highest performance.

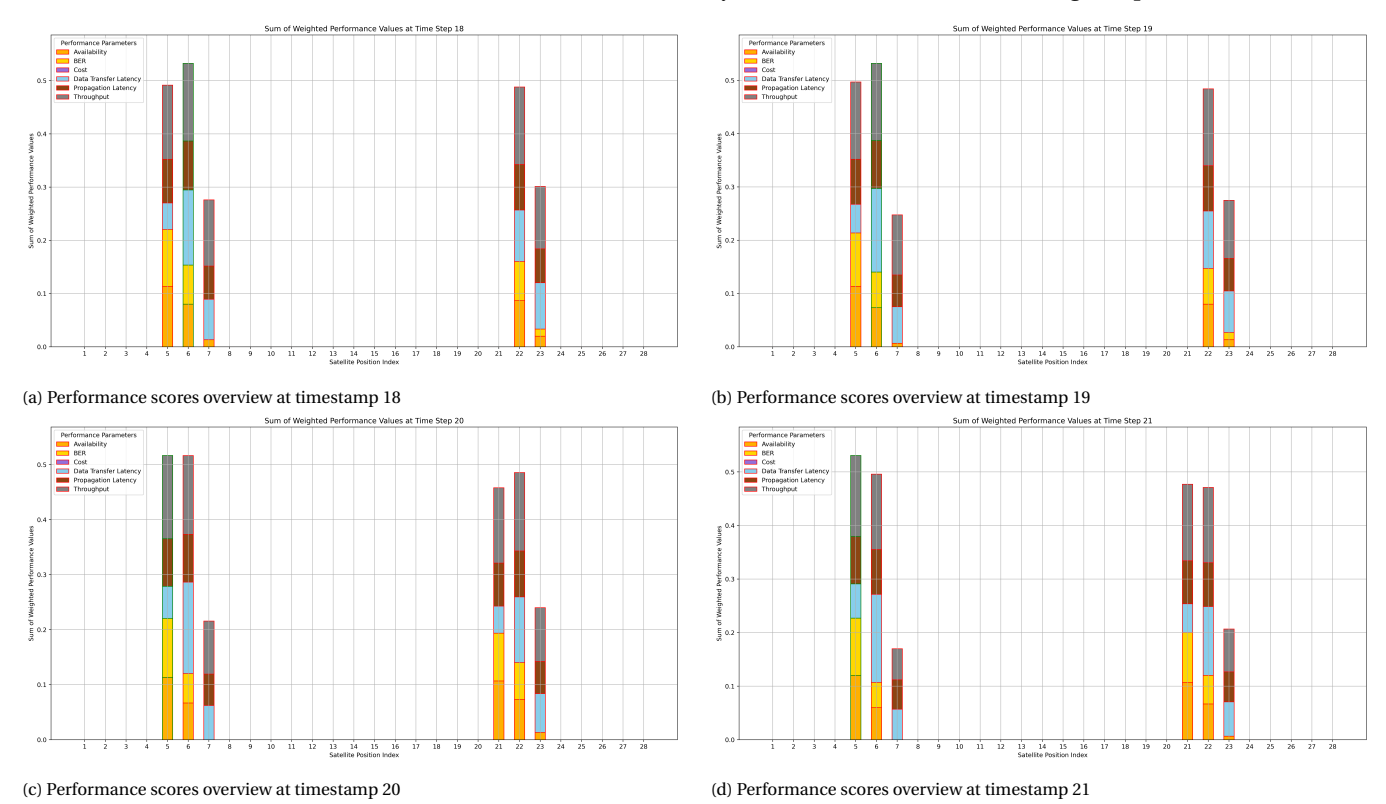


Figure F.3: Performance scores of 4 subsequent time instances of a 28 satellites simulation configuration showing a link switch

32 F. Verification and Validation

F.0.5 Control performance parameter

From **Unit-106** and **Unit-108A** it was concluded that the model could benefit from the addition of a control parameter. It was observed within **Unit-106** that although all performance parameter values are put to zero a link gets selected. The link selected was simply the satellite with the lowest satellite index. In **Unit-108A** all satellites were removed from being applicable and the simulation got killed. Both issues can be resolved by adding a geometrical based control performance parameter which select a link if there is no performance score readily available while there are applicable satellites. It was decided that this implementation is not vital for the model to operate according to the set standards and is therefore left for future improvement.

F.0.6 Isolated performance parameter

In order to check if each performance parameter individually performs as was anticipated during the design phase, verification test **Unit-109** till **Unit-114** was performed. Within these test the weight of each performance parameter was set to 1 while the other performance parameters were put to zero. The simulation was performed in an isolated environment with a step size of 50 seconds and no link switching penalty applied. For each performance parameter a plot is provided with the results of the simulation, apart from the cost performance parameter. This was decided because only 1 constellation can be modelled within the current simulation and therefore no meaningful output is expected. Given that all performance scores for the cost performance parameter are equal due to only 1 constellation being modelled, the same behaviour as described for Unit-106 in the previous paragraph were seen. The provided plots will be compared to the isolated performance plot without link selection simulation provided in chapter 3. It was deliberately chosen not to provide a legend, as it was deemed no added value for the visibility of the plot. The only reminder needed is that the orbital plane spanning from satellite 1 to 14 is closer to the ALCT compared to the second orbital plane spanning form satellite 15 to 28.

The first performance parameter isolated is the availability performance parameter corresponding to test **Unit-109**. In Figure F.6 a simulation with the availability weight put to 1 can be seen. The first thing that can be observed is that the behaviour of the performance parameter is not exactly in line with Figure F.4. This can be explained due to the difference in isolated environment that the two simulations were performed. Namely, Figure 3.2 was generated by making use of a static input to provide the reader with a clean image how the performance parameter behaves. However, within an isolated link selection simulates the physical performance input is not static and thus the Monte Carlo simulation mentioned in Appendix B is performed for each applicable satellite at each instance of time. This leads to the behaviour that sometimes the availability vector for a satellite chances with a subsequent time instance. However, the overall behaviour of the availability performance is still gradually downwards as expected. Furthermore, the link switch is performed directly when a new satellite becomes available, which is in line with the highest availability performance at the start of a satellite becoming available.

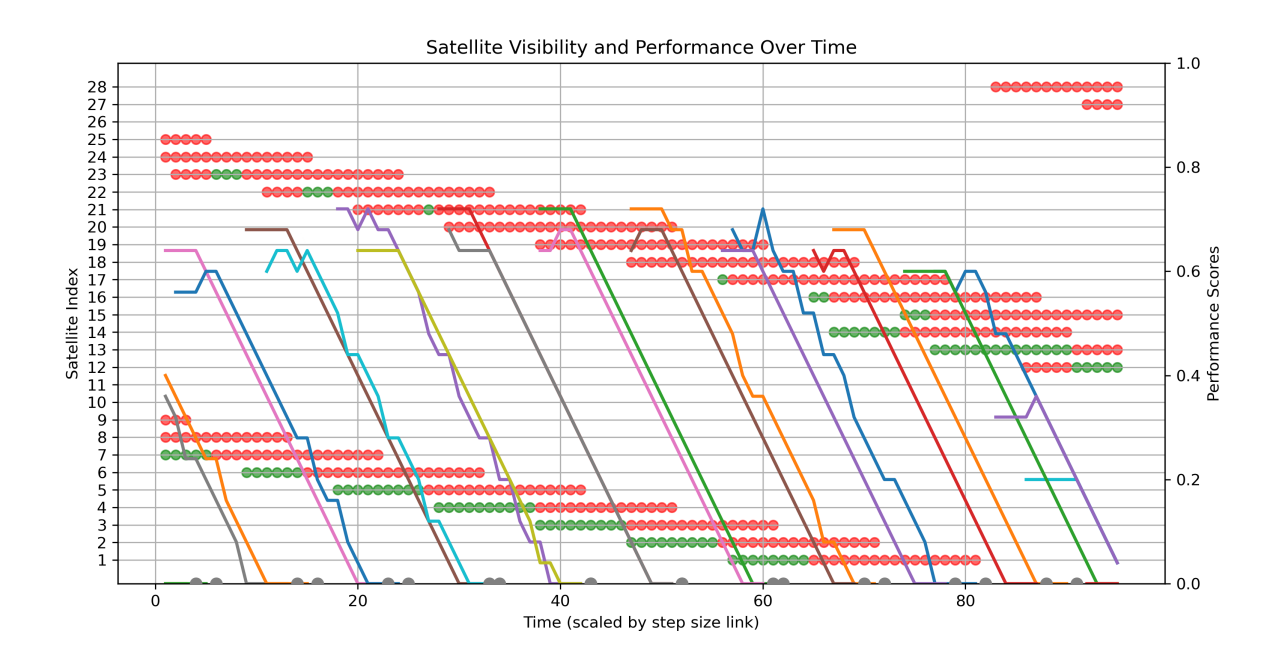


Figure F4: Mission simulation with a 28 satellites configuration while the availability performance parameter weight set to 1

The second isolated performance parameter is the BER performance parameter corresponding to test **Unit-110**. The same reasoning used for the availability performance parameter can be applied to the BERperformance behaviour in Figure E.5,

however the fluctuations are more severe in this case. This can be explained by closely looking at the mathematical definition provided in Equation 3.3. Namely, if only 1 of 2.5 * 10E9 bits is not delivered the requirement is not met. It was therefore evaluated if this performance parameter requires a more lenient condition by matching it for example to the provided maximum acceptable BER. However, it was chosen not to do so as making this condition more lenient would simply build in additional link margin, which is not the purpose of this specific performance parameter. As can be seen from the plot, the link switch is performed once a new satellite becomes available, which is in line with expectations as the performance score is highest at the beginning of the visibility period.

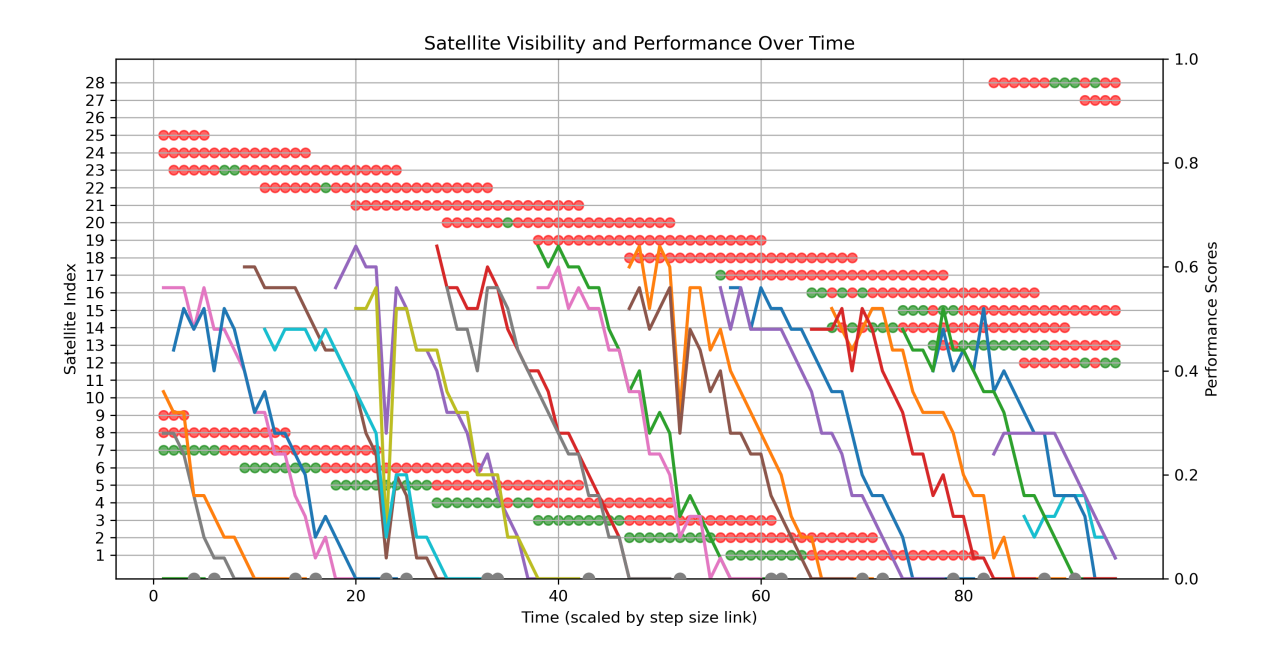


Figure F5: Mission simulation with a 28 satellites configuration while the bit error rate performance parameter weight set to 1

Below in Figure F.6 the isolated performance of a simulation with the data transfer latency weight put to 1 can be seen. The first thing that can be observed from test **Unit-112** is that the behaviour of the performance parameter is in line with Figure 3.4. Furthermore, as expected the link switch (apart from the first link) is performed a couple of time instances after a new satellite has become available, matching the point where the current active link starts to loose it performance and the new satellite starts to improve.

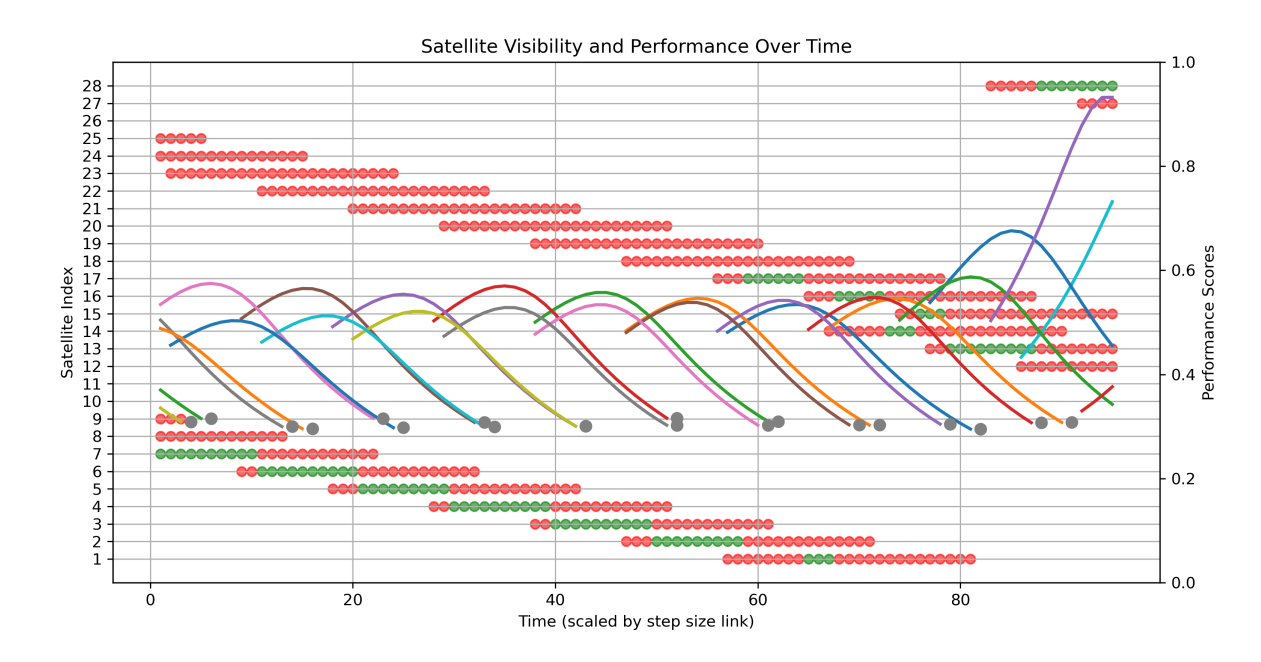


Figure F.6: Mission simulation with a 28 satellites configuration while the data transfer latency performance parameter weight set to 1

34 F. Verification and Validation

Below in Figure F7 the isolated performance of a simulation with the propagation latency weight put to 1 can be seen. It can be observed from test **Unit-112** that the behaviour of the performance parameter is in line with the behaviour shown in Figure 3.5. Furthermore, as expected the link switch (apart from the first link) is performed near the middle of the time instances a satellite is available. It is interesting to see, that due to no acquisition penalty being in place, sometimes the decrease in propagation latency performance of orbital plane 1 (the closer one) is such that the new available satellite in orbital plane 2 gets selected.

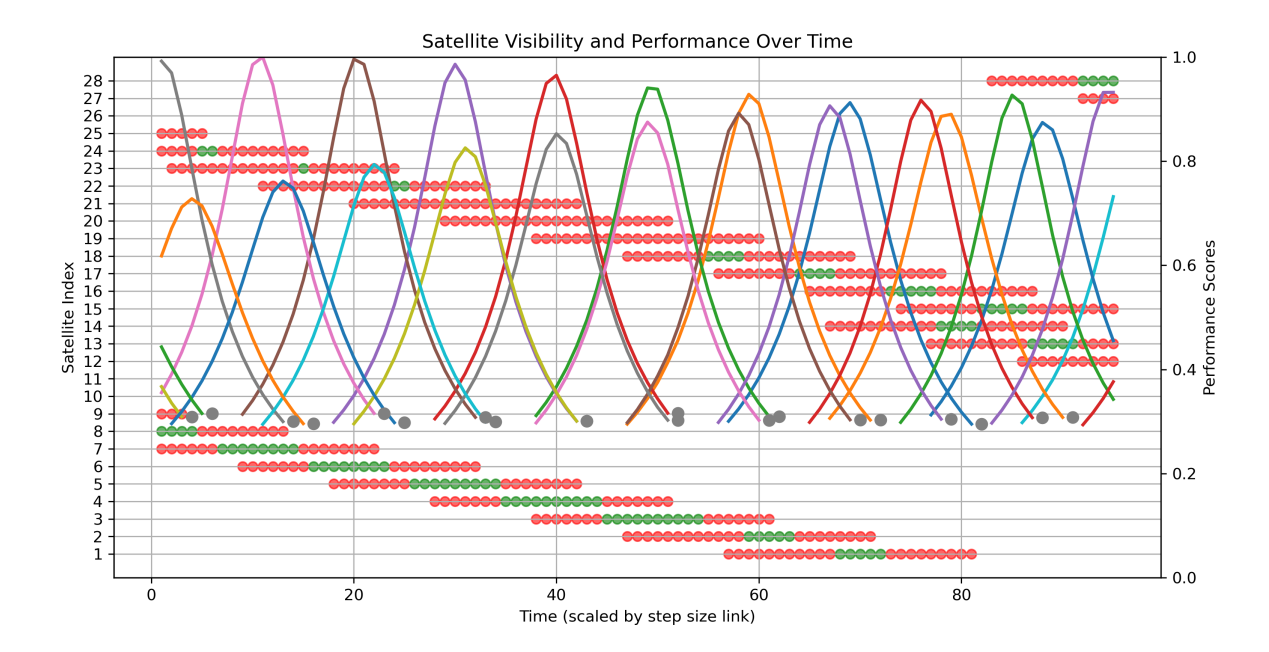


Figure E7: Mission simulation with a 28 satellites configuration while the propagation latency performance parameter weight set to 1

The last plot corresponds to **Unit-114**, the isolated throughput performance parameter which is provided in Figure F.8. The first thing that can be observed is that the behaviour of the performance parameter is in line with Figure 3.6. Furthermore, as expected most of the link switches (apart from the first link and the switch to satellite 4) is performed after a couple of time instances that a new satellite has become available to the ALCT.

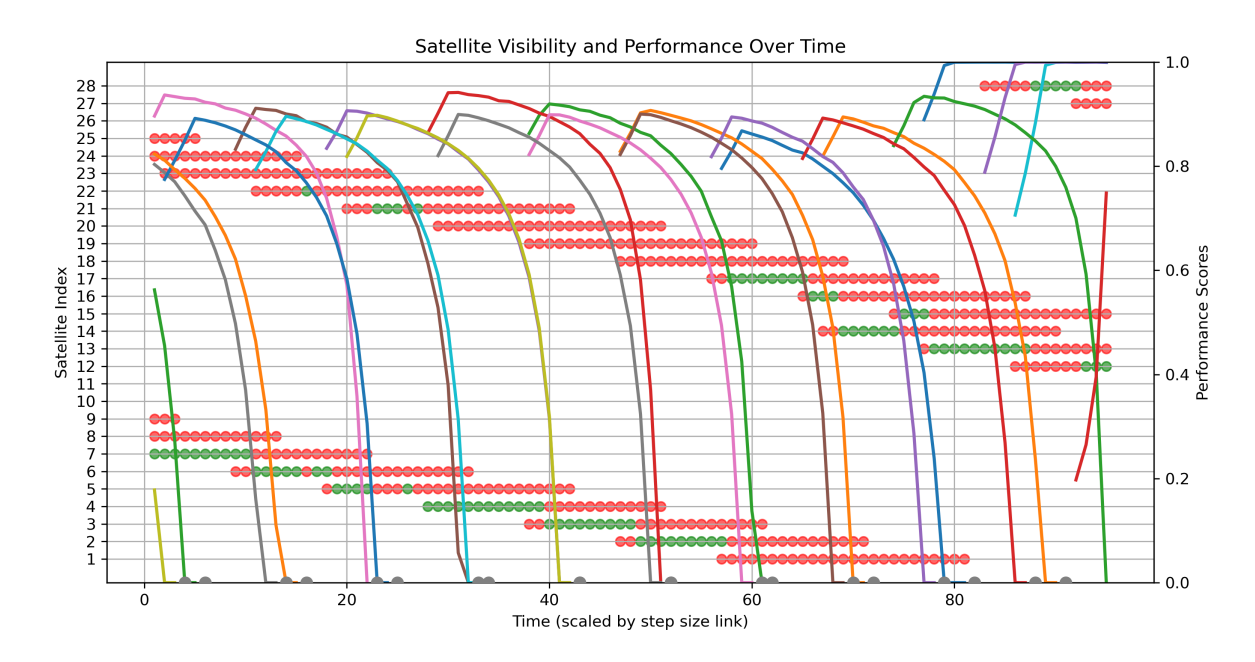


Figure F8: Mission simulation with a 28 satellites configuration while the throughput performance parameter weight set to 1

F.0.7 Unit 404 to 409

Looking at verification **Unit 404 to 409**, it was checked whether the behaviour of all the performance parameters corresponds to their physical behaviour in an isolated condition. This isolated condition means that the performance parameters are calculated outside of the link selection simulation loop and are simply computed based on a static physical input. Given that a performance parameter can be translated to a normalized value, a penalized value and a normalized penalized value it must be checked if all those values correspond to their physical behaviour. The behaviour of the cost performance parameter has been omitted from this analysis as only 1 constellation was modelled and therefore it holds no verification results to show. The normalized behaviour for the latency performance parameters has already been provided in section 3.3. Figure F.9 and F.10 are provided to clearly show the translation from the physical behaviour to the normalized and penalized values. Note this is done with a set of 8 satellites in the same orbital plane for visualization purposes, identical to the configuration used in chapter 3.

Looking at the behaviour of the availability performance (Q_A) in Figure F.9, a downward slope can be observed at the top left image. The availability performance starts at its highest value and afterwards decreases with each subsequent instance of time. This continuous downwards slope can therefore also be seen in the normalized performance behaviour \hat{Q}_{A_i} . The normalization performance is calculated by dividing the performance with the maximum applicable length of one of the satellites available during the mission. Looking at the performance compared to the penalized performance on the bottom left, it can be observed that for each satellite the performance is 4 points lower. This translates to the simulation being run on a 5 second time interval while having an T_{acq} of 20 seconds, translating to a penalty of 4 instances of time during which satellite i is not available to the ALCT. Therefore, the normalized penalized performance shown in the bottom right corner starts at a lower value compared to the normalized performance. These four figures therefore show that the isolated performance of the availability behave accordingly to the envisioned behaviour and the test was passed successfully.

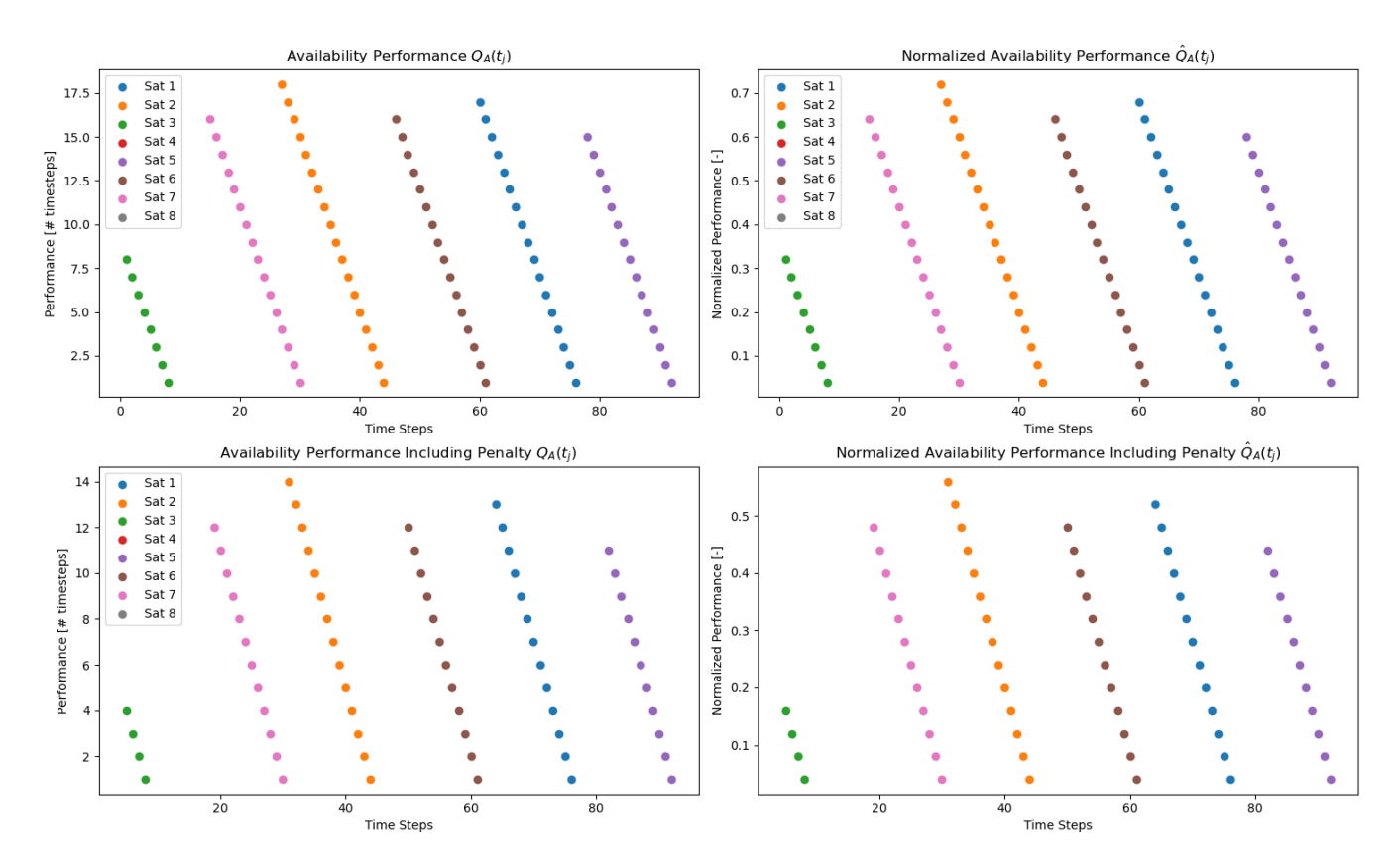


Figure F.9: Availability Performance including normalization and penalization

Looking at the behaviour of the BER performance (Q_{BER}) in Figure F10, a similar behaviour can be observed compared to the availability performance. The BER performance starts at its highest value and afterwards decreases with each subsequent instance of time. This continuous downwards slope should therefore also be visible in the normalized behaviour \hat{Q}_{A_i} . The normalization performance is calculated by dividing the performance with the maximum applicable length of one of the satellites available during the mission, resulting a value between 0 and 1. The upper right image provides the behaviour of the normalized BER performance, and as expected it is a decreasing slope for each satellite range between 0 and 1. Looking at the performance compared to the penalized performance on the bottom left, it can be observed that for each satellite and every instance of time the performance is 4 points lower. This translates to the simulation being run on

36 F. Verification and Validation

a 5 second time interval while having a acquisition time (T_{acq}) of 20 seconds, translating to a penalty of 4 instances of time during which satellite i is not available to the ALCT. Therefore, the normalized penalized performance shown in the bottom right corner starts at a lower value compared to the normalized performance. These four figures therefore show that the isolated performance of the BER behave accordingly to the envisioned behaviour and the test was passed successfully.

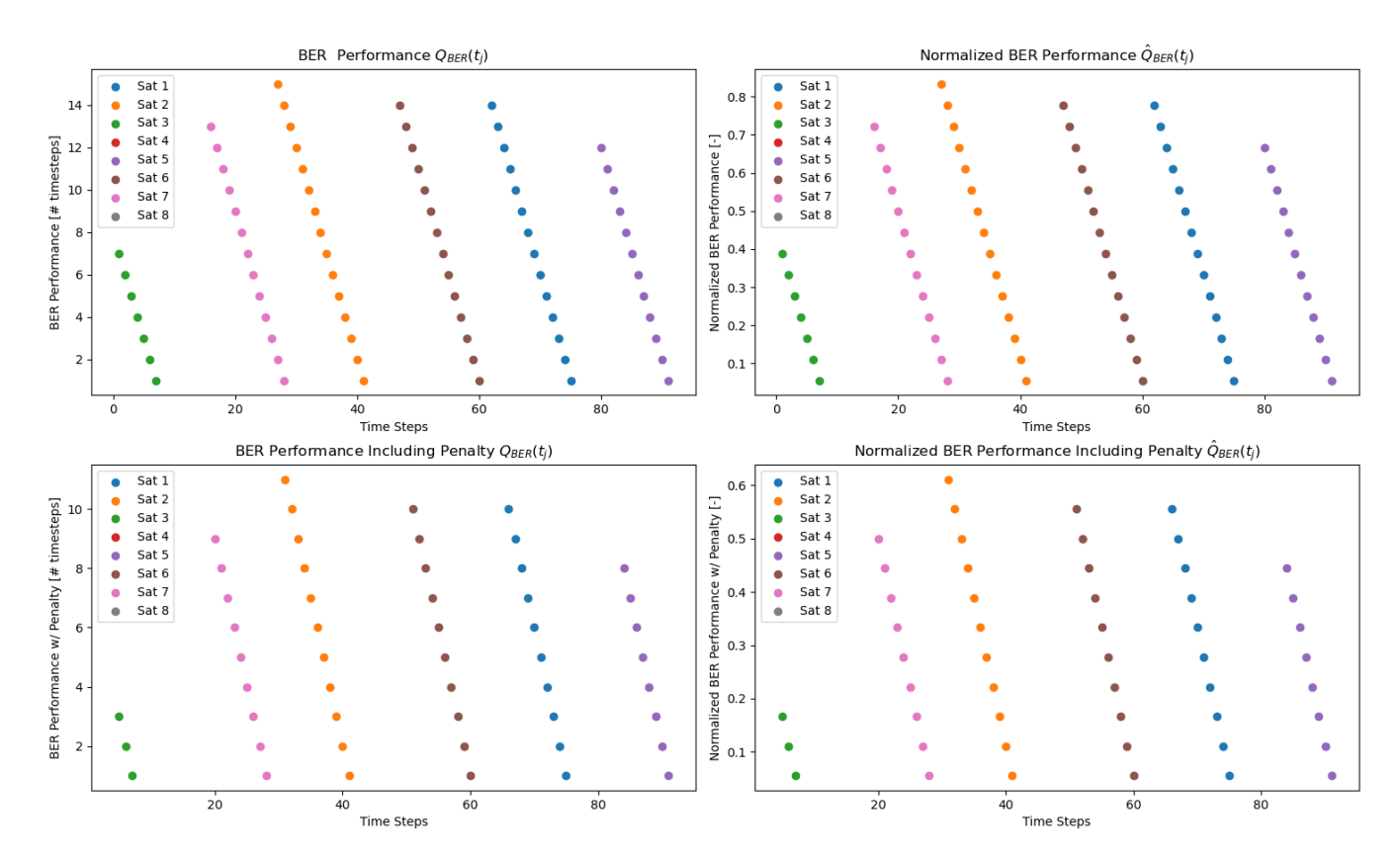


Figure F.10: Bit Error Rate Performance including normalization and penalization

E.1. Verification Overview 37

F.1 Verification Overview

Verification tag	Test Description	Priority	Test	Expected Result	Performed (Y/N)	Passed (Y/N)	Outcome	Solution	Implemented (Y/N)
Unit- 001	Does the list of activated satellites correspond to the links selected?	1	Check in debug mode and generate print statements during simulations	Yes	Y	Y	Number of activated satellites needs to be converted to index +1 to correctly map it onto the link selected	Store both values, the satellite index (for future calculations) and the satellite number which is index +1	Y
Unit- 002	Is the list of activated satellite equal in length to the entire mission time?	3	Generate plot with active satellites over time	Yes	Y	Y	As long as the list of time is equal in length to the list of activated satellites, the acti- vated satellite plot can be generated		
Unit- 003	Is the number of active links equal or smaller than the number of total available satellites within the constellation?	3	Generate plot with active satellites over time	Yes	Y	Y	Figure 4.1 and 4.4 show that only 1 satellite is activated at each instance of time		
Unit- 004	Is the number of active links equal or smaller than the number of total applicable satellites	3	Generate plot with active satellites over time	Yes	Y	Y	Figure 4.1 and 4.4 show that only 1 satellite is activated at each instance of time		
Unit- 005	Is the sum of activated satellites plus the number of different links (i.e. acquisition time) smaller or equal to the mission time	1	Write control function	Yes	Y	N	Model automatically makes the new satellite active independent of acquisition time. Currently the total acquisition time is removed at the end which is composed of the multiplication between the acquisition time by the number of different links.	Implement a check if the satellite made active is equal to the previous timestep, if not, directly count the downtime	N
Unit- 006	What if the active satellite is constant throughout the entire mission?	2	Mimic output of the link se- lection class and use as in- put	Performance and availability very low	N				
Unit- 007	What if there is no active satellite throughout the entire mission?	2	Mimic output of the link se- lection class and use as in- put for performance class	No performance	N				
Unit- 008	To what extent is there an output difference with the "single sat module" turned on	1	Mimic output of the link se- lection class and use as in- put for performance class	Multiple satellites removed and impact on computational effort required	Y	Y	Model loops through various time instances much faster. The combined performance value is missing if this mode is turned on for some instances of time.		
Unit- 009	To what extent is there an output difference with the "falling satellite" turned on	1	Build setting as input for JSON config file	Multiple satellites removed and impact on computa- tional effort required	Y	N	Model loops through various time instances much faster. Model simulates entire mission, however error occurs in assigning the right physical performance to the set of reduced satellites. Error is invoked due to removal of applicable satellites	Rewrite satellite removal definition and link physical performance to a certain satellite	Y
Unit- 010	To what extent is there an output difference with the "Outperforming" turned off	3	Generate print statement	Multiple satellites removed and impact on computa- tional effort required	Y	Y	No satellite gets removed based on this setting and therefore no computational gain	Evaluate if setting is required or requires an iteration	N
Unit- 011A	How does the output in terms of availability/throughput (average and total)/ BER compare to existing models	1	Check against Wieger based on literature	Link selection model has increased performance	Y	Y	The use case with the optimized link selection model shows significant improvement in both availability and throughput		
Unit- 011B	How does the output in terms of availability/throughput (average and total)/ BER compare to existing models	3	Use output of link selec- tion class as input in source code Wieger	Link selection model has increased performance	N				

 $Table \ E1: Overview \ of performed \ unit \ tests, convergence \ analysis \ and \ validation \ on \ the \ mission \ level \ of \ the \ link \ selection \ model$

Verification tag	Test Description	Priority	Test	Expected Result	Performed (Y/N)	Passed (Y/N)	Outcome	Solution	Implemented (Y/N)
Unit-101	Does the model select the satellite with the highest performance score	1	Check in debug mode and generate plot	Yes	Y	Y	Clearly visible from Figure F.3 that satellite with highest performance score is made active		
Unit-102	Does the sum of the separate link times equal the service time	1	Write function	Yes	Y	N	Same behaviour as with Unit-005. The model makes the satellite active while it not being available yet.	Perform this calculation by making use of the availability vector, in which in be- tween a link change an outage period oc- curs	Y
Unit-103	Does the average link time multiplied with the number of links equal the service time?	2	Write function	Yes	Y	N	Same behaviour as with Unit-005. The model makes the satellite active while it not being available yet.	Perform this calculation by making use of the availability vector, in which in be- tween a link change an outage period oc- curs	Y
Unit-104	Are the normalized performance parameters value used for the active satellite?	1	Check in debug mode	Yes	Y	Y			
Unit-105	Are the normalized penalized performance parameter values used for the inactive satellites?	1	Check in debug mode	Yes	Y	Y			
Unit-106	What if all performance parameter values are put to zero, which link get selected?	3	JSON configuration file	No link gets selected	Y	N	The model selects from the list of applicable satellites the satellite with the lowest satellite index	Implement a control performance parameter which is always turned "ON" if no other performance parameter is propagated. Control parameter based on geometrical performance (range/elevation angle)	N
Unit-107	What if all performance parameter values are put to one, which link get selected?	3	JSON configuration file	Simulation gets killed (constraint sum of weights performance values =1)	Y	N	The constraint is not built as a hard kill for the model	Build a check point where the model checks if the sum of the performance parameter weight is 1	N
Unit-108A	What if the rising/falling satellite performance assumption breaks? ('falling satellite setting "ON"')	1	This is checked by Unit-109 and Unit-110 while hav- ing 'falling satellite setting "ON"	Satellites are removed and at a certain point there are no more applicable satel- lites, simulation gets killed	Y	Y	Independent of results found in Unit-009, the expected behaviour was observed	Implement a control performance parameter which is always turned "ON" if no other performance parameter is propagated. Control parameter based on geometrical performance (range/elevation angle)	N
Unit-108B	What if the rising/falling satellite performance assumption breaks? ('falling satellite setting "OFF"')	1	This is checked by Unit-109 and Unit-110 while hav- ing 'falling satellite setting "OFF"	Normal simulation	Y	Y	Link switch is performed if a new satellite becomes applicable		
Unit-109	When will the link switch if the availability weight is put to 1, and the rest to zero	1	JSON configuration file	Link switch is performed once a new satellite be- comes applicable	Y	Y	Figure F.4 shows that link is switched directly once a new satellite becomes available		
Unit-110	When will the link switch if the BER weight is put to 1, and the rest to zero	1	JSON configuration file	Link switch is performed once a new satellite be- comes applicable	Y	Y	Figure F.5 shows that link is switched directly once a new satellite becomes available		
Unit-111	When will the link switch if the Cost weight is put to 1, and the rest to zero	1	JSON configuration file	All performance scores are equal	N				
Unit-112	When will the link switch if the Data Transfer Latency weight is put to 1, and the rest to zero	1	JSON configuration file	Link switch is performed after a couple of time in- stances a satellite has be- come applicable (center- left)	Y	Y	Figure F.6 shows that link is switched after a couple of time instances after a new satellite has become available		
Unit-113	When will the link switch if the Propagation Latency weight is put to 1, and the rest to zero	1	JSON configuration file	Link switch is performed in the center of the applicable period for each satellite	Y	Y	Figure F.7 shows that link is switched in the middle of the time a satellite is applicable		
Unit-114	When will the link switch if the Throughput weight is put to 1, and the rest to zero	1	JSON configuration file	Link switch is performed after a couple of time in- stances a satellite has be- come applicable (center- left)	Y		Figure F.8 shows that link is switched after a couple of time instances after a new satellite has become available		

F.1. Verification Overview 39

Verification tag	Test Description	Priority	Test	Expected Result	Performed (Y/N)	Passed (Y/N)	Outcome	Solution	Implemented (Y/N)
Unit-115	What if the current active satellite becomes invisible/ not applicable, and all other satellites are removed due to falling performances?		To be identified	To be identified	N				
Unit-116	Is the difference in performance for a link, once there are 2 optical heads, equal to its performance with only normalized non-penalized values	3	Check within debug mode and generate print statement	No	N				

 $Table \ E2: Overview \ of performed \ unit \ tests, convergence \ analysis \ and \ validation \ on \ the \ service \ level \ of \ the \ link \ selection \ model$

Verification tag	Test Description	Priority	Test	Expected Result	Performed (Y/N)	Passed (Y/N)	Outcome	Solution	Implemented (Y/N)
Unit-201	Are the individual performance parameters combined equal to the performance score used in the link selection?	2	Generate plot with performance per time instance	Yes	Y	Y	Figure F.3 shows that the link is switched from sat 6 to sat 5 from time index 19 to 20, aligning with the visibility plot in Figure F.2		
Unit-202	Is the weight multiplied with performance parameter equal to the weighed performance parameter?		Generate plot with performance per time instance	Yes	Y	Y	calculated values perfectly match weight times performance		
Unit-203	Is the performance calculation equal if the "No Link" and "Active satellite num- ber" loop are switched		Generate plot	Yes	Y	Y			
Unit-204	Is the propagated link within the list of visible satellites?	2	Generate visibility and active satellite plot		N				
Unit-205	Is the active link within the list of applicable satellites?	2	Generate applicability and active satellite plot		N				

 $Table \ E3: Overview \ of performed \ unit \ tests, convergence \ analysis \ and \ validation \ on \ the \ link \ level \ of \ the \ link \ selection \ model$

Verification tag	Test Description	Priority	Test	Expected Result	Performed (Y/N)	Passed (Y/N)	Outcome	Solution	Implemented (Y/N)
Unit-301	Are all applicable satellites visible?	3	Generate applicability and active satellite plot		N				
Unit-302	Does the correct loop gets entered based on the previous time step stating "No Link" or "Active satellite number" or "Active satellite number" and "previous_indices = current_indices"?	3	Check in debug mode	Yes	Y	Y	Correct loop gets entered		

Table F.4: Overview of performed unit tests, convergence analysis and validation on the access level of the link selection model

Verification tag	Test Description	Priority	Test	Expected Result	Performed (Y/N)	Passed (Y/N)	Outcome	Solution	Implemented (Y/N)
Unit-401	What is the impact of a decay factor of 1 on the throughput performance parameter	3	JSON configuration file		N				
Unit-402	What is the impact of a decay factor of 0.5 on the throughput performance parameter	3	JSON configuration file		N				
Unit-403	What is the impact of a decay factor of 0.15 on the throughput performance parameter	3	JSON configuration file		N				
Unit-404	Does the availability performance parameter (both normal, normalized and penalized) correspond to the physical layer outcome	1	Generate isolated performance parameter plot	Yes	Y	Y	Plots provided in Figure F.9		
Unit-405	Does the BER performance parameter (both normal, normalized and penalized) correspond to the physical layer outcome	1	Generate isolated performance parameter plot	Yes	Y	Y	Plots provided in Figure F.10		
Unit-406	Does the Cost performance parameter (both normal, normalized and penalized) correspond to the physical layer outcome	1	Generate isolated performance parameter plot	Yes	N				
Unit-407	Does the Data Transfer Latency performance parameter (both normal, normalized and penalized) correspond to the geometrical outcome	1	Generate isolated performance parameter plot	Yes	Y	Y	Plots provided in Figure 3.4		
Unit-408	Does the Propagation Latency performance parameter (both normal, normalized and penalized) correspond to the input	1	Generate isolated performance parameter plot	Yes	Y	Y	Plots provided in Figure 3.5		
Unit-409	Does the Throughput performance parameter correspond to the physical geometrical outcome	1	Generate isolated performance parameter plot	Yes	Y	Y	Plots provided in Figure 3.6		
Unit-410	What if the actual throughput for all time steps is set equal to the client requirement?	3	Mimic prerequisites class output and use as input for link selection		N				
Unit-411	What if the actual Bit Error Rate for all time steps is set equal to the client requirement	3	Mimic prerequisites class output and use as input for link selection		N				

Table E5: Overview of performed unit tests, convergence analysis and validation on the performance level of the link selection model

F.1. Verification Overview 41

Verification tag	Test Description	Priority	Test	Expected Result	Performed (Y/N)	Passed (Y/N)	Outcome	Solution	Implemented (Y/N)
Unit-501	What happens if a simulation run is performed with random throughput values	2	Mimic prerequisites class output and use as input for link selection		N				
Unit-502	What happens if a simulation run is performed with random BER values	2	Mimic prerequisites class output and use as input for link selection		N				
Unit-503	What happens if a simulation run is performed with random P_r values	2	Mimic prerequisites class output and use as input for link selection		N				
Unit-504	What happens if a simulation run is performed with all throughput values set to zero	3	Mimic prerequisites class output and use as input for link selection		N				
Unit-505	What happens if a simulation run is performed with all BER values set to zero	3	Mimic prerequisites class output and use as input for link selection		N				
Unit-506	What happens if a simulation run is performed with all P_r values set to zero	3	Mimic prerequisites class output and use as input for link selection		N				

 $Table \ E6: Overview \ of performed \ unit tests, convergence \ analysis \ and \ validation \ on \ the \ physical \ layer \ of \ the \ link \ selection \ model$

Verification tag	Test Description	Priority	Test	Expected Result	Performed (Y/N)	Passed (Y/N)	Outcome	Solution	Implemented (Y/N)
Unit-601	What is the impact on the output if the timestep is increased to 1s	3	JSON configuration file	Runtime error	N				
Unit-602	What is the impact on the output if the timestep is increased to 50s	2	JSON configuration file	Normal simulation but impact on model accuracy	Y	Y	The simulation shows correct selection behaviour in line with expectations, however, some throughput behaviour at the start of end of link show high fluctuations. Furthermore, the penalty assumptions break if the acquisition time is less than 50 seconds		
Unit-603	What is the impact on the mission output if the timestep is increased to 500s	3	JSON configuration file	Normal simulation but impact on model accuracy	N				
Unit-604	What is the impact on the mission output if constellation is increased to 1000 satellites		JSON configuration file	Runtime error	N				

 $Table \ E.7: Overview \ of performed \ unit \ tests, convergence \ analysis \ and \ validation \ on \ the \ input \ level \ of \ the \ link \ selection \ model$

Appendix G

Variable Description

G.1 Greek Variables

Table G.1: Description of Greek Variables

Greek Symbols	Description	Unit
α_A	The client input weight applied to the Availability performance pa-	[-]
	rameter	
α_{BER}	The client input weight applied to the Bit Error Rate performance pa-	[-]
	rameter	
α_C	The client input weight applied to the Cost performance parameter	[-]
α_{DTL}	The client input weight applied to the Data Transfer Latency perfor-	[-]
	mance parameter	
α_{PL}	The client input weight applied to the Propagation Latency perfor-	[-]
	mance parameter	
α_R	The client input weight applied to the Throughput performance pa-	[-]
	rameter	

G.2. Latin Variables 43

G.2 Latin Variables

Table G.2: Description of Latin Variables

Latin Symbols	Description	Unit
$BER_{act}(t_j)$	The actual Bit Error Rate at a specific time index	[-]
BERreq	The required Bit Error Rate defined by the client	[-]
BR	The bit rate required limited by the transmitter's hardware capabili-	[bits/s]
	ties	
c_s	The speed of light	[m/s]
C_{var_k}	The variable cost per second to maintain a link between an ALCT and	[€/s]
	a satellite of constellation k	
$C_{var_{max}}$	The maximum variable cost per second to maintain a link between	[€/s]
	an ALCT and a satellite of constellation k, captured form all constel-	
	lations available within the mission span	
C_{fix_k} $C_{fix_{max}}$	The fixed cost to establish a link between an ALCT and a satellite of	[€]
	constellation k	
$C_{fix_{max}}$	The maximum fixed cost to maintain a link between an ALCT and a	[€]
	satellite of constellation k, captured form all constellations available	
	within the mission span	
d_{LCT-S_i}	Distance between an ALCT and satellite i	[m]
$d_{LCT-S_{min}}$	Smallest distance between a satellite and an ALCT, over the entire	[m]
	mission span	
$E_i(t_j)$	The decision variable which is either 1 if a link is active between satel-	[-]
	lite i and an ALCT, or 0 if no link is active between satellite i and an	
	ALCT.	
$J_i(t_j)$	The cost function for satellite i at time index j	[-]
P_{thr}	The power threshold which resembles the system sensitivity above	dBm
	which a link between satellite i and the ALCT can be made. This is de-	
	rived from the Required Bit Error Rate BER_{req} defined by the client.	_
P_{pen}	The power penalty applied to the P_{RX} to compensate for micro-scale	dBm
	losses.	_
P_{RX}	The power at the receiver including the power penalty (P_{pen})	dBm

G. Variable Description

Table G.3: Description of Variables (1/2)

Variable	Description	Unit
$q_{A_i}(t_j)$	The availability performance parameter of satellite i, at a specific time index	[-]
$Q_{A_i}(t_j)$	The propagated availability performance parameter of satellite i, over a duration of time at a specific time index	[-]
$\hat{Q}_{A_i}(t_j)$	The normalized propagated availability performance parameter with respect to t_{V_i} , for satellite i at a specific time index	[-]
$q_{BER_i}(t_j)$	The Bit Error Rate performance parameter of satellite i, at a specific time index	[-]
$Q_{BER_i}(t_j)$	The propagated Bit Error Rate performance parameter of satellite i, over a duration of time at a specific time index	[-]
$\hat{Q}_{BER_i}(t_j)$	The normalized propagated Bit Error Rate performance parameter with respect to t_{A_i} , for satellite i at a specific time index	[-]
q_{C_i}	The cost performance parameter of satellite i, independent of the time index	[€]
$\hat{q}_{C_i} \ Q_{DTL_i}(t_j)$	The normalized cost performance parameter with respect to Q_{Cmax} The data transfer latency performance parameter of satellite i, at a specific time index	[-] [ms]
$\hat{Q}_{DTL_i}(t_j)$	The normalized data transfer latency performance parameter with respect to $q_{PL_{min}}$, for satellite i at a specific time index	[-]
$q_{PL_i}(t_j)$	The propagation latency performance parameter of satellite i, at a specific time index	[ms]
$\hat{q}_{PL_i}(t_j)$	The propagation normalized latency performance parameter with respect to $q_{PL_{min}}$, for satellite i at a specific time index	[-]
$q_{R_i}(t_j)$	The throughput performance parameter of satellite i, at a specific time index	[-]
$Q_{R_i}(t_j)$	The propagated throughput performance parameter of satellite i, over a duration of time at a specific time index	[-]
$\hat{Q}_{R_i}(t_j)$	The normalized throughput performance parameter with respect to $t_{A,max}$, for satellite i at a specific time index	[-]
$R_{act}(t_j)$	The realised throughput at a specific index of time	[bits/s]
R_{req}	The required number of bits received per second, defined by the client	[bits/s]
R_{avg}	The average throughput over a TBD period of time	[bits/s]
R_{avg,L_i}	The average throughput over the link time with active satellite i [bits/s]	[bits/s]
R_{avg,t_S}	The average throughput over the service time	[bits/s]
R_{avg,t_M}	The average throughput over the mission time	[bits/s]
R_{ACC}	The accumulated throughput over a TBD period of time	[bits]
R_{ACC,L_i}	The accumulated throughput over the link time with active satellite i [bits/s]	[bits]
R_{ACC,t_S}	The accumulated throughput over the service time	[bits]
R_{ACC,t_M}	The accumulated throughput over the mission time	[bits]
R_C	The potential theoretical throughput of a link based on the Shannon-Hartley theorem	[bits/s]
s_i	The satellite with index number i	

G.2. Latin Variables 45

Table G.4: Description of Variables (2/2)

Variable	Description	Unit
t_{acq}	The time it takes to make a link acquisition	s
t_j	The time at index j	[-]
t_{A_i}	The duration that satellite i has an available link for an ALCT	S
$t_{A_i,s}$	The time index at which the link between satellite i and an ALCT becomes available	[-]
$t_{A_i,e}$	The time index at which the link between satellite i and ALCT becomes unavailable	[-]
$t_{A,max}$	The largest duration of time a satellite within the mission span is applicable	S
t_{L_i}	The duration that satellite i is linked to an ALCT	S
$t_{L_i,s}$	The time index at which the link between satellite i and an ALCT is established	S
$t_{L_i,e}$	The time index at which the link between satellite i and ALCT ends	s
t_{V_i}	The duration that satellite i is visible to an ALCT	S
$t_{V_i,s}$	The time index at which satellite i becomes visible to an ALCT	[-]
$t_{V_i,e}$	The time index at which satellite i becomes non-visible to an ALCT	[-]
$t_{V,max}$	The largest duration of time a satellite within the mission span is visible	S
t_S	The combined service duration of all linked satellites with an ALCT	S
t_M	The total mission duration, during which the link selection process is optimized	S
$t_{M_i,s}$	The time index at which the link selection optimization mission for an ALCT and a LEO constellation starts	[-]
$t_{M_i,e}$	The time index at which the link selection optimization mission for an ALCT and a LEO constellation ends	[-]
Δt	The step size over which the link selection optimization module is performed	s

Appendix H

Definitions

H.1 Availability

- Link Availability: The link availability is defined as the ratio of time that the link has a positive link margin compared to the total time of link visibility. The switch over point is determined by a comparison between P_{RX} (including power penalty for fading statistics) and the minimal acceptable detector BERthreshold. [% of visible time]
- **Power Received** (P_{RX}): The signal power received at the receivers terminal. Within this power received a power penalty is applied for scintillation, beam wander, angle of arrival, transmitter jitter and receiver jitter. [dBm]
- Threshold Signal Power (P_{thr}): The minimum sensitivity needed to receive the transmitted bits. [dBm]

H.2 Bit Error Rate

- Required Bit Error Rate (BER_{req}): The worstBERwhich is accepted by the client from a hardware perspective. This will be defined by the client in an initial phase. [Bits/s]
- Actual Bit Error Rate ($BER_{act}(t_j)$): The number of faulty bits received at a specific time index (t_j) . This is calculated by dividing the quantity of total number of bits received by the number of bits transmitted at (t_j) . [Bits/s]

H.3 Cost

- Link variable cost (C_{var_k}) : The amount of money charged per second to have a link with a satellite in constellation k. $[\notin/s]$
- Link fixed cost (C_{fix_k}) : The amount of money charged to acquire a new link with a satellite in constellation k. $[\xi]$

H.4 Latency

- **Propagation Latency** (q_{PL}): The delay caused by the transfer of bits. The latency consist out of multiple factors, which together stand for the total latency. The only latency factor taken into account for this research is the propagation latency, which is solely dependent on the link distance. The other latency factors such as transmission latency, data queuing latency etc are assumed to be equal for all links and therefore not interesting to use within the cost function as the cost function is a matter of comparing performance. [ms]
- Data Transfer Latency (Q_{DTL}): The average delay caused by the transfer of bits over an instance of time. [ms]
- Link Distance (d_{ALCT-S_i}): The geometrical distance between the ALCT and satellite at an instance of time. [m]

H.5 Throughput

• **Bit Rate** (BR): The number of bits send from the transmitter to the receiver. Therefore, the BR is limited by the transmitter's hardware capabilities [Bits/s]

H.6. Time instances 47

• **Required Throughput** (R_{req}): The required number of bits received per over a specific time instance. This will be defined by the client in an initial phase and can be converted to an average required bits at a specific time index. [Bits/[TBD]]

• Actual Throughput ($R_{act}(t_j)$): The realised throughput at a specific index of time (t_j), which takes into account the link conditions and system constraints. The formula used to calculate this is shown below in Equation H.1. [Bits/s]

Actual Throughput = Bit Rate – Actual Bit Error Rate
$$(H.1)$$

- Average [TBD] Throughput (R_{avg}): the total amount of bits that are transmitted/received over a predefined instance of time. [Bits/[TBD]]
- Total Link Throughput (R_{L_i}): The total amount of bits that are received over 1 link time. [Bits/link]
- **Total Aggregated Link Throughput** ($R_{L_i i}$): The total amount of bits that are received over a combined set of link times. [Bits]
- Total Mission Throughput (R_{ACC,t_M}): The total amount of bits that are received over the entire mission span. [Bits]
- Capacity (R_C): The capacity is defined as the potential theoretical throughput which is calculated with the Shannon-Hartley theorem, shown in Equation H.2. The capacity is thus dependent on the bandwidth and signal to noise ratio. Meaning that in case of a very large link margin, theoretically speaking we can very high data rates. Note, the capacity of a link is therefore not dependent on any other physical hardware and software or firmware. [Bits/s]

$$C_{theoretical} = B \cdot \log_2(1 + \frac{S}{N}) \tag{H.2}$$

H.6 Time instances

- **Mission Time** (t_M): The total mission duration during which the link selection optimization algorithm will be applied. This will be defined by the client in an initial phase. [s]
- **Service Time** (*t_S*): The combined service time of all active links during the mission time. [s]
- Visibility Time (t_{V_i}): The time that satellite i is visible, within line of sight, to an ALCT. [s]
- Availability Time (t_{A_i}) : The time that satellite i has a positive link margin and thus is available to make a link with an ALCT. [s]
- **Link Time** (t_{L_i}): The time that satellite i is linked to an ALCT. [s]

Appendix I

Configuration file

Parameter	Value	Unit
Constants		
R_earth	6367000.0	m
speed_of_light	299792458.0	m/s
q	1.602176634e-19	С
h	6.62607015e-34	J⋅s
k	1.38e-23	J/K
mu_earth	3.986004418e14	m^3/s^2
t_day	24.0	h
Omega_t	6.283185307179586	rad
omega_earth	7.27220521664304e-05	rad/s
Numerical Simulation Setup	'	<u>'</u>
start_time	0.0	S
end_time	21600.0	S
step_size_link	50.0	S
step_size_SC	7.0	S
integrator	Runge Kutta 4	-
step_size_channel_level	0.0001	S
interval_channel_level	5.0	s
frequency_filter_order	2	-
Link Analysis Parameters		
analysis	total	-
link_number	all	-
ac_LCT	general	-
link	up	-
LCT Laser Parameters - AC		,
wavelength_ac	1.553e-06	m
data_rate_ac	2500000000.0	bps
P_ac	20.0	W
D_ac	0.08	m
clipping_ratio_ac	2.0	-
obscuration_ratio_ac	0.1	-
M2_defocus_ac	1.0	-
M2_defocus_acquisition_ac	11.66	-
angle_div_ac_acquisition	0.0003	rad
focal_length_ac	0.12	m
angle_pe_ac	4.0e-06	rad
std_pj_ac	3.4e-06	m
std_pj_spot_ac	2.5e-05	m
eff_quantum_ac	1.0	-
T_s_ac	300	K
FOV_ac	1.0e-08	rad

Parameter	Value	Unit
FOV_ac_acquisition	0.0065	rad
eff_transmission_ac	0.8	-
WFE_static_ac	1.0e-07	m
WFE_static_acquisition_ac	1.5e-07	m
h_splitting_ac	0.9	-
detection_ac	Preamp	-
mod_ac	OOK-NRZ	-
M_ac	150.0	-
F_ac	4.0	-
delta_wavelength_ac	5.0e-09	m
R_L_ac	50.0	ohm
sensitivity_acquisition_ac	3.16227766016e-10	W
LCT Laser Parameters - SC		
wavelength_sc	1.553e-06	m
data_rate_sc	2500000000.0	bps
P_sc	20.0	W
D_sc	0.08	m
clipping_ratio_sc	2.0	-
obscuration_ratio_sc	0.1	-
M2_defocus_sc	1.0	-
M2 defocus acquisition sc	11.66	-
angle_div_sc	2.5e-05	rad
angle_div_sc_acquisition	0.0003	rad
focal_length_sc	0.12	m
angle_pe_sc	3.6e-06	rad
std_pj_sc	3.3e-06	m
std_pj_spot_sc	2.5e-05	m
eff_quantum_sc	0.7	-
T_s_sc	300	K
FOV_sc	1.0e-08	rad
FOV_sc_acquisition	0.0065	rad
eff_transmission_sc	0.8	-
WFE_static_sc	1.0e-07	m
h_splitting_sc	0.9	-
detection_sc	Preamp	-
mod_sc	BPSK	_
M_sc	285.0	-
F_sc	2.0	-
BW_sc	250000000000	Hz
delta_wavelength_sc	5.0e-09	m
R_L_sc	50.0	ohm
sensitivity_acquisition_sc	3.16227766016e-10	W
Aircraft Parameters		
method_AC	opensky	-
h_AC	10000.0	m
vel_AC	[0.0, 220.0, 0.0]	m/s
lat_init_AC	78.5094	deg
lon_init_AC	60.54131	deg
aircraft_filename_load	/Users/jaristensen/Desktop/Visual_Studio/Thesis/	-
	Link_Selection_Simulation_version2.1/	
	ac_trajectories/OSL_ENEV.csv	
aircraft_filename_save	/Users/jaristensen/Desktop/Visual_Studio/Thesis/	-
	Link_Selection_Simulation_version2.1/ sc_trajectories/SDA.json	
Constellation Parameters		
constellation_data	NONE	-
method_SC	tudat	-
		1

50 I. Configuration file

Parameter	Value	Unit
SC_filename_load	/Users/jaristensen/Desktop/Visual_Studio/Thesis/	-
	Link_Selection_Simulation_version2.1/ sc_trajectories/SDA.json	
SC_filename_save	/Users/jaristensen/Desktop/Visual_Studio/Thesis/	-
	Link_Selection_Simulation_version2.1/sc_trajectories/SDA.json	
constellation_type	LEO_cons	-
h_SC	1200000.0	m
inc_SC	85	deg
number_of_planes	2	-
number_sats_per_plane	14	-
variable_link_cost_const1	1.667	-
fixed_link_cost_const1	100	-
TLE_filename_load	C:\Users\wiege\Documents\TUDelft_Spaceflight\Thesis\	-
	ac_sc_data\constellation_TLE_data\oneweb_tle.json	
Link Selection Parameters		<u>'</u>
elevation_min_angle	0.0	deg
elevation_threshold	5.0	deg
acquisition_time	20	s
Atmospheric Parameters		
scale_height	6600.0	m
att_coeff	0.005	-
I_sun	0.5	-
I_sky	0.0	-
n_index	1.002	<u> </u>
Methods Choices	11002	
margin_buffer	3.0	-
desired_frac_fade_time	0.01	-
BER_thres	[1.0e-09, 1.0e-06, 1.0e-03]	-
coding	no	-
latency_interleaving	0.1	s
N	255	-
K	223	<u> </u>
symbol_length	8	bit
turbulence model	Hufnagel-Valley	-
wind_model_type	Bufton	-
turbulence_freq_lowpass	1000.0	Hz
jitter_freq_lowpass	100.0	Hz
jitter_freq2	[100.0, 300.0]	Hz
jitter_freq1	[900.0, 1100.0]	Hz
method_att	[900.0, 1100.0] ISA profile	
	static	-
method_clouds dist_scintillation	lognormal	-
dist_scintiliation dist_beam_wander	rayleigh	-
	• •	-
dist_AoA	rayleigh	-
dist_pointing Performance Parameters	rayleigh	-
	0.167	
client_input_availability	0.167	-
client_input_BER	0.167	-
client_input_cost	0.167	-
client_input_data_transfer_latency	0.167	-
client_input_propagation_latency	0.167	-
client_input_throughput	0.167	-
Throughput Decay Rate		
decay_rate	0.0	-
Visualization		
folder_path	animations	-
Acquisition		

Parameter	Value	Unit
T_acq	20	S

Conclusion and Recommendations

Free-space-optics (FSO) satellite communication presents a transformative potential in achieving high bandwidth, low latency, and secure data transfer on a global scale. The optimization of link selection between a airborne laser communication terminal (ALCT) and a satellite constellation is critical to leveraging the high potential of FSO communication services compared to the current operational radio frequency technology. This link selection process needs to take into account future physical performance of the potential link, a set of client requirements and there preferred optimization criteria. Despite the inherent complexity and computational demands associated with optimizing this link selection process, which involve numerous physical and geometric performance parameters, a Linear Programming (LP) formulation was deemed an effective solution.

This LP formulation consist of a decision variable, an objective function and a set of constraints. This decision variable determines if an applicable satellite is made active or not. The objective function is a maximization of the defined cost function over the entire mission span. This cost function is a multiplication of the performance parameters matrix and the associated client weight matrix. These performance parameters are divided in three groups, the cost, which simulates the financial impact of the mission. Secondly, the coverage which models the total link availability over the mission span and lastly the link quality. This link quality consist of bit-error-rate (BER), throughput and latency, where the latency is split into propagation latency and data transfer latency. Each of these performance parameters are assigned with a weight based on the client mission preferences. The constraints associated to this LP formulation are derived from the mission specific physical environment and time domain. This LP formulation serves as the backbone of the model which further consist of an input, prerequisites, settings and result section. The input is modelled as a JSON configuration file in which all mission specific parameters are defined. The prerequisites are adjustable propagation modules for the movement of both the ALCT and low-earth orbit (LEO) constellation, and the physical behaviour of potential links. The settings module is brought into life to be able to control the computational effort required to perform a simulation.

The model's efficacy was validated through tests involving two 80-minute missions using the same ALCT and input configurations. These tests utilized the SDA constellation with one and two orbital planes. These simulations achieved availability rates of 86.11% and 85.26% respectively. The accumulated throughput for these scenarios was 10.12 and 9.87 Tbits, respectively. A thorough verification process has been performed, assessing the correctness of the individual models, their integration and the accompanying results. However, very preliminary validation has been performed by comparing it only to 1 model found in literature. From this validation it could be concluded that the impact of this link selection model on the performance of FSO communication is significant and resulted in a 10% and 14.7% performance increase in terms of accumulated throughput and availability. Once the technology around link selection models between air-to-space layers is at an improved technical readiness level, a more complete validation should be performed by comparing it to measurements from experimental demonstrations.

These results underscore the LP formulation's robustness in dynamically selecting optimal links, thereby maximizing the availability and throughput of the communication link. The successful application of this model in different constellations highlights its versatility and effectiveness, establishing it as a foundational component for future FSO satellite communication link selection models. This work paves the way for further enhancements in global connectivity and bandwidth through optimized FSO satellite communication services. However, in order to really make use of the complete potential of FSO communication some additional fundamental work needs to be done. The model is build in a very modular way, which allows it to be extended both from a development as a use case perspective. Namely, the model can be further developed by introducing additional performance parameters, including multiple constellations within the simulation and by adding a control parameter based on readily available geometrical data. Furthermore, additional settings can be initiated and the selection within the applicability module can be increased, to make the model less computational extensive. However, it is also believed that the model can gain significant computational run time by a refactoring based on real software development coding rules.

To enhance the added value of this link selection model it needs to incorporate a complete routing network spanning from ground to deep space communications. In order to achieve such an extension, the model needs to be assessed if is ap-

plicable on a broader scope and an assessment needs to be made which parts are missing. For example, an ground to air link requires different modelling as cloud attenuation become more dominant, while the availability performance changes significantly if GEO satellites are taken into the equation as their visibility is static.